CHAPTER IV:

RESULTS

4.0 Results:

In order to carry out the study, it was found that the understanding of trends, crop calendar and vulnerability of the agricultural area to climate change should be taken note of to make the study precise. So each component has been discussed separately.

4.1 Trend analysis in different crops:

The present study was undertaken with a view to analyze the trends in area, production and yield of different crops of the study area during period 2000 to 2012. This analysis when done for the country, state and district showed variations. This type of information generated proves to be significant for the policy makers for developing their strategies. Such type of analysis therefore was done for major crops observed during the study viz Cotton (*Gossypium hirsutum* L.), Castor (*Ricinus communis* L.) and Banana (*Musa paradisiaca* L.).

4.1.1 COTTON

a) At country level

Among all the major states of India, Maharashtra Gujarat, and Andhra Pradesh occupy the first, second and third position respectively, accounting for over 75% cotton sown area (**Figure 14**).

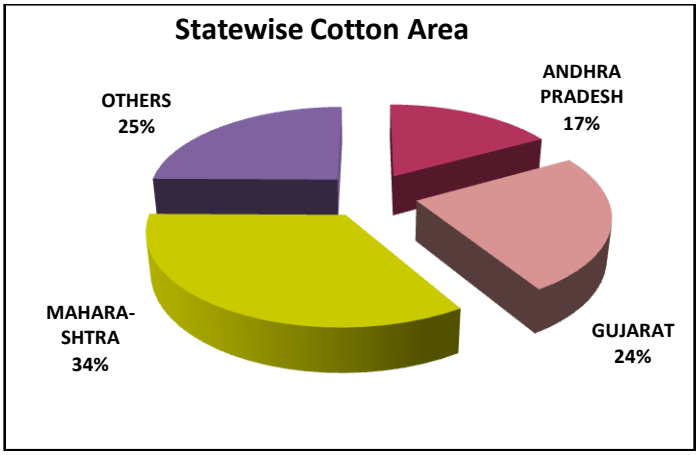

Fig 14. Statewise Area under Cotton (in '000 hectares) in India 2011-12

Trends in area under cotton crop in the country during 2000-2012 witnessed significant increase in the area covered by this crop (**Figure 15**). A 41.9% of increase from 2000-01 to 2011-12 was observed.

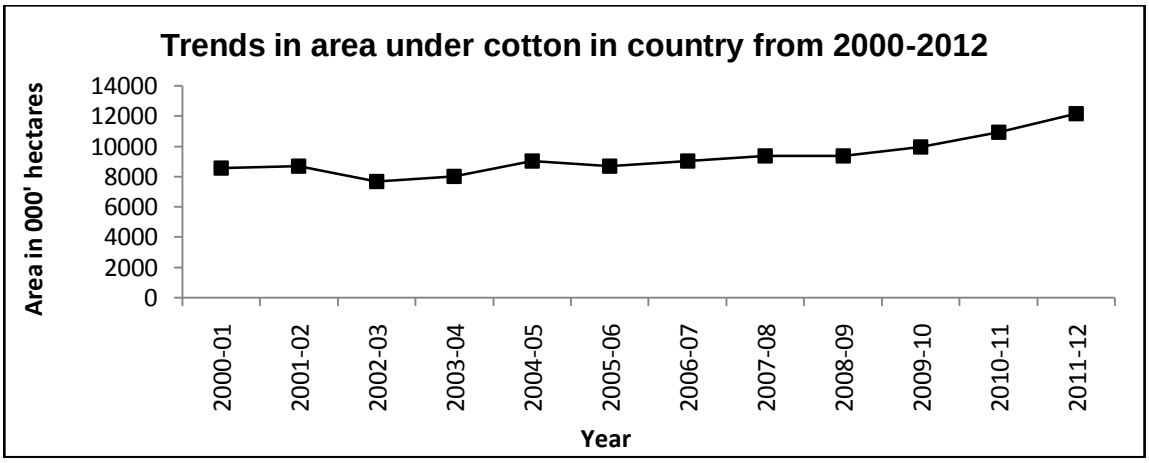

Fig 15. Trends in area under cotton in country from 2000-2012

b) At state level

Gujarat has achieved significant quantitative increase in cotton production over the years**.** The analysis has revealed an 85.9% increase in an area under cotton and 793.3% increase in cotton production during 2000-2001 to 2011-2012 respectively (**Figure 16 and 17**).

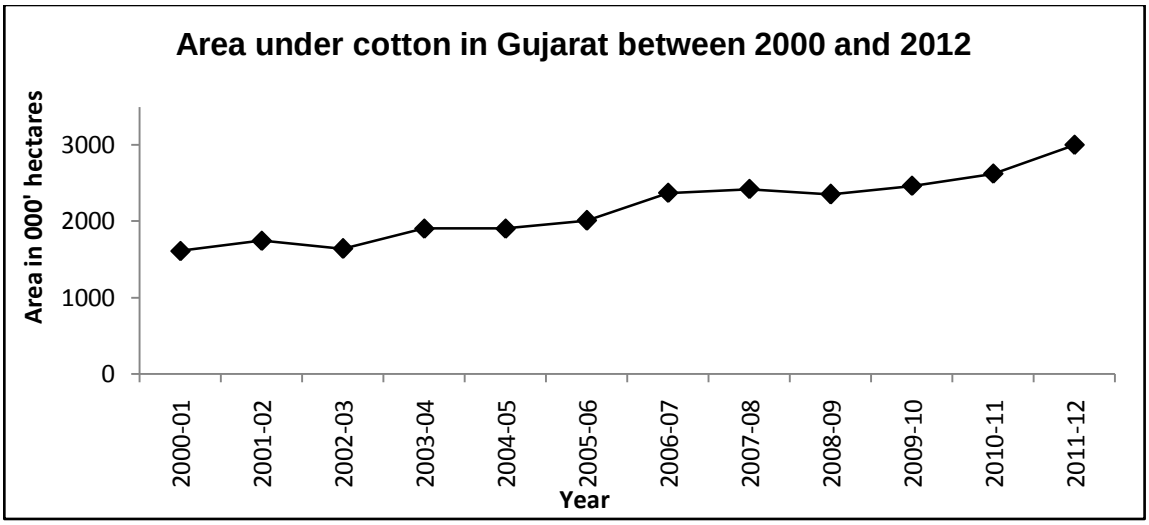

Fig 16. Area under cotton in Gujarat between 2000 and 2012

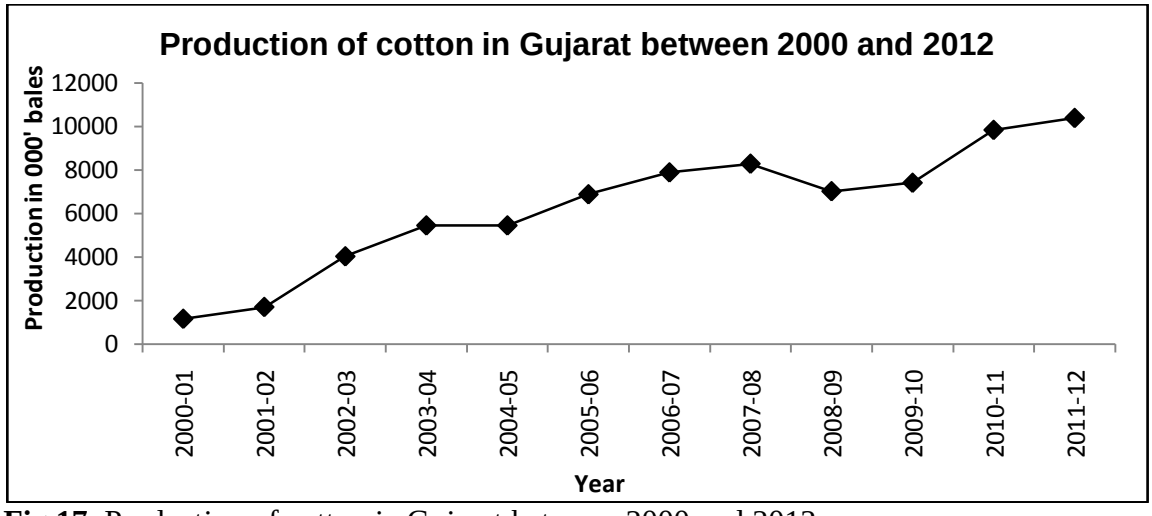

Fig 17. Production of cotton in Gujarat between 2000 and 2012

c) At district level

Vadodara district showed slight ups and downs in the cotton grown area but as such an overall increase in an area was observed from 2000 to 2012 (**Figure 18**). Concomitantly the production of crop has also drastically increased (**Figure 19)**. A 268.3% increase in the production of cotton bales each of 170 kg has also been noted.

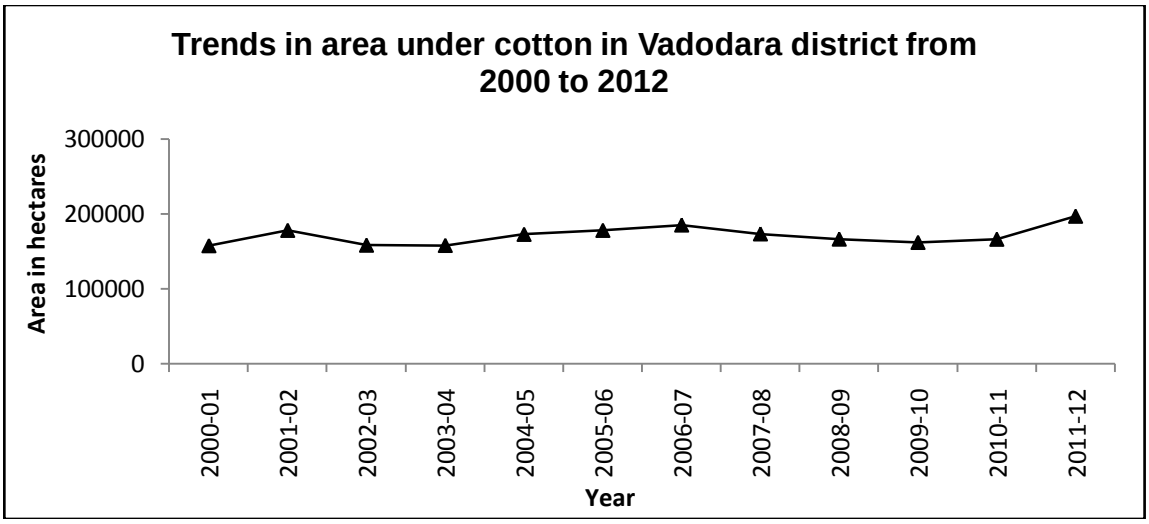

Fig 18. Trends in area under cotton in Vadodara district from 2000 to 2012

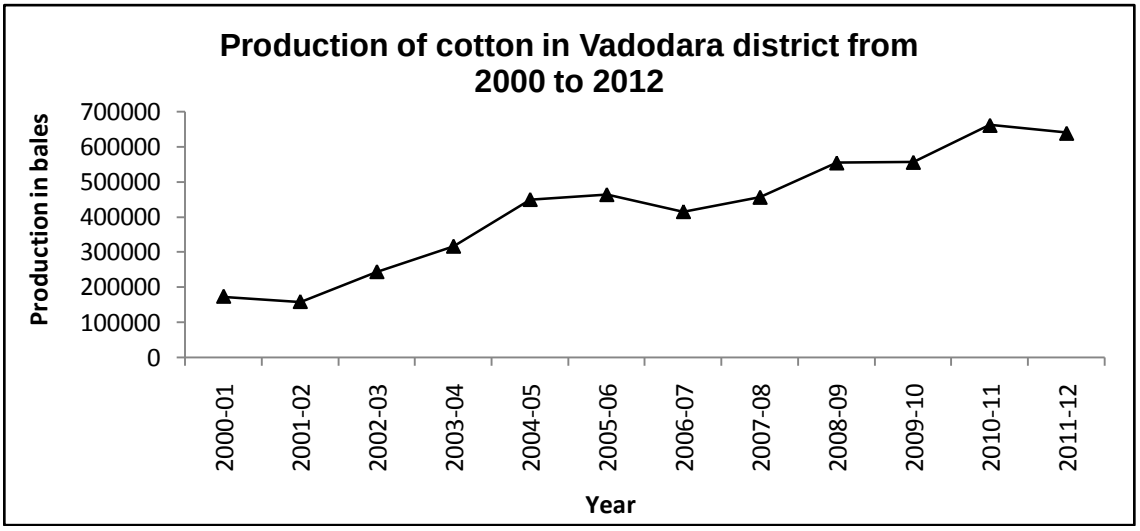

Fig 19. Production of cotton in Vadodara district from 2000 to 2012

Cotton crop showed upward trend in cottonseed yields from 2000 to 2011. Yield climbed up by 261.8% in these years. Slight decrease in yield was observed in the year 2011-12 (**Figure 20**).

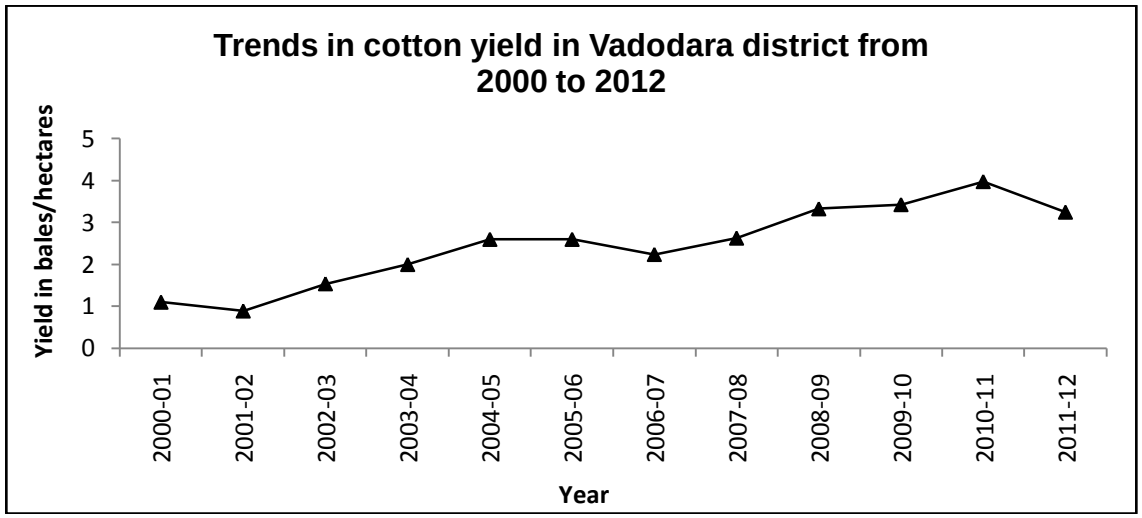

Fig 20. Trends in cotton yield in Vadodara district from 2000 to 2012

4.1.2 CASTOR

a) At country level

Gujarat covers the maximum area under castor (60%) compared to the whole country in the year 2011-12 which signifies the role of the state in terms of castor production in the country (**Figure 21**). Castor area in India increased from 678 thousand ha (2002-03) to 1459 thousand ha (2011-12) showing an increase of 115.9% percent (**Figure 22**).

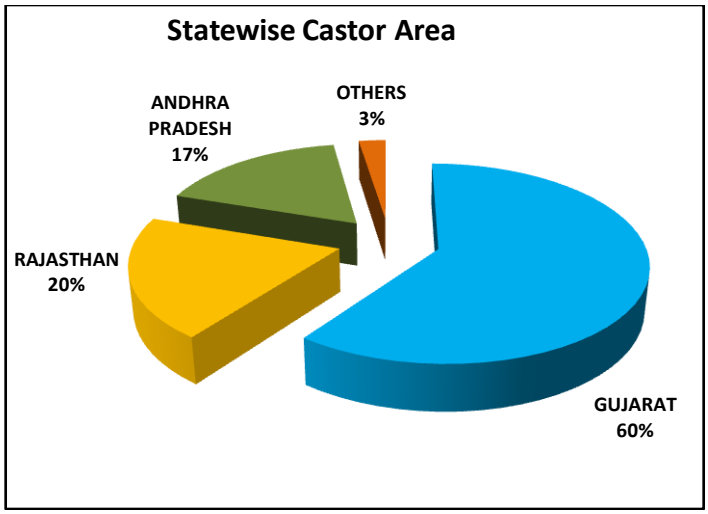

Fig 21. Statewise Area under Castor (in '000 hectares) in India 2011-12

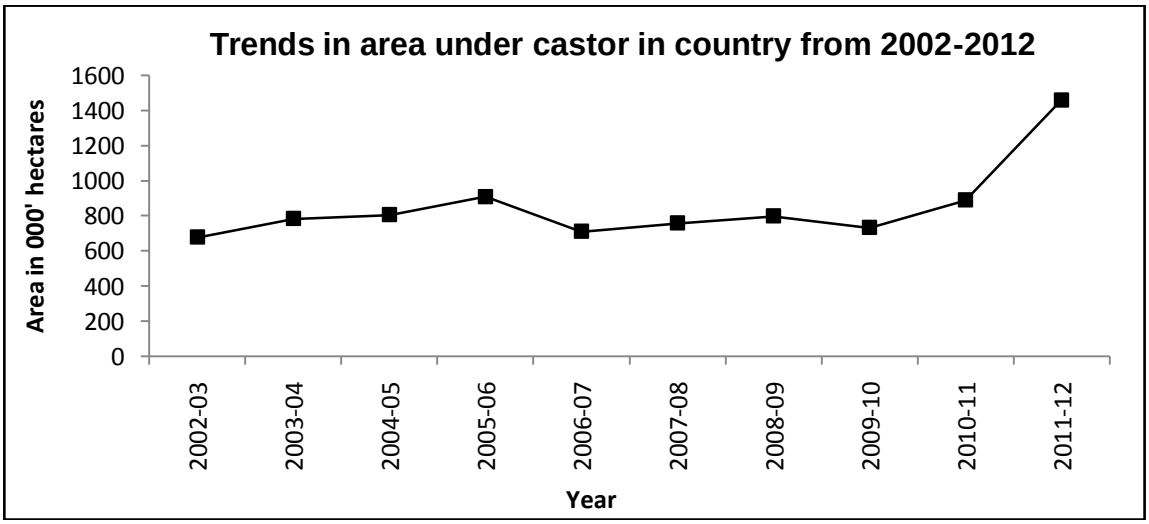

Fig 22. Trends in area under castor in country from 2002-2012

b) At state level

In Gujarat the area under castor crop decreased by 47.2% during the period of 2000-2003. The decrease in the area correspondingly resulted into the decrease in the production during the same period. In year 2011-12, a huge increase in an area has been noted which was the greatest among the years studied (**Figure 23**). Concurrently the production estimates of this oil seed has also increased during this year and the production recorded was the highest annual production over these years (**Figure 24**).

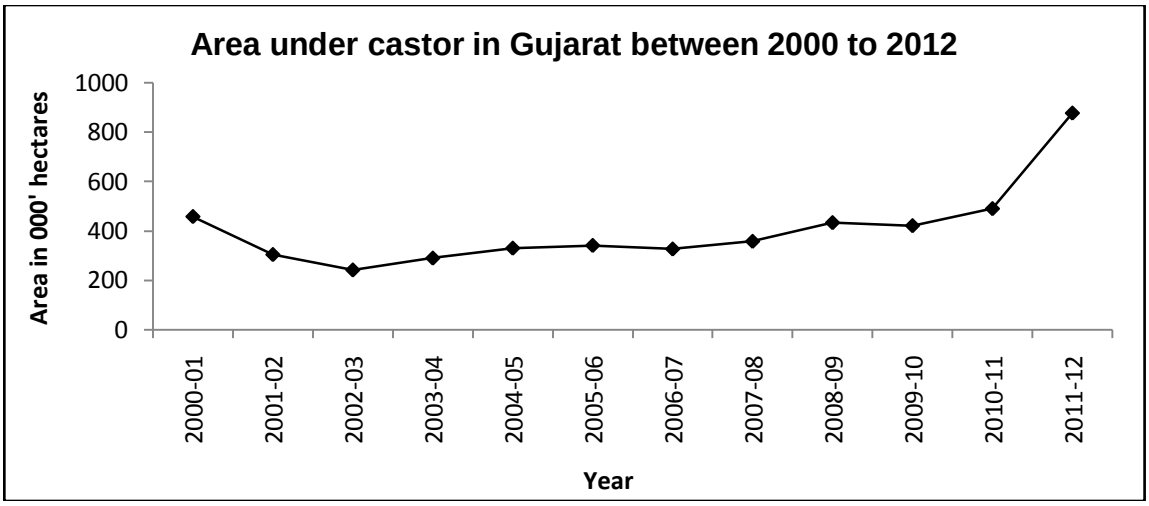

Fig 23. Area under castor in Gujarat between 2000 and 2012

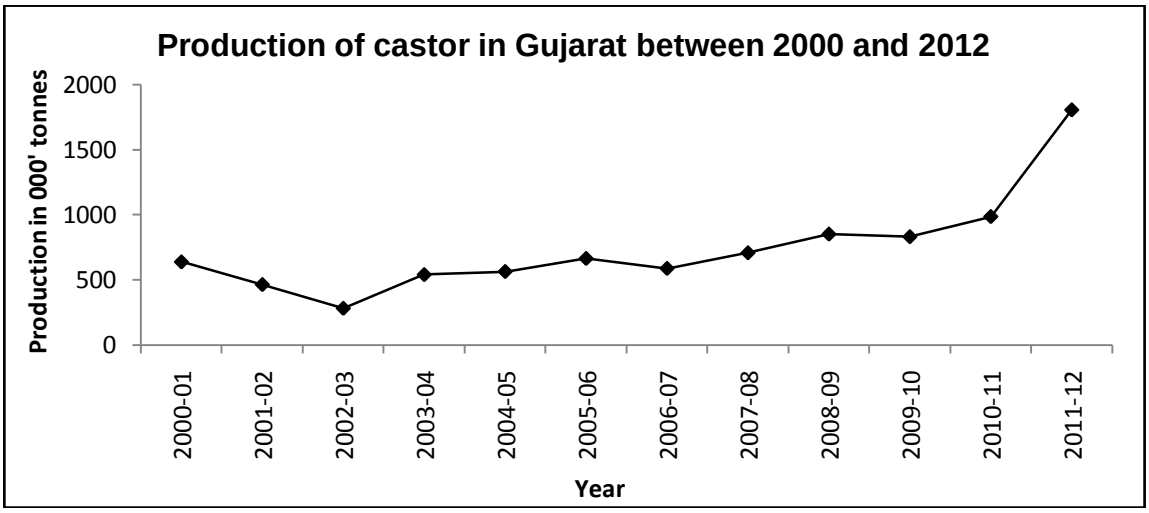

Fig 24. Production of castor in Gujarat between 2000 and 2012

c) At district level

At district level, though there occurred variations in the area, the production and the yield in relation to castor crop, on average an increasing trend was observed from 2000 to 2012 (**Figure 25, 26 & 27**).

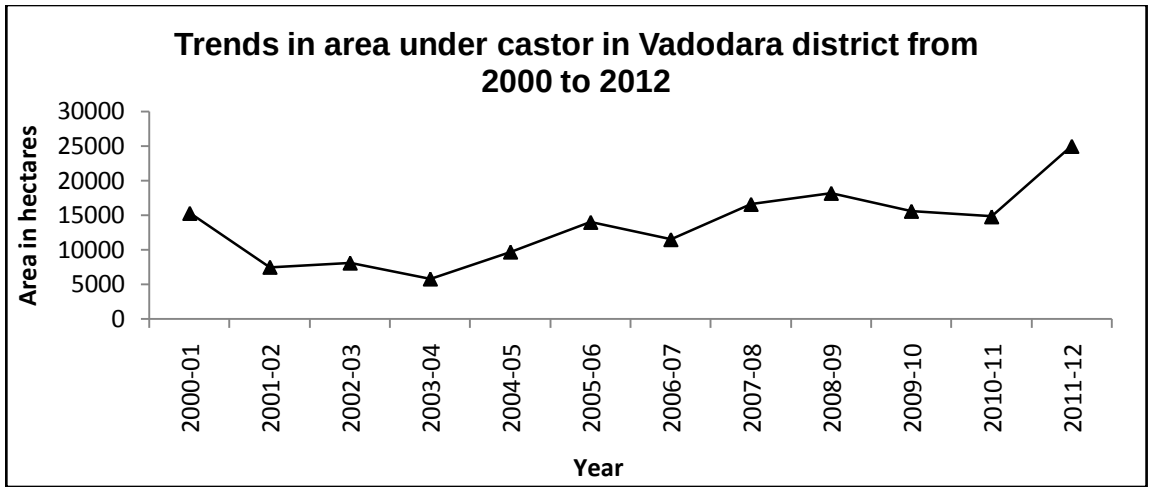

Fig 25. Trends in area under castor in Vadodara district from 2000 to 2012

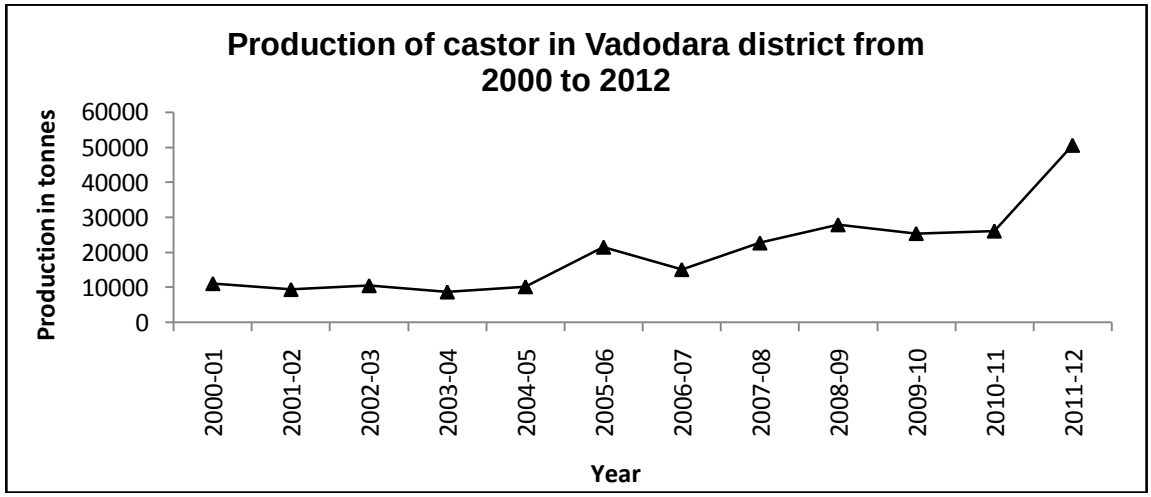

Fig 26. Production of castor in Vadodara district from 2000 to 2012

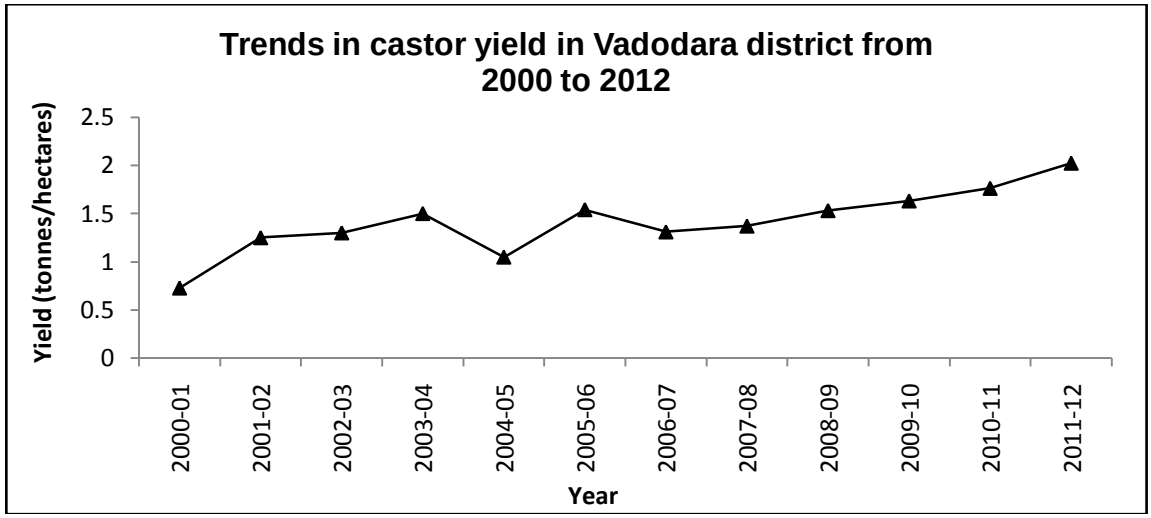

Fig 27. Trends in castor yield in Vadodara district from 2000 to 2012

4.1.3 BANANA

a) At country level

Statewise distribution of banana in the country has highlighted that Gujarat covers only 7% of total area under banana plantation (**Figure 28).** In India, trends in banana area have shown gradual increase in an area sown under banana till 2008-09. A gradual decrease in an area has been recorded from 2009 to 2012 (**Figure 29**).

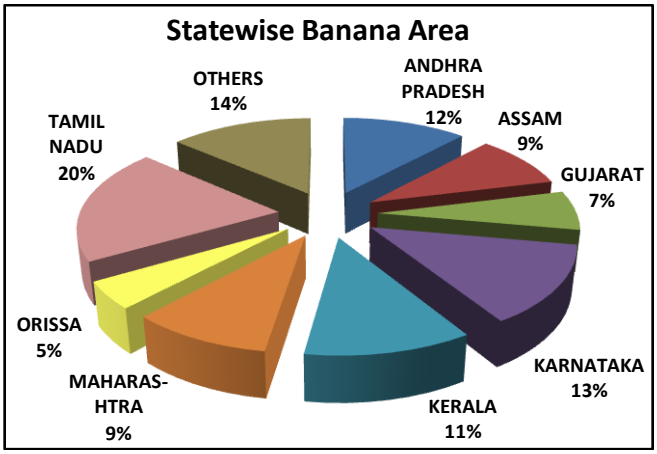

Fig 28. Statewise Area under Banana (in '000 hectares) in India 2011-12

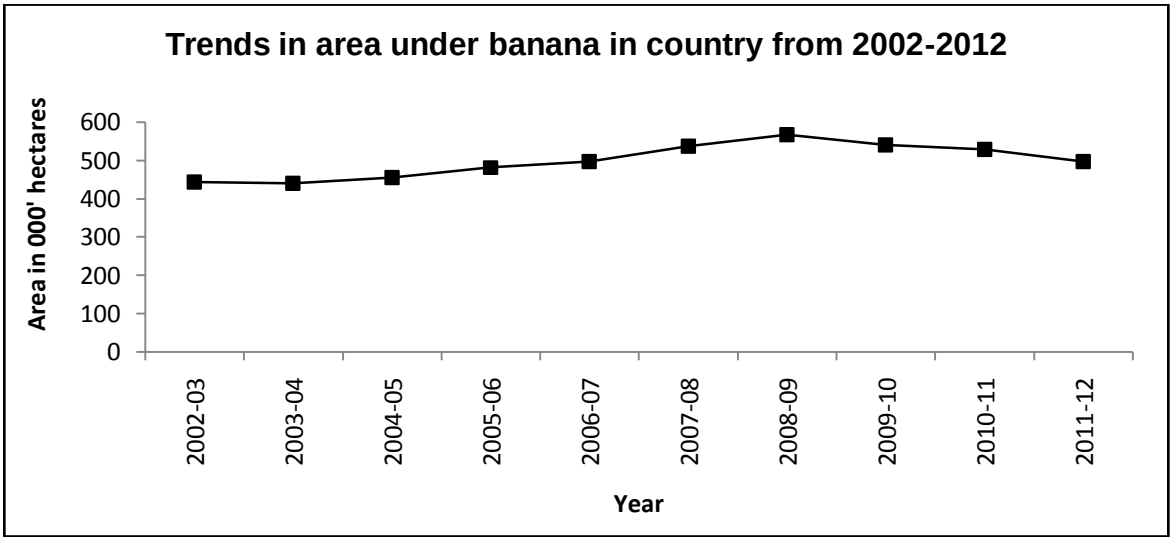

Fig 29. Trends in area under banana in country from 2002-2012

b) At state level

Area under banana plantation in Gujarat showed variation from 2000-2012 but an average increase of 25.4% in banana covered area and 60.5% in banana production has been observed with annual instability (**Figure 30 and 31**).

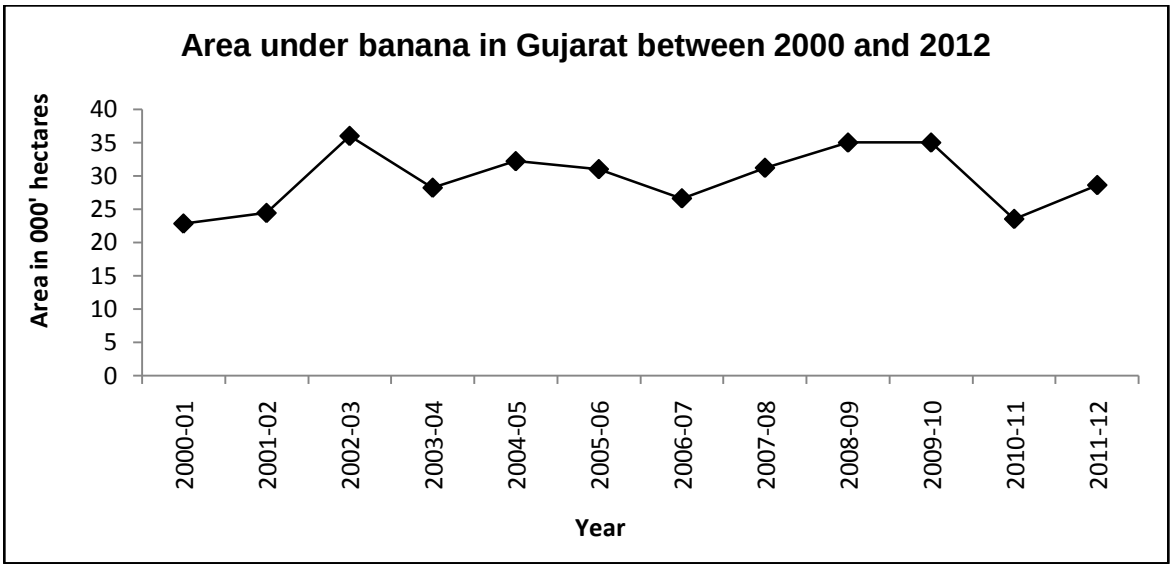

Fig 30. Area under banana in Gujarat between 2000 and 2012

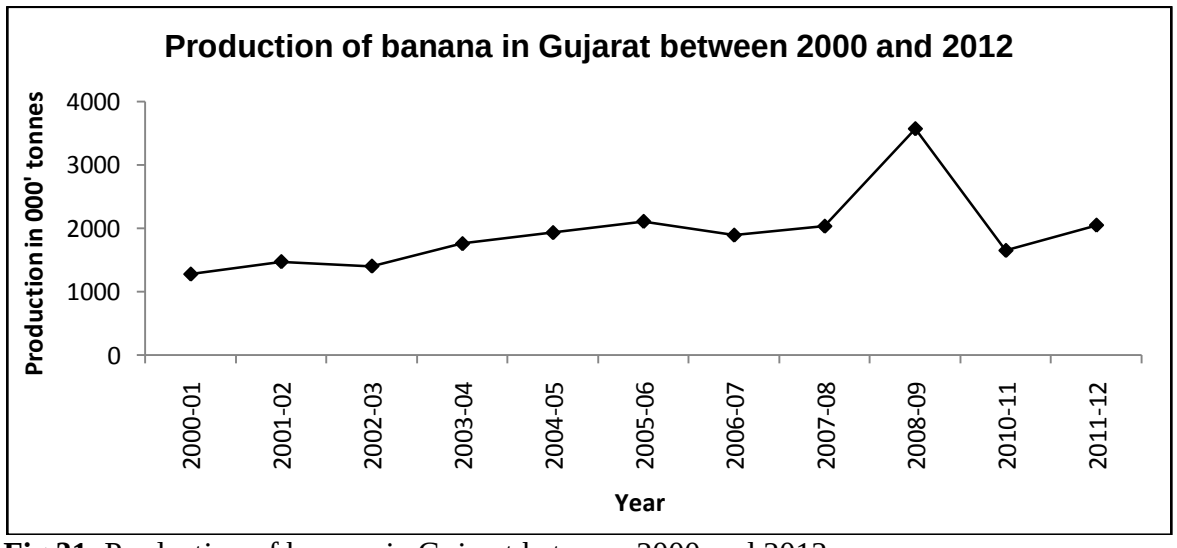

Fig 31. Production of banana in Gujarat between 2000 and 2012

c) At district level

Area, production and yield of Banana showed an instability in the trend over the years (**Figure 32, 33 and 34**). An overall decrease of 52.4% and 56.7% was observed in an area and the production respectively during the period 2000-12 along with decrease of 9.2% in the yield**.**

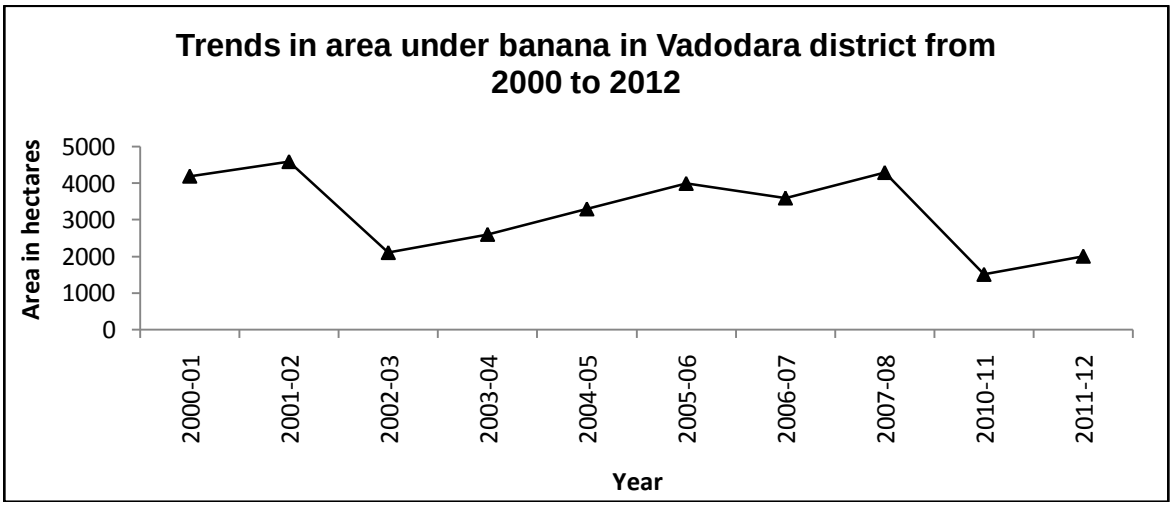

Fig 32. Trends in area under banana in Vadodara district from 2000 to 2012

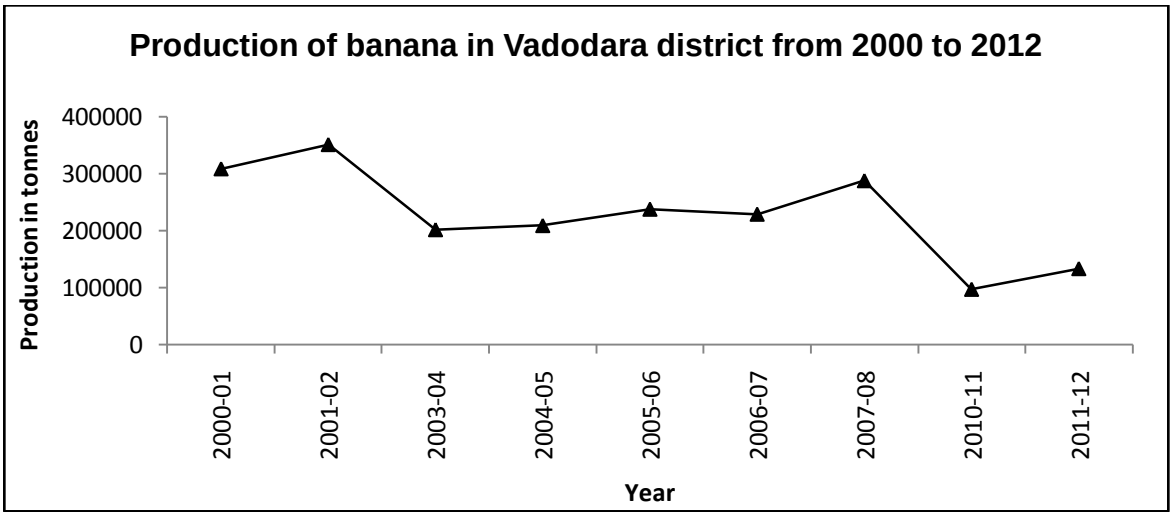

Fig 33. Production of banana in Vadodara district from 2000 to 2012

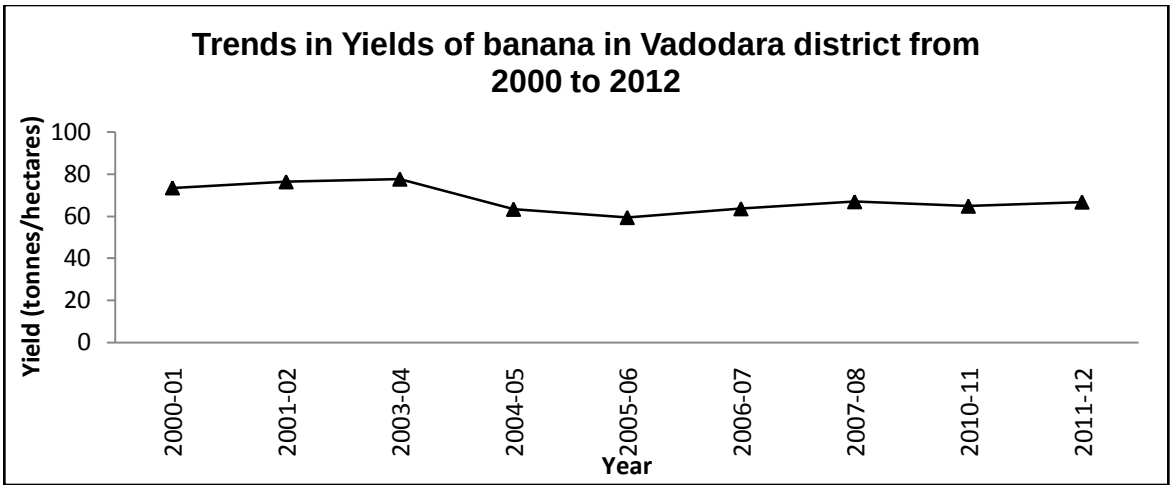

Fig 34. Trends in yields of banana in Vadodara district from 2000 to 2012

4.2 Crop Calendar:

The applications of space technology in the field of agriculture are wide viz. crop discrimination, crop inventory, crop parameter retrieval and assessing long-term changes in the crop environment. Remote sensing data can prove to be more valuable with a priori knowledge of the crop calendars. These calendars can be an important input for judicious planning related to the selection of the crop stage for the study and for the procurement of the satellite data for time critical events of the crop calendar (Karila et al., 2014). Correct acquisitions of the data in terms of crop stage and condition become significant to generate proper outputs from the study.

The crop calendars for the selected crops have been generated as depicted in **Figure 35**. The planting season for cotton in the study area begins around the mid-March and runs through the end of June. Cotton harvest occupies the time frame from the end of September through the end of December. Castor crop is sowed in July and August and harvesting is begun around the 1st of January and concluded around the end of February. The planting of banana begins in mid-June and continues till end of August. Its harvesting is carried out between months of February and April.

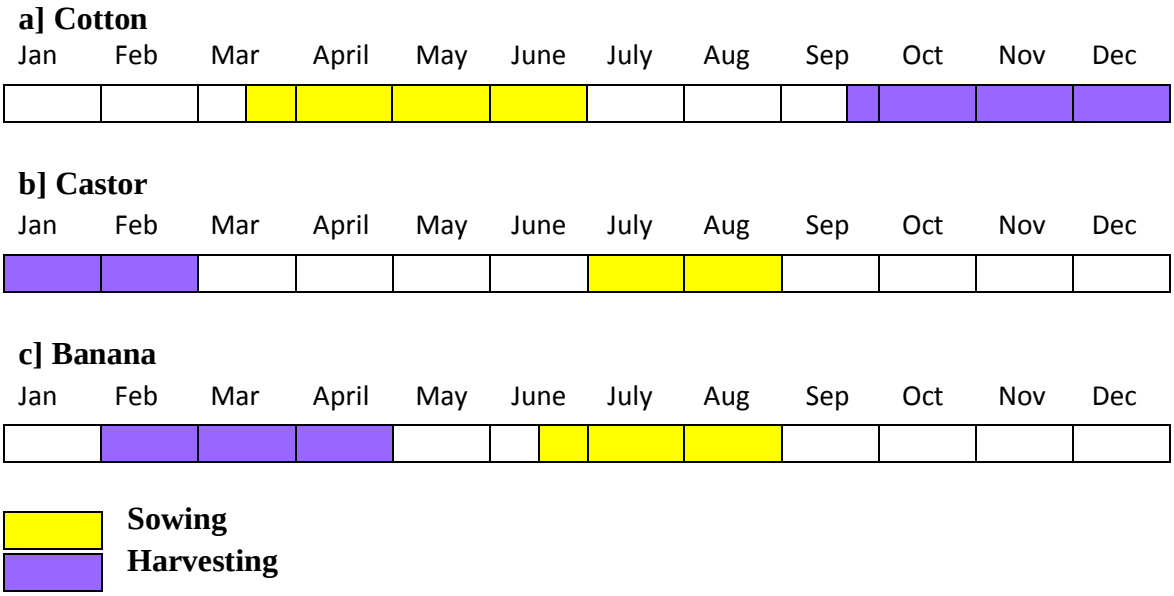

Fig 35. Crop Calendar of (a) cotton (b) castor (c) banana crops

4.3 Vulnerability assessment:

Crop development is directly linked to the capability of agricultural fields to withstand the changes in the climate which can be understood through vulnerability assessment of these agrifields. Such type of studies can assess the climate change related risks to the crops. It requires the input in the form of exposure and sensitivity of these fields to climate variability. It also requires adaptive capacity of farmers to protect the crops against the climate change. The vulnerability assessment of the agricultural fields of Vadodara and other nearby districts viz. Anand, Kheda, Panchmahal, Dahod, Bharuch and Narmada brought out their vulnerability in terms of vulnerability index. Data required for this assessment like exposure, sensitivity and adaptive capacity of an individual district was analyzed and vulnerability index generated exhibited the role and impact of each component in the value of vulnerability index (**Plate 1**). The values of this index ranged between -0.47 and +0.26. Accordingly, the districts were categorized into four classes viz. least vulnerable, less vulnerable, moderately vulnerable and highly

vulnerable. In the present study it was observed that agrilands of Vadodara district were least vulnerable with vulnerability index of -0.47. The reason for its least vulnerability was its high adaptive capacity. The excellent socioeconomic profile indicators viz. literacy rate, access to basic amenities and infrastructure are the prime factors leading to increased adpative capacity in this area. Thus despite of high sensitivity and moderate exposure, the adaptive capacity has contributed towards the reduction in vulnerability. Such parameters when accessed for districts independently have shown that categorization of vulnerability index is directly correlated to the variation in all three components viz. exposure, sensitivity and adaptive capacity as observed in **Table 6** below.

Table 6. Status of vulnerability and its components in different districts

Sr. No.	District	Exposure	Sensitivity	Adaptive Capacity	Vulnerability
1.	Vadodara	Moderate	High	High	Least vulnerable
2.	Anand	Low	Moderate	Moderate	Less vulnerable
3.	Kheda	Low	Moderate	Moderate	Less vulnerable
4.	Panchmahal	High	Moderate	Moderate	Moderately vulnerable
5.	Dahod	High	Low	Low	Highly vulnerable
6.	Narmada	High	Low	Low	Highly vulnerable
7.	Bharuch	Moderate	Moderate	Moderate	Moderately vulnerable

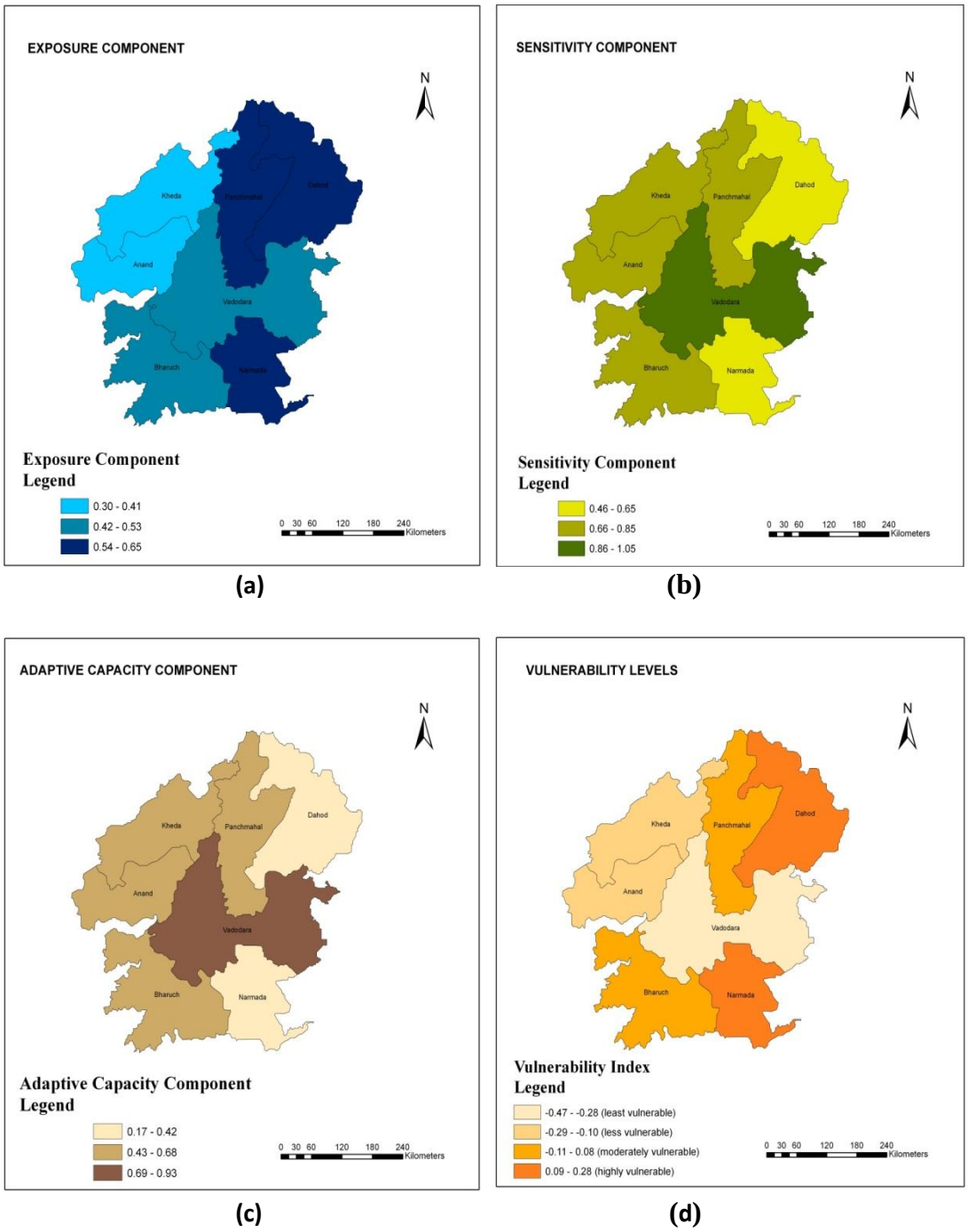

Plate 1. (a) Exposure Map on basis of climate and demographic profile of selected districts (b) Sensitivity Map on basis of ecosystem and agriculture profile of selected districts (c) Adaptive Capacity Map on basis of socio-economic factors of selected districts (d) Final Vulnerability Index Map generated on integration of exposure, sensitivity and adaptive capacity components

4.4 Advantages of microwave data in crop assessment:

In tropics, the only disadvantage of the optical data is its reliance on the sun's energy which limits image acquisition at user defined time (Forkuor et al., 2014). The reason being the frequent cloud cover during monsoon, thereby obscuring the entire growing season (Murakami et al., 2001; Ippoliti-Ramilo et al., 2003; Diuk-Wasser et al., 2004). Crop mapping is important in the cloud covered areas for continuous monitoring of agricultural fields. In order to achieve accurate classification rates, it is essential to have uninterrupted i.e. cloud free coverage of an area under investigation for successive passes of the satellite (Ulaby et al., 1982). The use of radar data helps in rectifying this interruption problem as it is unsusceptible to the presence of clouds in the atmosphere (Karjalainen, 2004; Malhi and Kiran, 2013). In addition to this, their operations are independent of solar illumination and hence imagery acquisition becomes possible throughout the day. This data provides a unique perspective of the landscape and many opportunities for quantitative terrain analysis (Soria-Ruiz et al., 2009). The utility of SAR data in the present study proved to be fruitful in understanding both the landuse as well as crop classification of selected area specifically in kharif season. No doubt optical data also yielded good results in seasons other than monsoon.

4.4.1 Land Use Classification using Optical Data:

The successful utilization of optical imageries for land use mapping has been reported by several authors (Khorram et al., 1991; Treitz et al. 1992; Defries and Townshend, 1994; Homer et al., 1997; Kuplich et al., 2000). Kaul and Sopan (2012) have categorized LISS III data into seven landuse classes viz. Barren land, Settlement, Salt Affected Area, Forest land, Waterbody, Harvested land and Agricultural land for

Jalgaon district. Landuse classification of the present selected area when carried out brought out a precise status of agriculture in the area. Supervised output of Landsat 5 TM delineated six landuse classes viz. cropland, fallow field, builtup area, wasteland, waterbody and scrubland in the year October 2009 (**Plate 2**). The statistics generated showed 83.1% of land under agriculture which included both cropland and fallow field categories with an overall accuracy of 85.0% and kappa statistics as 0.77. Higher accuracy was unable to be achieved because of mixing of cropland with scrubland, and fallow field with wasteland and builtup areas. This could be also attributed to coarse resolution of data.

LISS IV, high resolution data at this point proved to be better as it increased separability of agriculture from other landuse categories (**Plate 3**). It also aided in improvement of accuracy by 10.2% when compared to Landsat data. The accuracy was 93.3% with Kappa Statistics 0.89. Another interest aspect which was noted was that in case of LISS IV data, with increased separability the percentage area under agricultural land got reduced when compared to Landsat 5 TM as observed in **Table 7**.

Table 7. Area in hectares and percentage for Landsat and LISS IV data under different land use classes

Sr. No.	**Class Names**	**Landsat 5 TM**		**LISS IV**	
		Area (ha)	**Area (%)**	**Area (ha)**	**Area (%)**
1	Cropland	26704.62	42.3	25341.53	40.4
2	Fallow field	25763.76	40.8	24004.23	38.3
3	Builtup	2163.33	3.43	1879.445	3
4	Waterbody	537.93	0.85	692.0425	1.1
5	Scrubland	3942	6.24	5641.838	9
6	Wasteland	4036.05	6.39	5145.54	8.21
	Total	**63147.69**	**100**	**62704.63**	**100**

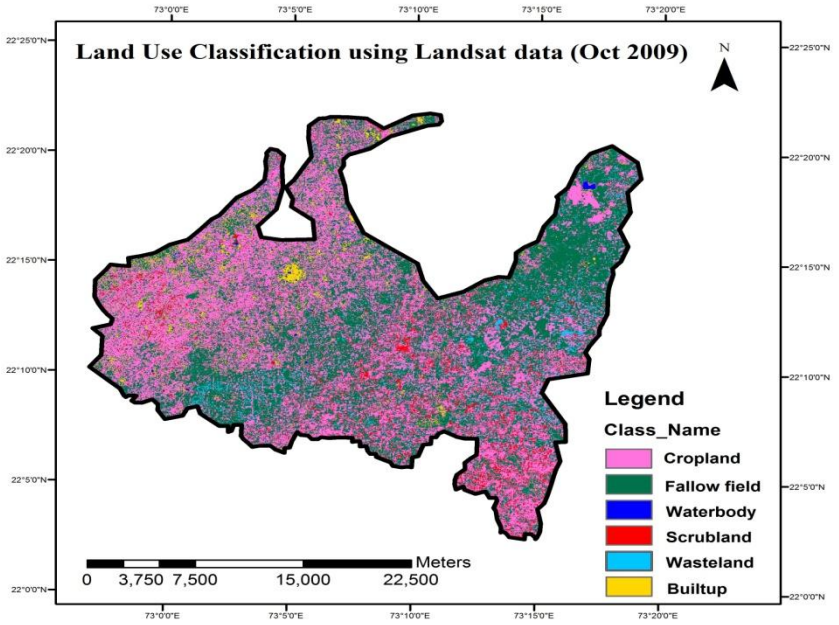

Plate 2. Landuse map generated using Landsat 5 TM data for Oct 2009

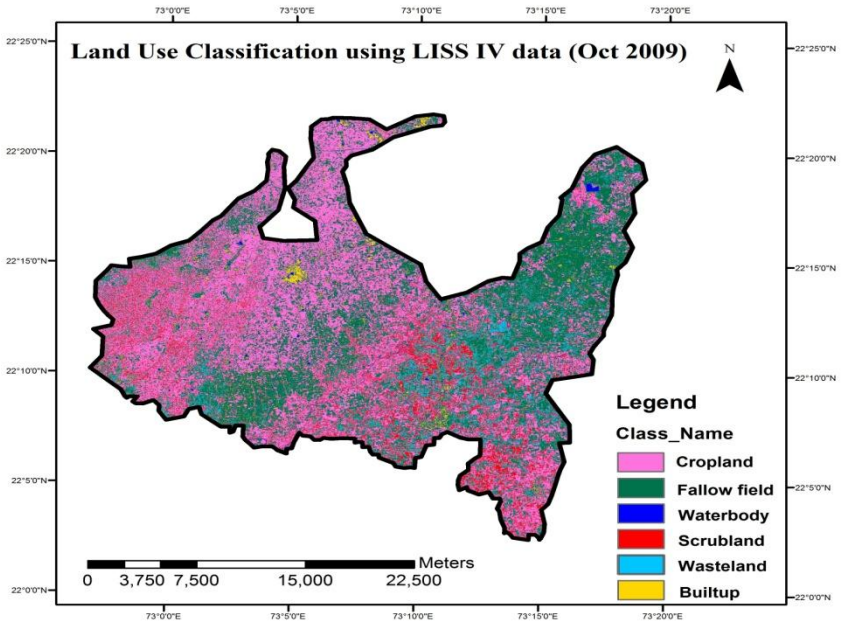

Plate 3. Landuse map generated using LISS IV data for Oct 2009

Crop type classification was found to be subtle despite of high resolution due to field heterogeneity resulting into mixing of signatures. Several workers have also reported such difficulties in crop type classification due to small-scale traditional agricultural holdings such as the densely populated rural landscapes of India (Pax-Lenney and Woodcock, 1997; Heller et al., 2012). Small agricultural fields and diversity in crop types are the components contributing to the subtleness in crop type classification while mapping large areas.

An attempt to achieve crop type classification when carried out at village level gave good results. A precise distinction between major crop fields was observed. In the present work such classification was carried out for Dabhasa village of Vadodara district.

4.4.2 Crop Classification at microlevel using Optical Data:

Microlevel classification for Dabhasa village using Landsat 5 TM showed classes of three different crop types viz. cotton, castor and banana (**Plate 4**). The other agricultural areas were classified as fallow fields and other crops. The other classes consisted of builtup area, scrubland and wasteland. Accuracy of this classified output could not exceed 73.3% and Kappa statistics was 0.64. It was seen that out of total village area, 13.7%, 9.91% and 4.2% area was covered by cotton, castor and banana respectively. The classification accuracy improved by 6.7% by using high resolution LISS IV data. Overall accuracy for LISS IV classified output was 80.0% and kappa statistics 0.74. This accuracy could have been still better with the use of more ground control points (GCPs). Area under cotton, castor and banana identified using LISS IV classified output

was 11.6%, 10.2 % and 4.9% respectively. Statistics for the output of both optical data has been given in **Table 8**.

Table 8. Area in hectares and percentage in Dabhasa village for Landsat and LISS IV data under different classes

Sr. No.	Class Names	Landsat 5 TM		LISS IV	
		Area (ha)	Area (%)	Area (ha)	Area (%)
1	Cotton	167.8	13.7	140.893	11.6
2	Castor	121.07	9.91	124.013	10.2
3	Banana	51.37	4.2	59.3875	4.88
4	Other crops	219.13	17.9	237.575	19.5
5	Fallow field	298.33	24.4	271.748	22.3
6	Wasteland	109.14	8.93	128.373	10.6
7	Scrubland	134.23	11	162.67	13.4
8	Builtup	121.116	9.91	91.5282	7.53
	Total	**1222.19**	**100**	**1216.19**	**100**

Similar to optical classified outputs, the classified outputs generated from microwave data could also delineate different landuse and crop types.

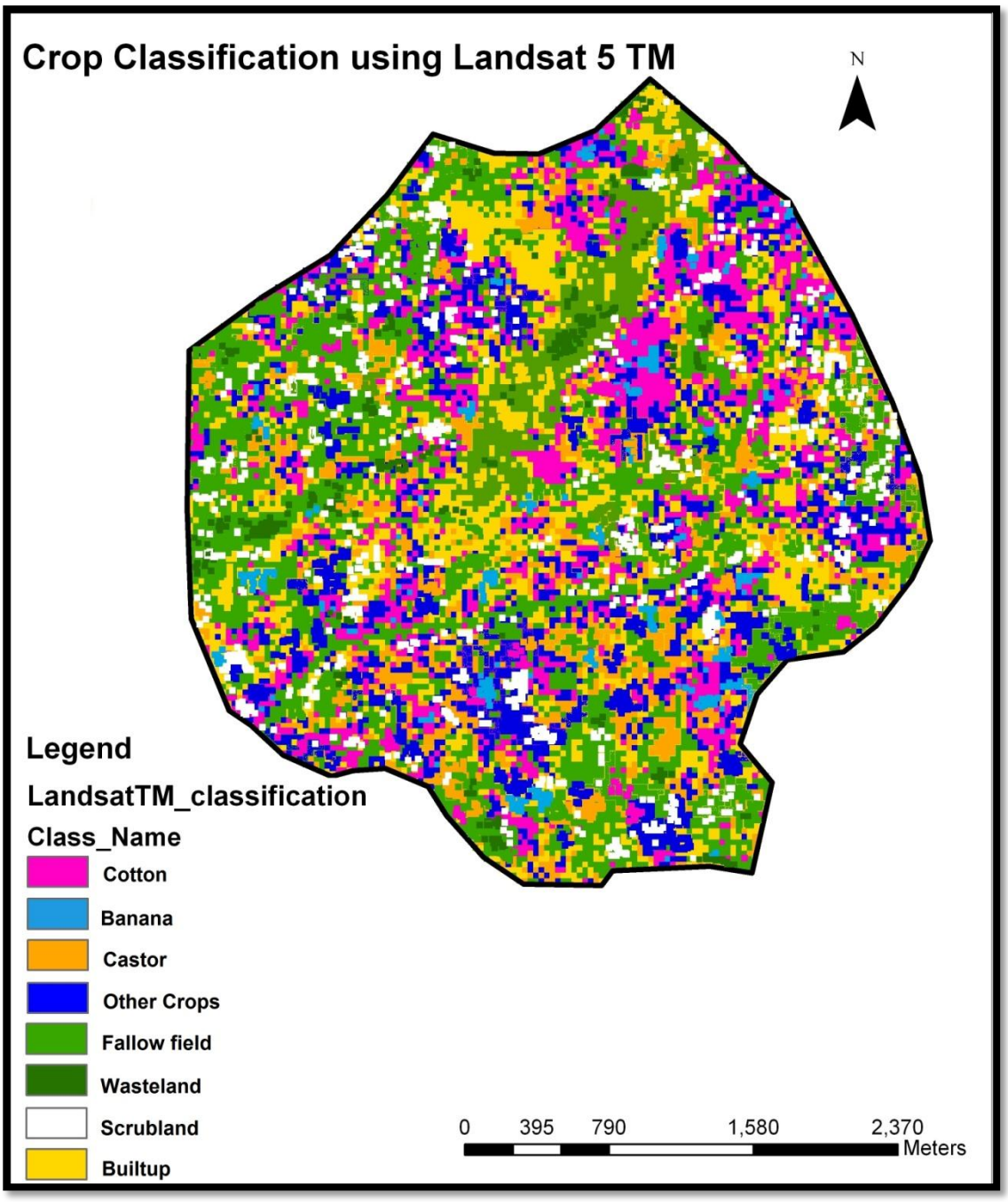

Plate 4. Crop map generated using Landsat 5 TM data for Dabhasa village

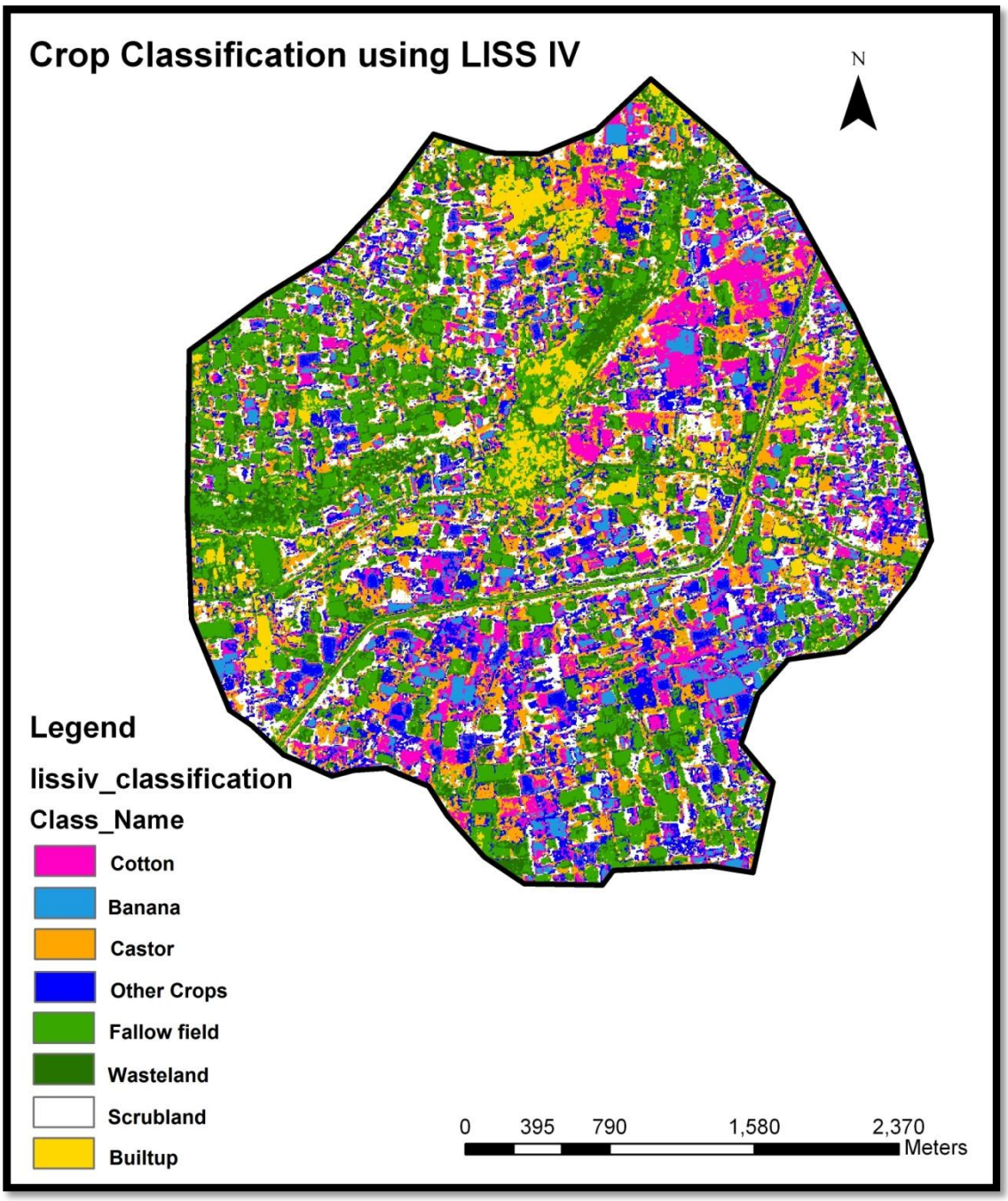

Plate 5. Crop map generated using LISS IV data for Dabhasa village

4.4.3 Land Use Classification using Radar Data:

In the present work, dual polarized C-band (5.3 GHz) Envisat ASAR data was subjected to landuse classification using two different digital techniques viz. Supervised Maximum Likelihood and Wishart supervised classification. Basic landuse types viz., cropland, fallow field, waterbody, builtup and scrubland were discriminated from the data. Both the techniques exhibited variation in their performance. Out of the two techniques used, ASAR data yielded comparatively poor results using MLC when compared to Wishart classifier. Accuracies in MLC and Wishart were 73.3% and 83.1% respectively and kappa statistics 0.61 and 0.79 respectively. The classified outputs generated using different techniques are as shown in **Plate 6 (a and b)**. Total land area identified as agricultural area was 67% in case of MLC and 68.6% in case of Wishart classifier (**Table 9**). Wishart classifier exhibited a better performance both at individual as well as at overall classification accuracy along with kappa coefficients (**Table 10)**.

Table 9. Statistics generated using Maximum Likelihood and Wishart Supervised classifiers for land use classification of Envisat ASAR data

Sr. No.	**Class Names**	**Maximum Likelihood**		**Wishart**	
		Area (ha)	**Area (%)**	**Area (ha)**	**Area (%)**
1	Cropland	15613.36	22.0	17430.1	23.3
2	Fallow field	44053.83	62.0	33911.6	45.3
3	Scrubland	4176.50	5.9	19908.3	26.6
4	Builtup	5102.84	7.2	1717.67	2.3
5	Waterbody	2090.40	2.9	1852.24	2.48
	Total	**71036.93**	**100.0**	**74819.94**	**100**

The backscatter values of different landuse types varied significantly. Highest backscattering was observed in builtup and lowest in waterbody. Fallow field, scrubland and cropland exhibited these values in a decreasing order. This could be derived from

mean and standard deviation values of each class. **Figure 36 and 37** has depicted this fact very distinctly.

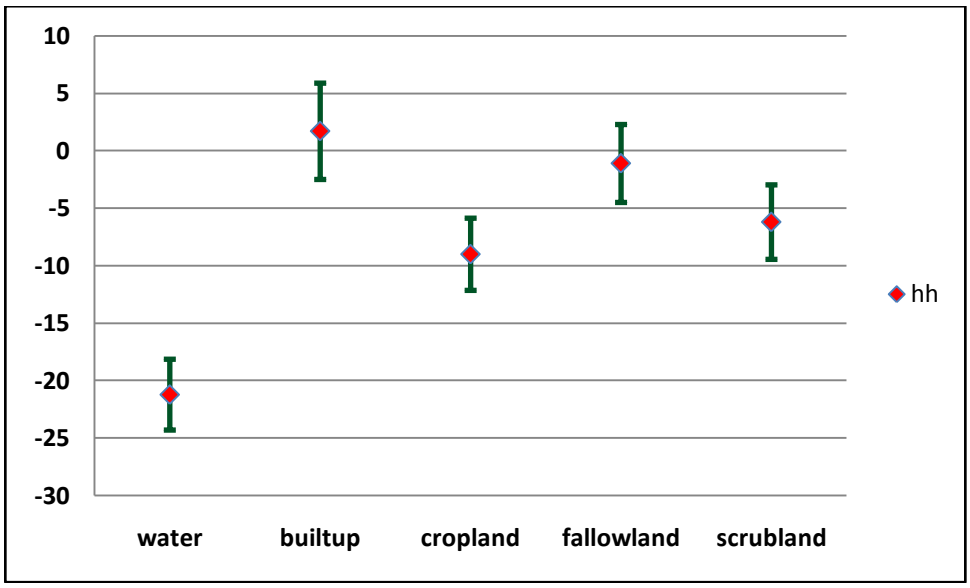

Figure 36. Mean and standard deviation of HH σ° for various classes

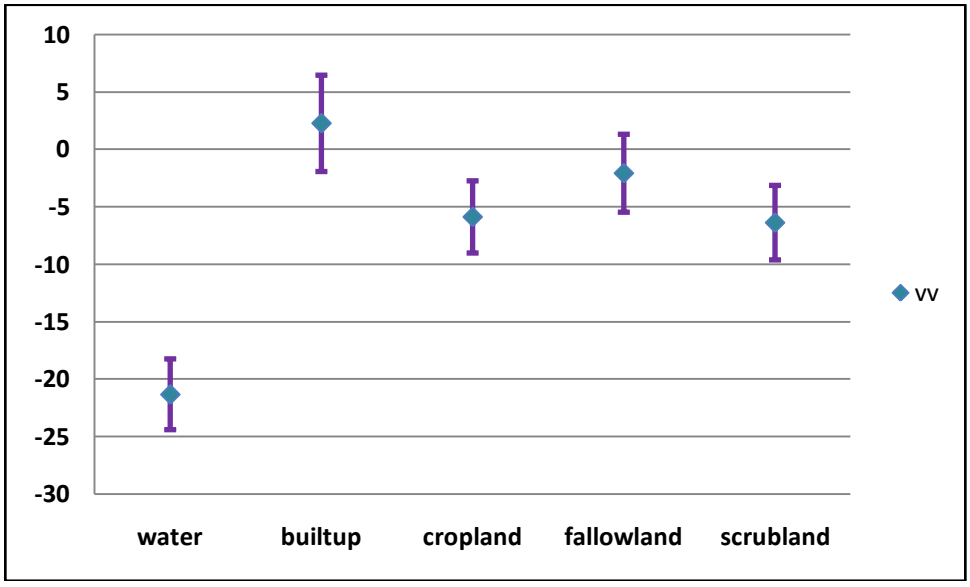

Figure 37. Mean and standard deviation of VV σ° for various classes

On an average, VV component exhibited higher and HH component exhibited lower backscatter values across the various classes. HH is less than VV in builtup and cropland classes. The mean values of the cropland and scrubland in HH component

were very close. Similarly this closeness increased in VV component. In other classes viz. waterbody and scrubland, backscatter for both HH and VV were similar. Although there is clear separation for the mean values of all the classes, it was difficult to classify data on backscatter alone. Similar observations were also made for various landuse classes generated by Turkar et al. (2013). Standard deviation of various features was high and overlapped with mean values of other features. Standard deviation of scrubland got mixed up with the mean of cropland.

Discrimination between vegetated and non-vegetated areas was enabled using dual polarization data, has already been proved by several workers (Vyjayanthi, et al., 2012) and is confirmed in the present study once again. But a precise separability between crop and scrubland could not be achieved due to volume scattering. This proves the fact that in contrast to the dependence of optical data on spectral signatures, radar backscatter signatures are strongly dependent on physical properties of target like roughness, orientation and its dielectric properties (Srivastava et al., 2006). These reasons might have contributed to the subtleness in the delineation between cropland and scrubland as they exhibit equal volume scattering. This is also one of the reasons for better identification of builtup areas by SAR. An user accuracy of 94.6% was achieved in Wishart classification for builtup areas. Little mixing of builtup area occurred with few other classes. Builtup areas with wide flat roof were confused with fallow land because of similar scattering mechanism. Some shadow of builtup areas (such as buildings) was also prone to be classified as fallow land whereas few buildings having specific orientations not aligned in the azimuth direction or having complex structures such as rough roofs were assimilated into volume scattering class and thus assigned to

the vegetation classes i.e. cropland and scrubland. Some vegetated areas got as classified as fallow land because of very poor density of scrubland or seedling stages of cropland in these areas. Few cropland and scrubland with high soil moisture were misclassified as water in the classification result. But, the overall classification results were satisfactory to distinguish landuse classes with minimal accuracy of 70% for all the classes. The discrimination of vegetation classes viz. cropland and scrubland using backscattering coefficient of ASAR data though was satisfactory but this could be further improved by making use of multi-temporal ENVISAT-ASAR.

Table 10. Confusion matrix describing Wishart classification performance

	Water body	Builtup	Scrubland	Fallow field	Cropland	Producer Accuracy (%)	Overall Accuracy (%)	Kappa coeff.
Waterbody	99.94	0.00	0.06	0.00	0.01	100		
Builtup	0.00	70.47	0.57	22.97	5.99	72.17		
Scrubland	0.21	2.82	75.45	12.49	9.02	76.53		
Fallowfield	0.00	2.24	10.14	87.04	0.58	87.88		
Cropland	0.00	0.00	18.03	3.56	78.42	78.79		
User Accuracy (%)	100	94.60	72.82	70.16	84.78			
							83.13	**0.79**

The potentials of radar data in discriminating different land use types is being emphasized by the results of the present study. ASAR data standalone can contribute significantly towards better land use classification. As discussed previously in the case of optical data, crop classification could not be feasibly performed over large areas due to high crop heterogeneity found in the present study area. Similarly, radar data could not classify different crop categories at macrolevel. Thus to enable this classification at crop type level, classification was carried out at microlevel.

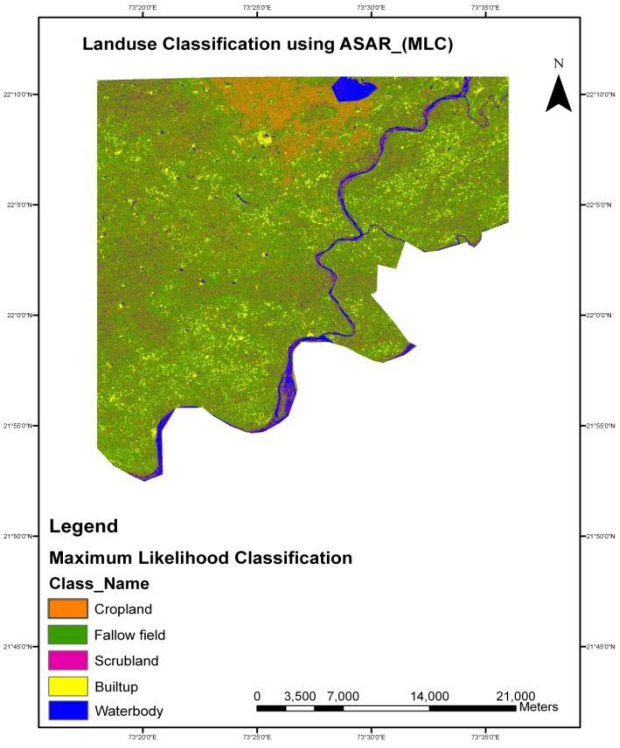

[a]

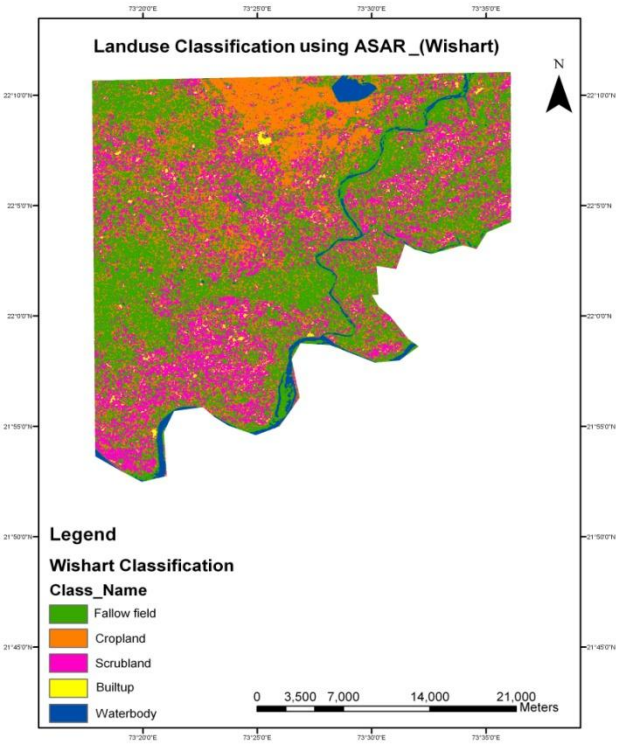

[b]

Plate 6. Land Use Map derived from ENVISAT ASAR data using [a] Maximum likelihood classifier [b] Wishart Classifier

4.4.4 Crop Classification at microlevel using Radar Data:

Backscatter sensed by SAR data are largely a function of the size, shape, orientation and dielectric constant of the scatterer (Haack, 2007). Hence, radar backscatter intensities for vegetation will vary based on the size, shape and orientation of the canopy components (e.g., leaves, stalks, fruit, etc.). Crops with different canopy architecture can be distinguished on the basis of their backscatter intensities (McNairn et al., 2009; Bargiel and Hermann, 2011).

In the present study, ground survey data was used for identifying the agricultural fields in the ASAR image and extracting the backscattering signatures. Based on this survey, crop classification performed at small scale using MLC identified cotton, banana and fallow fields. All other cropped agricultural fields were classified as other crops class. Remaining classes identified were scrubland, waterbody and builtup areas (**Plate 7**).

It is well-known that microwave data is sensitive to crop structure (Haldar et al., 2012b). Area statistics (**Table 11**) generated for the classification showed maximum area covered under banana plantation. Though banana showed distinct bright backscatter due its sizable leaves but it was confused with few other crops having large leaves like castor. Thus misclassification occurred because of similar backscattering mechanism. The fallow fields are discernable but few other crops with high moisture content or due to water cover are classified as waterbody. The fallow fields have very distinct radar backscatter and hence are classified without considerable mixing. Statistics generated for this classification showed accuracy of 65% with 0.59 kappa statistics. Reason for the non-achievement of required accuracy can be use of single SAR image (Del Frate et al.,

2003). In this context, the constraints in the classification techniques by ASAR when used exclusively with respect to agricultural areas can be overcome with the use of multi-frequency, multi-polarization or multi-anlge measurements (Foody et al., 1994; Freeman et al., 1994; Jia et al., 2009). Multi-temporal radar data can also be beneficial in improving classification accuracy reason being peculiar variations induced in backscattering by growth cycle of particular crop (Shao et al., 2001; Wang et al., 2010). Therefore, multi-configuration SAR data can improve accuracy of crop classification (Jia et al., 2012).

Table 11. Area in hectares and percentage in the selected area for ASAR data under different classes

Sr. No.	**Class Names**	**Area (ha)**	**Area (%)**
1.	Cotton	59.4	9.2
2.	Banana	115.0	17.9
3.	Other crops	118.7	18.5
4.	Fallowfield	142.8	22.2
5.	Scrubland	168.5	26.2
6.	Builtup	22.1	3.4
7.	Waterbody	16.9	2.6
	Total	**643.5**	**100**

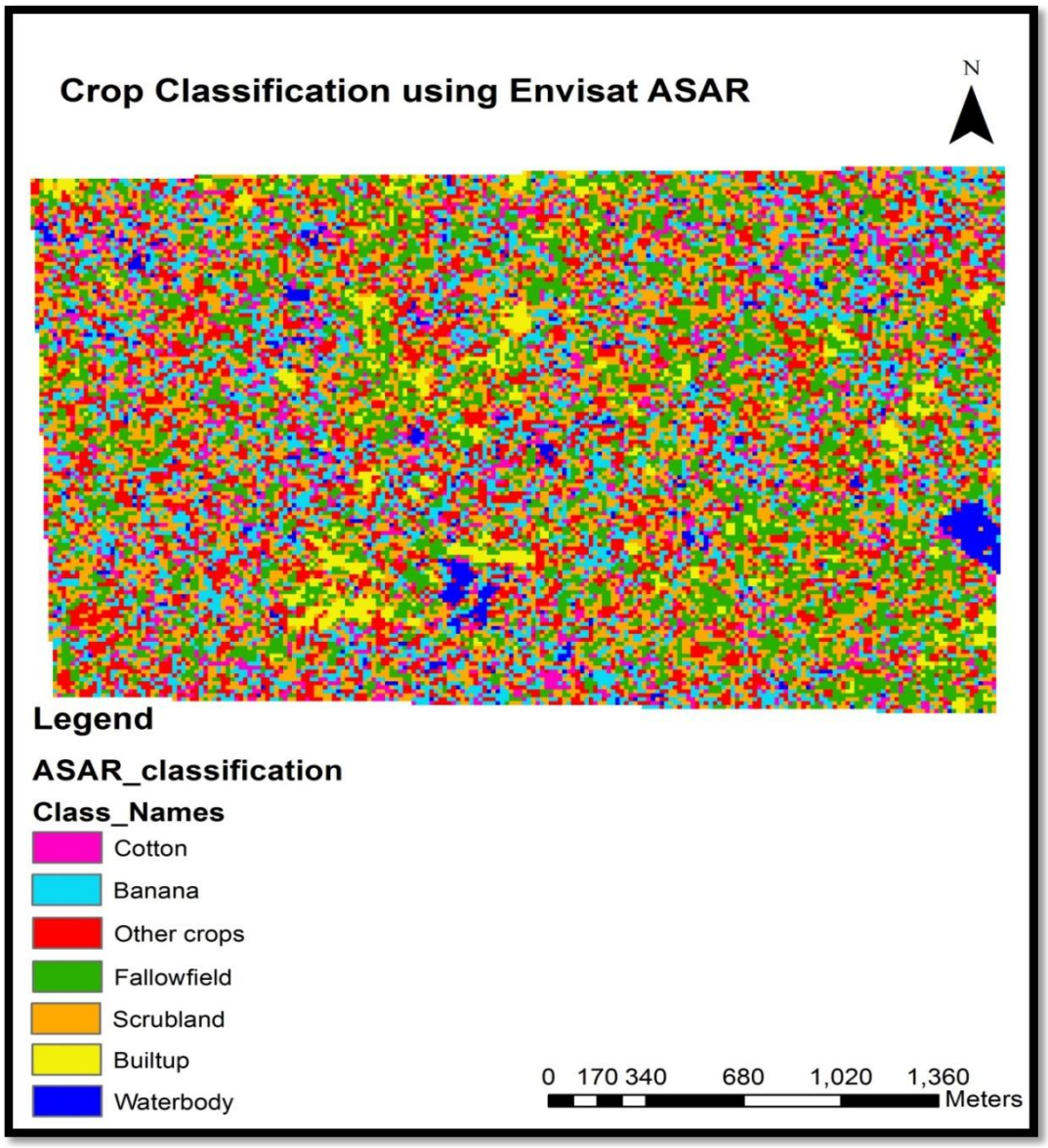

Plate 7. Crop map generated using Envisat ASAR data

4.5 Conventional and Non-conventional approach for estimation of crop parameters:

The present research involved the estimation of crop biophysical and biochemical parameters from the ground measurements i.e. the conventional method and from the satellite imagery using optical and microwave remote sensing i.e. the non-conventional method. The non-conventional approach was identified to be better potent and time efficient means for the retrieval of crop parameters.

4.5.1 Retrieval of crop parameters using conventional technique:

Crop biophysical (LAI, RWC and Biomass) and biochemical (CC) parameters are the indicators of the crop condition along the growing season (Thenkabail et al., 2000; McNairn et al., 2012). Earlier the conventional method was used to estimate these variables, such assessment many a times seemed to be destructive (Zheng and Moskal, 2009). Looking at the essentiality of the knowledge of these parameters in understanding of the crops and related environmental dynamics at any spatial scale it would be beneficial to study them using the non-conventional non-destructive method. In the present work, therefore LAI, RWC, Biomass and CC have been estimated using both the conventional and the spatial non-destructive approach to compare the results from the same and see the future prospects at a large scale.

Conventionally crop biophysical and biochemical parameters were estimated for Cotton, Castor and Banana sampled out from the different fields (**Plate 8**). Descriptive statistics are presented for the ground based biophysical and biochemical data by crop type.


Cotton Fields


Castor Fields


Banana Fields

Plate 8. Different agricultural fields of the study area

The LAI, RWC and CC values for cotton plants estimated from ground measurements are shown in **Table 12**. The LAI values in the cotton field captured a data range (0.2 to 4.76) around a total mean value of 2.59. The RWC and CC status analyzed from the same crop in the laboratory also showed a variation in data values. CC ranged from 9.07 to 22.47 mg g^{-1} with mean value of 15.8 mg g^{-1} while RWC ranged from 27.16 to 83.6% with total mean of 48.97%.

Table 12. Ground measured biophysical and biochemical parameters of cotton crop at different agricultural fields

Sr. No.	LAI	CC (mg g^{-1})	RWC (%)
1.	3.17±0.08	14.55±3.9	70.22±0.89
2.	3.18±0.03	20.23±0.6	44.82±1.52
3.	4.45±0.19	17.79±6.6	83.69±1.42
4.	3.93±0.05	16.71±6.9	43.31±1.63
5.	4.69±0.19	22.35±2.8	81.89±1.11
6.	1.58±0.11	11.47±4.8	30.92±1.55
7.	0.32±0.33	5.017±3.0	37.43±10.03
8.	0.58±0.35	11.19±3.7	73.02±6.44
9.	1.19±0.80	11.53±1.4	71.04±1.28
10.	0.11±0.09	9.07±1.8	79.59±2.21
11.	2.29±0.89	16.13±2.4	82.46±1.89
12.	1.74±0.62	14.3±3.3	29.89±2.14
13.	3.27±0.15	20.93±1.3	32.35±1.19
14.	4.13±0.11	22.47±1.7	70.036±1.62
15.	4.24±0.03	22.3±1.6	82.89±1.70
16.	4.76±0.22	22.3±2.3	30.88±1.53
17.	1.16±0.13	17.95±2.6	31.72±1.88
18.	1.77±1.08	13.03±2.9	82.15±0.57
19.	2.85±1.17	17.21±5	81.63±0.63
20.	3.25±0.68	17.31±3.3	28.99±0.41
21.	2.85±1.91	17.3±4.8	45.99±1.62
22.	0.64±0.003	12.74±1.3	68.85±0.29
23.	0.67±0.005	12.67±0.6	43.31±1.06
24.	3.22±0.08	15.55±3.2	77.34±0.73
25.	2.62±0.09	11.97±1	83.56±1.07
26.	0.2±0.0001	10.98±1.7	60.38±2.08
27.	3.64±0.09	17.83±2.6	74.55±2.16
28.	3.4±0.19	14.35±2.2	74.87±1.15
29.	2.36±1.35	13.07±4.5	49.98±1.25

30.	1.84±1.76	15.89±5.2	68.84±3.18
31.	2.58±2.21	15.78±1.9	66.33±2.31
32.	1.08±1.59	13.11±0.1	46.53±3.02
33.	2.41±0.76	12.68±0.8	78.72±5.67
34.	2.65±1.92	17.81±5	41.13±1.10
35.	4.58±0.48	19.81±3.8	49.42±2.55
36.	4.11±0.1	20.24±0.6	27.16±5.08
37.	4.26±0.21	18.31±1.1	40.65±1.59

Table 13 shows the ground measured LAI, RWC and CC values for castor crop along with their standard deviation values. Castor LAI measured ranged between 1.08 and 4.63, with a mean of 2.61. The average CC ranged between 8.75 and 54.55 mg g^{-1}, with a grand mean value of 32.32 mg g^{-1}. The range of RWC in the crop was between 1.35 and 29.9% with mean of 16.58 %.

Table 13. Ground measured biophysical and biochemical parameters of castor crop at different agricultural fields

Sr. No.	**LAI**	**CC (mg g^{-1})**	**RWC (%)**
1.	2.03±0.26	12.94±0.69	25.12±0.39
2.	2.19±0.54	11.37±0.23	21.03±1.29
3.	2.47±0.23	12.19±0.41	12.95±0.71
4.	2.88±0.32	16.14±5.62	16.45±1.48
5.	1.37±0.19	10.94±0.79	21.95±0.64
6.	1.08±0.08	8.75±0.7	22±0.71
7.	2.13±0.43	12.81±1	1.35±0.21
8.	1.79±0.75	9.94±0.09	1.95±0.21
9.	1.36±0.09	35.68±0.61	12.94±0.98
10.	2.11±0.41	27.94±10.5	19.37±1.65
11.	3.09±0.17	35.25±8.13	27.87±0.89
12.	3.25±0.35	45.15±2.05	29.9±0.71
13.	3.51±0.87	48.57±5.33	21.25±0.9
14.	3.99±0.23	54.55±0.41	16.8±3.2
15.	3.05±0.13	44.51±3.5	6.2±0.3
16.	2.23±0.66	45.03±3.82	6.33±1.42
17.	3.55±0.49	41.45±9.4	23±0.57
18.	4.05±0.07	50.13±5.48	29.24±0.76
19.	4.63±0.18	51.32±1.3	18±3.54
20.	2.95±0.07	49.34±7.41	2.1±0.14
21.	1.25±0.03	29.32±5.97	2±1.41
22.	1.75±0.53	15.94±6.72	12.76±13

23.	2.06±1.03	24.53±17.9	24.2±5.57
24.	2.59±0.12	13.2±5.29	18.77±3.67
25.	3.48±0.37	38.4±23	1.93±0.51
26.	3.15±0.76	51.17±1.7	11.15±2.96
27.	4.06±0.08	51.5±3.04	22.75±5.03
28.	3.92±0.78	54.13±0.9	21.77±1.25
29.	3.5±0.87	47.33±10.3	14.53±11.5
30.	2.87±0.71	37.13±10.9	9.763±5.73
31.	1.93±0.67	39.13±11.2	23.53±4.77
32.	1.4±0.53	16.13±2.4	19.27±1.54
33.	2.13±0.71	27.9±17.1	11.37±15.4
34.	2.05±1.06	28.87±20.3	21.53±1.2
35.	1.77±1.16	30.3±24.2	22.3±3.25
36.	2.35±0.49	34.6±19.9	23.49±5.25

The ground measured LAI, RWC and CC values for banana plants are as seen in **Table 14** along with their standard deviation values. For banana, it was found that LAI ranged between 1.89 and 4.99 with mean value of 3.78. Its CC range was between 6.79 mg g^{-1} and 34.0 mg g^{-1} with mean value calculated as 20.4 mg g^{-1}. RWC varied from 41.7% to 98.4 % with mean of 70.0%.

Table 14. Ground measured biophysical and biochemical parameters of banana crop at different agricultural fields

Sr. No.	**LAI**	**CC (mg g^{-1})**	**RWC (%)**
1.	3.45±0.55	6.79±1.6	42.6±2.4
2.	3.00±0.76	6.79±1.6	43.5±27.6
3.	3.95±1.16	17.6±17.0	60.7±34.0
4.	4.05±0.18	22.8±4.6	83.8±5.5
5.	4.30±0.26	19.0±4.4	80.5±3.5
6.	4.33±0.59	18.5±4.9	77.1±4.4
7.	4.87±0.67	29.0±4.0	45.8±15.3
8.	4.70±0.89	33.0±10.0	95.5±11.3
9.	4.71±0.66	30.1±10.0	69.9±6.6
10.	3.89±0.46	28.7±7.80	88.9±8.3
11.	4.99±0.33	22.1±13.0	60.8±9.1
12.	2.91±0.56	22.4±8.30	55.1±13.2
13.	2.49±0.54	6.27±1.0	62.8±15.2
14.	3.34±0.42	11.2±7.2	58.4±6.4
15.	3.96±0.04	13.5±5.3	41.7±2.9
16.	2.69±0.41	12.7±5.6	52.8±13.6

17.	2.77±0.20	10.5±2.5	49.8±16.6
18.	2.72±1.32	9.6±5.3	64.1±10.6
19.	1.89±0.57	9.78±1.7	70.5±5.4
20.	3.80±1.47	22.4±7.2	75.5±8.9
21.	4.02±0.55	34.0±5.3	90.1±2.0
22.	4.39±0.51	22.7±1.3	75.1±5.6
23.	4.48±0.16	30.7±3.2	91.1±3.9
24.	4.91±0.77	30.9±8.7	92.1±16.4
25.	4.68±0.39	32.0±4.5	94.4±8.0
26.	4.29±0.24	33.0±10.0	98.4±7.6
27.	3.15±0.32	17.8±2.6	71.5±6.7
28.	3.14±0.88	14.3±2.2	78.1±11.5
29.	3.69±0.61	23.1±16.0	60.8±5.7

Biomass values for cotton and banana crop are given in **Table 15**. Biomass for cotton ranged from 2001.2 to 6804.2 kg/ha with mean value of 4592.8 kg/ha. For banana, it ranged between 2041.2 and 5443.3 kg/ha with mean value of 3585.4 kg/ha.

Table 15. Ground measured biomass for cotton and banana plants at different agricultural fields

Sr. No.	Cotton biomass (kg/ha)	Banana biomass (kg/ha)
1.	5443.3	2721.7
2.	4762.9	3402.1
3.	4013.0	3041.2
4.	5429.3	5041.2
5.	6804.2	2621.0
6.	3402.1	2721.7
7.	5002.7	4762.9
8.	3505.0	4721.6
9.	4488.9	2041.2
10.	5113.2	5443.3
11.	2001.2	2142.2
12.	6305.0	4662.9
13.	4396.4	2190.0
14.	3996.3	5430.3
15.	3516.3	2241.5
16.	5102.5	4652.9
17.	3896.1	2701.7
18.	5082.5	2921.0
19.	5003.1	4662.9

These conventional measurements of the crop parameters were time-consuming and very tedious. Knowing about the predictive power of remote sensing, an attempt was made to retrieve these parameters using the spatial non-destructive non-conventional approach.

4.5.2 Retrieval of crop parameters using non-conventional technique:

The non-conventional technique viz. Remote Sensing has been found to be potentially valuable in estimating these biophysical variables by several workers (Ahlrichs and Bauer, 1983; Cheng et al., 2003; Tang et al., 2004; Zhang et al., 2006; Francesco et al., 2006; Monteiro et al., 2012). In the present study, Optical and Microwave remote sensing yielded good results related to the retrieval of crop biophysical and biochemical parameters in Cotton, Castor and Banana. Extracted RS parameters from Landsat 5 TM, LISS IV and radar data were correlated to LAI, CC and RWC which are important parameters strongly linked to the final grain yield. The satellite optical LANDSAT 5 TM and LISS IV along with the radar data gave a good comparative account of each data in terms of their limitations and advantages and are taken up separately.

4.5.2.1 Crop Parameters retrieval from Optical data:

For the retrieval of the crop parameters from an optical data, widely used approach namely **empirical-statistical approach** was used. Empirical statistical relationships were established between spectral indices and ground estimated crop parameters.

Spectral indices significant for the retrieval of crop parameters were derived from both Landsat 5 TM and LISS IV using ERDAS-9.1 which are described below separately:

4.5.2.1.1 Spectral indices calculated from both Landsat 5 TM and LISS IV:

Vegetation indices calculated using combinations of red and NIR wavebands: RVI and NDVI; and one water index using combinations of NIR and SWIR wavebands: NDWI are explained below:

Normalized Difference Vegetation Index (NDVI): NDVI is utilized to monitor crop conditions and thus early warning on droughts and famines can be obtained by computing this index. A strong relationship also exists between NDVI and agricultural yield (Labus et al., 2002; Boschetti et al., 2009; Yin et al., 2012). Derivation of vegetation properties, such as length of growing season, onset date of greenness, and date of maximum photosynthetic activity is often done using NDVI time series for monitoring changes in agricultural systems (Lee et al., 2002; Xin et al., 2002; Hill and Donald, 2003; de Beurs and Henebry, 2004). NDVI for the study area were derived from both Landsat 5 TM and LISS IV (**Plate 9a & 10a**). The common range for green vegetation in the study area is 0.2 to 0.8. **Table 16** shows NDVI values extracted from both the data for three crops dominant in the study area.

Table 16. Derived NDVI using LANDSAT 5 TM and LISS IV data

Crop	Satellite Data	NDVI Range	Standard deviation
Cotton	Landsat 5 TM	0.11 - 0.42	0.07
	LISS IV	0.13 - 0.45	0.08
Castor	Landsat 5 TM	0.05 - 0.56	0.14
	LISS IV	0.07 - 0.53	0.12
Banana	Landsat 5 TM	0.13 – 0.47	0.09
	LISS IV	0.15 – 0.44	0.08

Ratio Vegetation Index (RVI): The RVI was probably the first index to be defined and is the most commonly used index. It is formed by ratioing Near Infrared (NIR) and Red. Use of this index is made by several researches for the retrieval of different vegetation

parameters (Jordan, 1969; Tucker, 1979). RVI extracted from Landsat 5 TM and LISS IV optical data is shown in **Plate 9b & 10b.** RVI values derived using these data for different crops are shown in **Table 17**.

Table 17. Derived RVI using LANDSAT 5 TM and LISS IV data

Crop	**Satellite Data**	**RVI Range**	**Standard deviation**
Cotton	Landsat 5 TM	1.0 - 2.7	0.33
	LISS IV	1.1 - 2.7	0.43
Castor	Landsat 5 TM	0.74 - 3.15	0.64
	LISS IV	0.82 - 3.7	0.65
Banana	Landsat 5 TM	1.1 - 2.58	0.40
	LISS IV	1.01 - 2.62	0.38

Normalized Difference Water Index (NDWI): Information regarding crop water content has a great utility in the field of agriculture. NDWI vary according to RWC and is the determinant of changes in the crop water content. It can be used in the detection of water stress caused by drought. The index generated ranged from -1.0 to 1.0 (**Plate 11**). The extracted NDWI values from Landsat data for the crops analyzed in the present research ranged from -0.19 to 0.38. Banana showed the highest NDWI values (**Table 18)**.

Table 18. Derived NDWI using LANDSAT 5 TM

Crop	**Satellite Data**	**NDWI Range**	**Standard deviation**
Cotton	Landsat 5 TM	-0.05 - 0.18	0.07
Castor	Landsat 5 TM	-0.19 - 0.2	0.09
Banana	Landsat 5 TM	-0.08 – 0.38	0.11

Correlation of these indices with different in situ estimates of a crop can be useful in the prediction of crop variables. The spatially derived spectral indices from the Landsat 5 TM and LISS IV optical data served to be an input for the retrieval of crop biophysical and biochemical parameters.

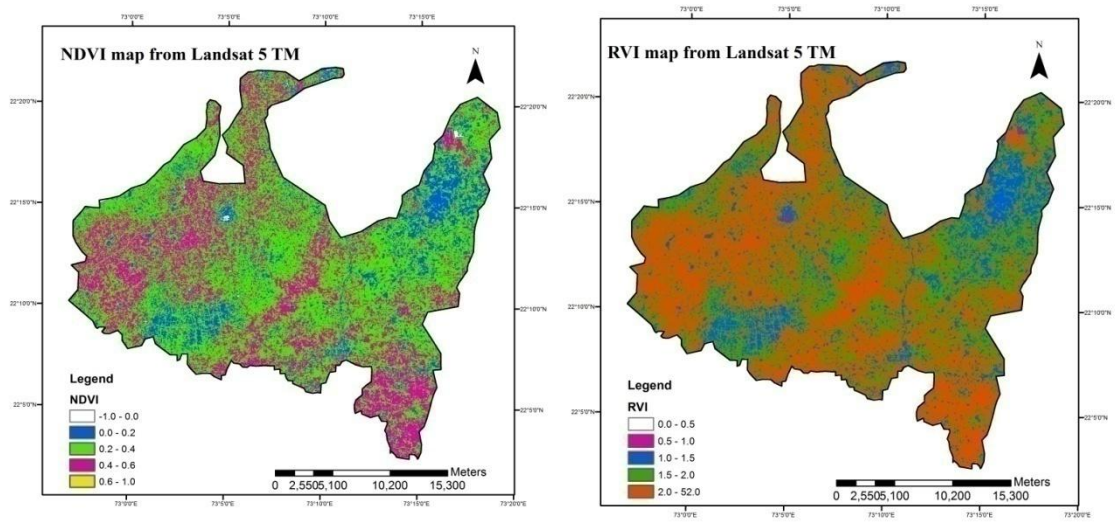

[a] **[b]**

Plate 9. Vegetation index map [a] NDVI [b] RVI derived from Landsat 5 TM (Oct 2009) for agricultural fields of Vadodara

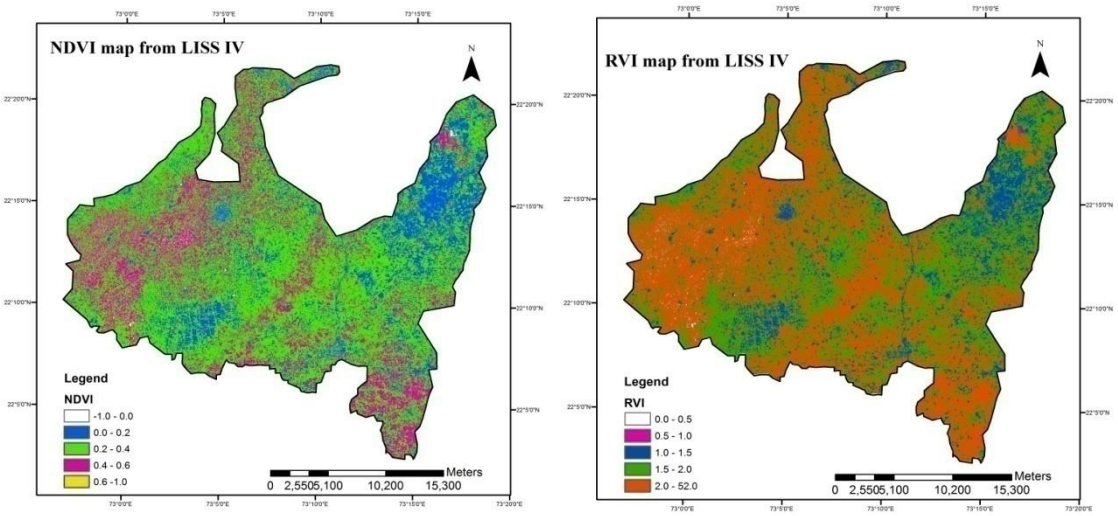

[a] **[b]**

Plate 10. Vegetation index map [a] NDVI [b] RVI derived from LISS IV (Oct 2009) for agricultural fields of Vadodara

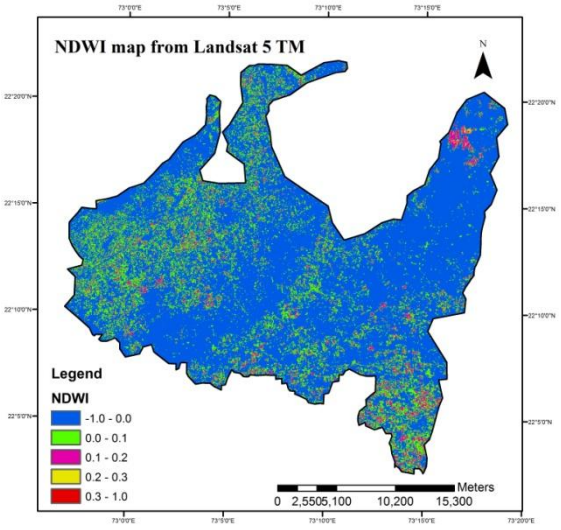

Plate 11. NDWI Map derived from Landsat 5 TM (Oct 2009) for agricultural fields of Vadodara

4.5.2.1.2 Retrieval of Crop parameters using Optical RS based Empirical-statistical models:

The utility of optical remote sensing data (LANDSAT 5 TM and LISS IV) for retrieving crop biophysical and biochemical parameters has been clearly observed in the present study. Such findings have also been reported by many earlier researchers (Dong et al., 2003; Ji-hua and Bing-fang, 2008; Meng et al., 2013). They have confirmed that the retrieval of these parameters using vegetation indices such as NDVI and RVI could be achieved with an acceptable accuracy.

4.5.2.1.3 LAI retrieval in different crops using Landsat 5 TM and LISS IV:

LAI is a key canopy descriptor that is used in determining foliage cover, and in predicting photosynthesis and evapotranspiration for assessing crop yield (Haboudane et al., 2004b, Wittamperuma et al., 2012). Its estimation from the remote sensing data has been the focus of many investigations in the recent years (Aboelghar et al., 2010, Vuolo et al., 2013). Linear models developed for the assessment of LAI in three crops by

correlating LAI with vegetation indices namely NDVI and RVI derived from Landsat and LISS IV optical data showed quite good correlation. Coefficient of determination (R^2) for these models varied from 0.555 to 0.805.

For any established statistical based model, its validation becomes very important as it entails to an algorithm development for large scale applications (Mohan et al., 2011). Validation carried out for all the developed models exhibited strong relationship between estimated and predicted crop parameters.

NDVI-LAI model: The correlation coefficients computed showed a positive correlation between ground based LAI and NDVI extracted from LANDSAT 5 TM with R^2 0.674, 0.724 and 0.718 in Cotton, Castor and Banana respectively (**Figure 38, 46 & 54)**. LAI when correlated with LISS IV derived NDVI also exhibited a positive correlation with R^2 0.805, 0.747 and 0.738 in Cotton, Castor and Banana respectively (**Figure 42, 50 & 58)**. This correlation of LAI with LISS IV derived NDVI was comparatively higher when compared to one with Landsat derived NDVI. The t-test for correlation coefficient conducted exhibited that the results were highly significant (p 0.01 level).

Validation of both the NDVI-LAI models was done and a good relationship was observed between ground measured LAI and LAI derived using developed NDVI-LAI model (For Landsat data, R^2=0.756, R^2=0.626 and R^2=0.667; and for LISS IV data, was R^2=0.679, R^2=0.634 and R^2=0.674 in Cotton, Castor and Banana respectively) (**Figure 39, 47, 55, 41, 51 & 59**). A good accuracy of 92.7%, 87.8% and 83.3% was observed for the developed Landsat data based biophysical model for Cotton, Castor and Banana respectively. For LISS IV data also, a good accuracy of 87.8%, 95.1% and 87.5% was observed for Cotton, Castor and Banana developed models respectively. Using

established RS based empirical-statistical relationships, LAI maps for Cotton, Castor and Banana were also generated using these linear models (**Plate 12a, 13a, 14a, 15a, 16a and 17a**).

RVI-LAI model: The linear regression relationships established between ground measured LAI of Cotton, Castor and Banana crops and RVI measured from Landsat 5 TM images showed comparatively less but good positive correlation (**Figure 40, 48 & 56)**. R^2 computed was 0.592 and 0.658 and 0.555 in Cotton, Castor and Banana respectively. LISS IV derived RVI showed better correlation with ground measured LAI of Cotton, Castor and Banana crops (**Figure 44, 52 & 60)**. R^2 computed was 0.696, 0.686 and 0.660 for Cotton, Castor and Banana respectively. Results for these correlations were also found to be highly significant (p 0.01 level). Validation carried for RVI-LAI models showed the correlation between ground LAI and RVI-LAI model predicted LAI (**Figure 41, 49, 57, 45, 53 & 61).** RVI-LAI models established using Landsat data showed an accuracy of 92.6%, 95.1% and 91.7% and those established using LISS IV data showed an accuracy of 87.8%, 92.7% and 91.7% for Cotton, Castor and Banana respectively. LAI maps were also developed using derived relationships between RVI and LAI (**Plate 12b, 13b, 14b, 15b, 16b and 17b**).

In terms of vegetation indices, comparison of R^2 values between the models revealed that NDVI was slightly superior to RVI in its correlation with LAI in both Landsat 5 TM and LISS IV data. Hence amongst indices, NDVI-LAI model proves to be better choice as an estimator of LAI when compared to RVI-LAI model. In terms of data, LISS IV data showed better potential for the estimation of LAI when compared to Landsat TM data.

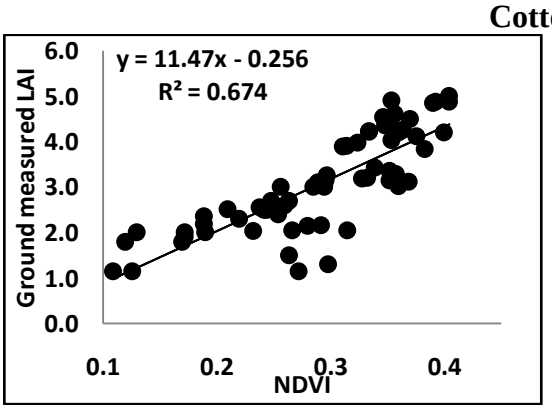

Fig 38. The linear relationship between Landsat 5 TM derived NDVI and cotton LAI

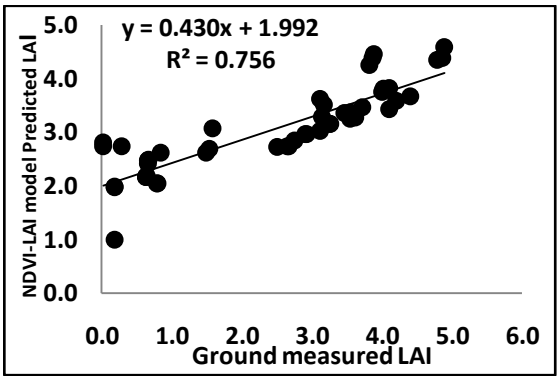

Fig 39. Validation of Landsat NDVI–LAI model using ground measured cotton LAI

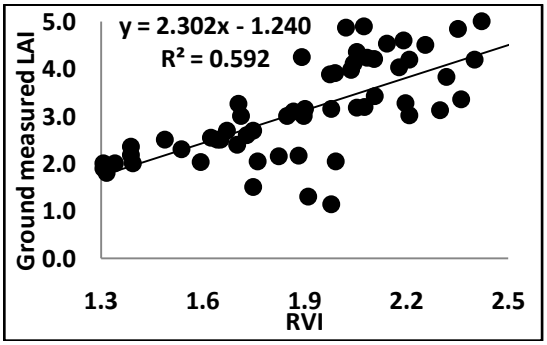

Fig 40. The linear relationship between Landsat 5 TM derived RVI and cotton LAI

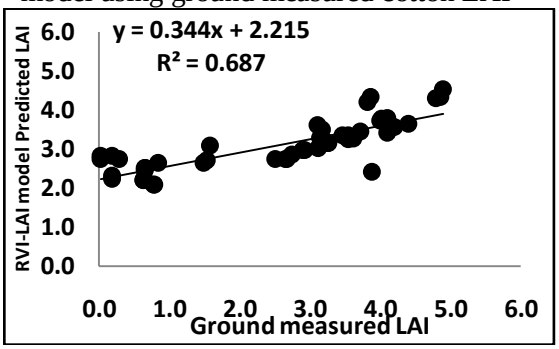

Fig 41. Validation of Landsat RVI–LAI model using ground measured cotton LAI

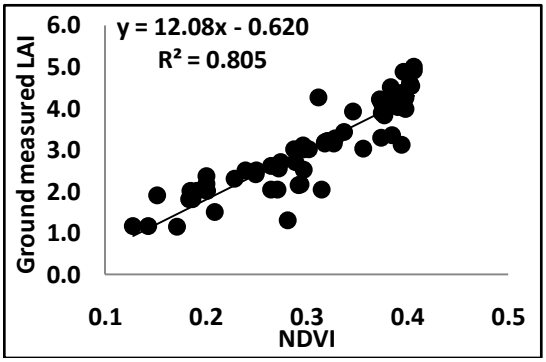

Fig 42. The linear relationship between LISS IV derived NDVI and cotton LAI

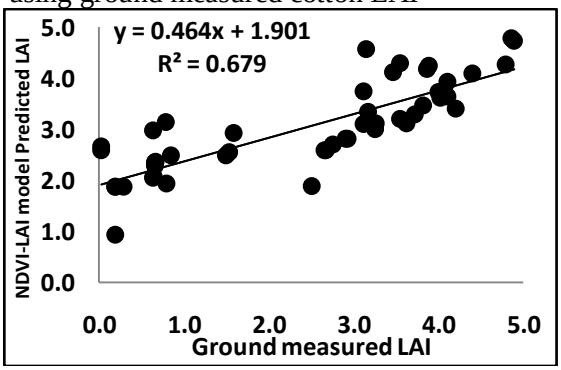

Fig 43. Validation of LISS IV NDVI–LAI model using ground measured cotton LAI

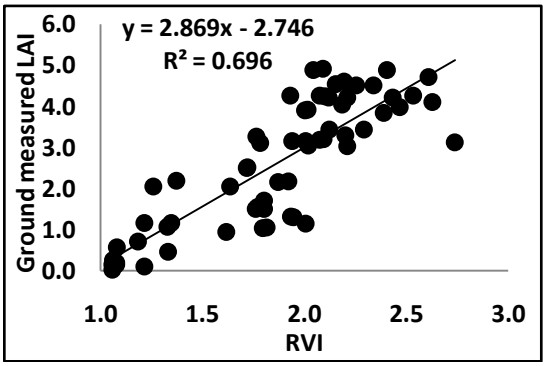

Fig 44. The linear relationship between LISS IV derived RVI and cotton LAI

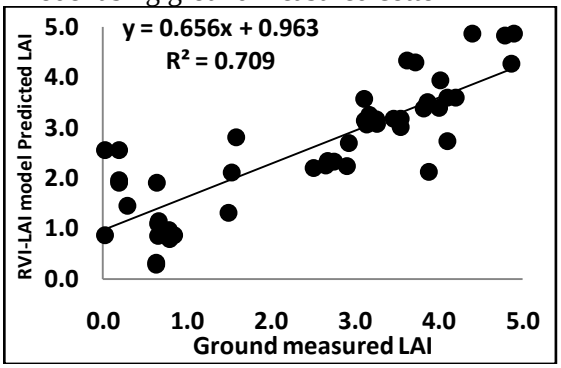

Fig 45. Validation of LISS IV RVI–LAI model using ground measured cotton LAI

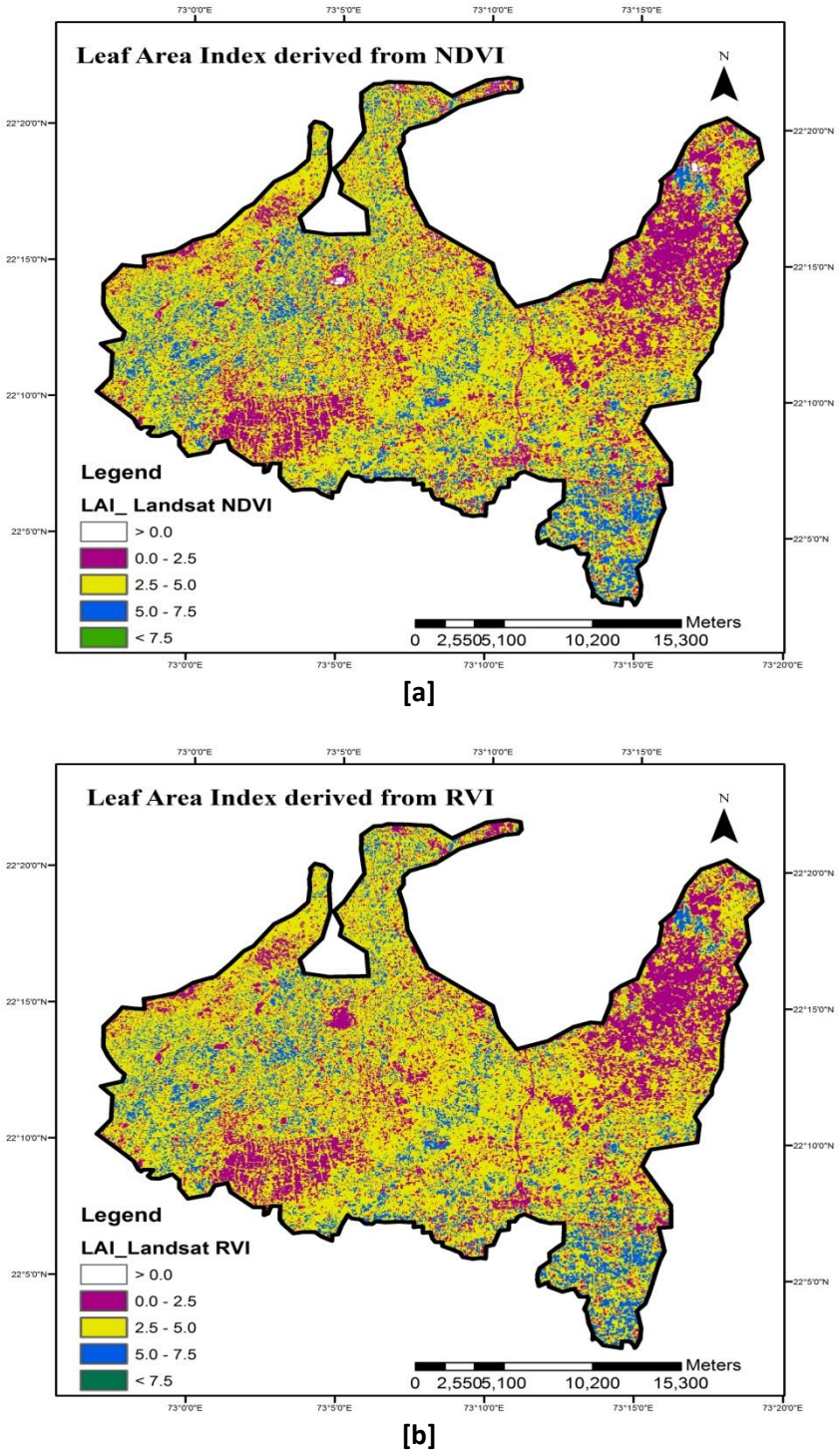

Plate 12. LAI Map generated from [a] Landsat 5 TM derived NDVI [b] Landsat 5 TM derived RVI for cotton agricultural fields of Vadodara

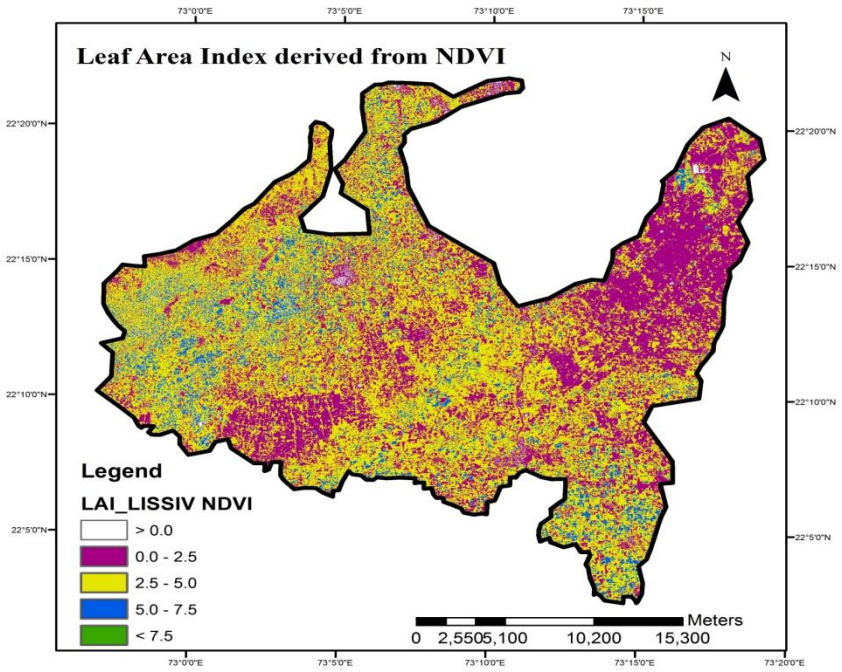

[a]

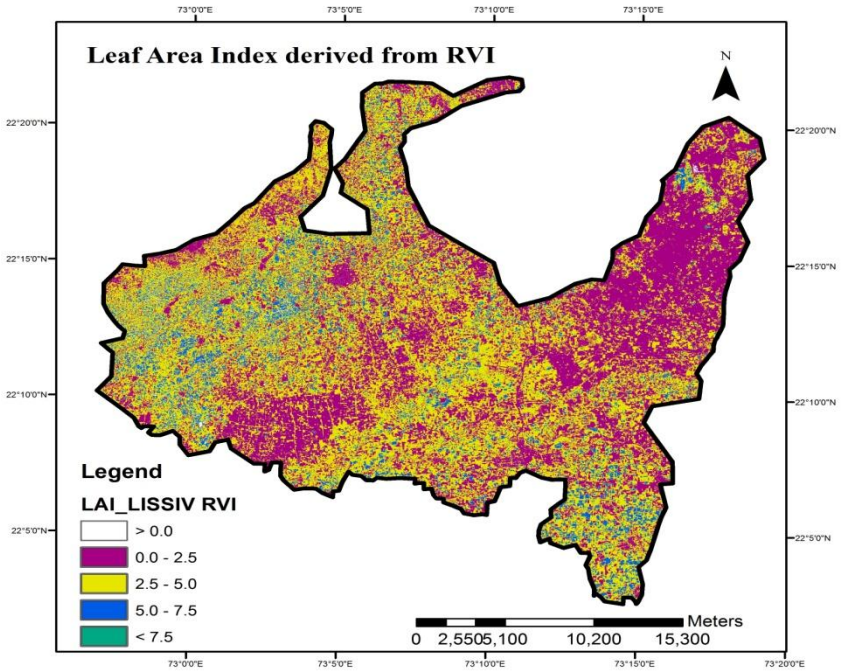

[b]

Plate 13. LAI Map generated from [a] LISS IV derived NDVI [b] LISS IV derived RVI (Oct 2009) for cotton agricultural fields of Vadodara

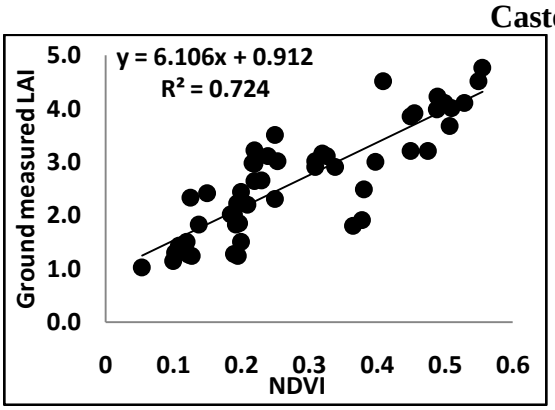

Fig 46. The linear relationship between Landsat 5 TM derived NDVI and castor LAI

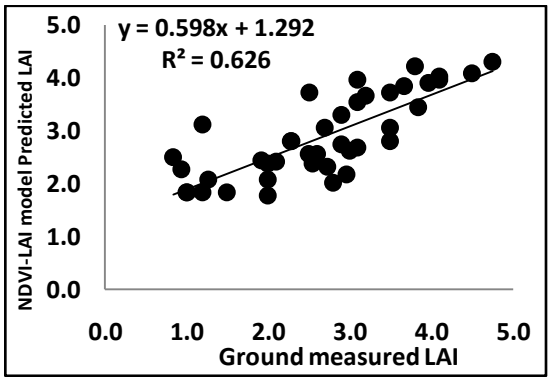

Fig 47. Validation of Landsat NDVI–LAI model using ground measured castor LAI

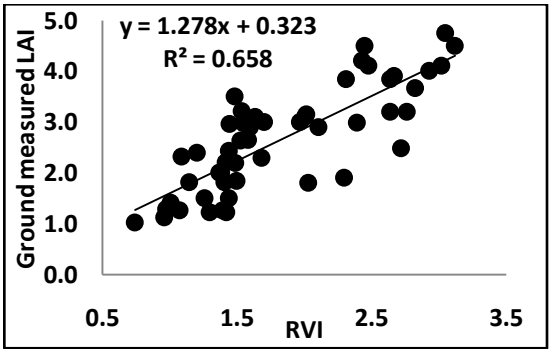

Fig 48. The linear relationship between Landsat 5 TM derived RVI and castor LAI

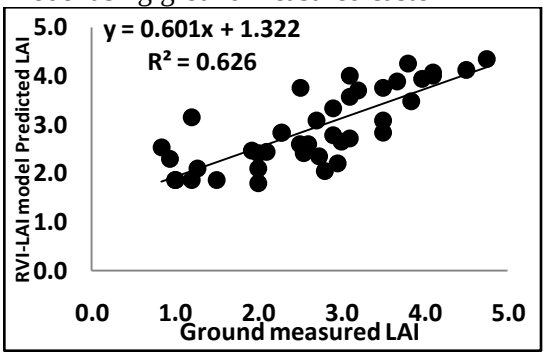

Fig 49. Validation of Landsat RVI–LAI model using ground measured castor LAI

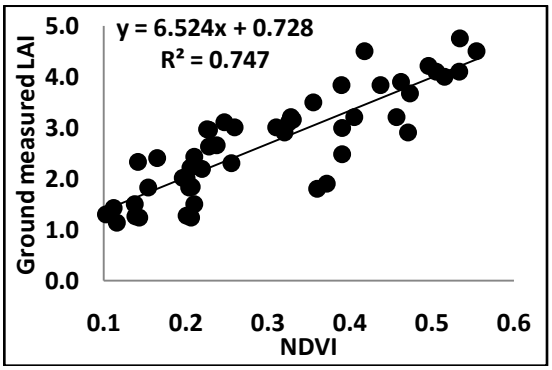

Fig 50. The linear relationship between LISS IV derived NDVI and castor LAI

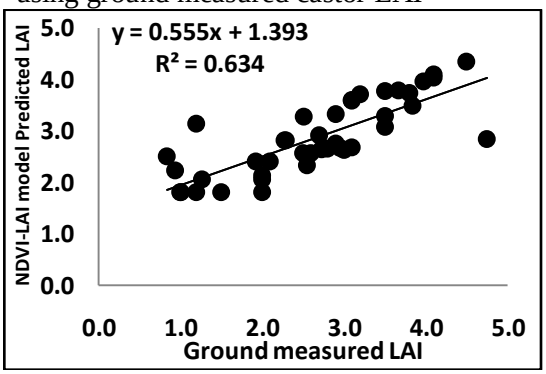

Fig 51. Validation of LISS IV NDVI–LAI model using ground measured castor LAI

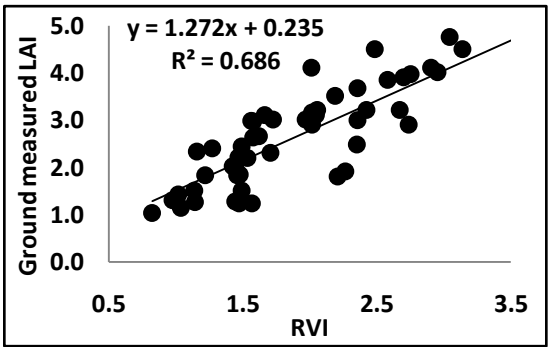

Fig 52. The linear relationship between LISS IV derived RVI and castor LAI

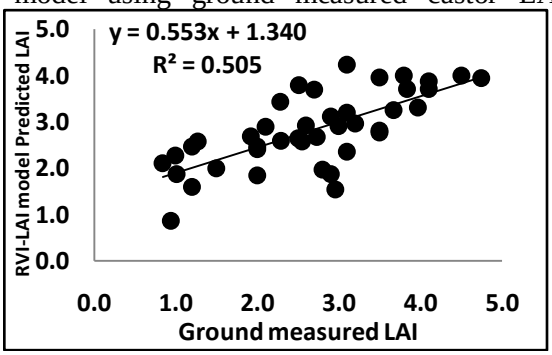

Fig 53. Validation of LISS IV RVI–LAI model using ground measured castor LAI

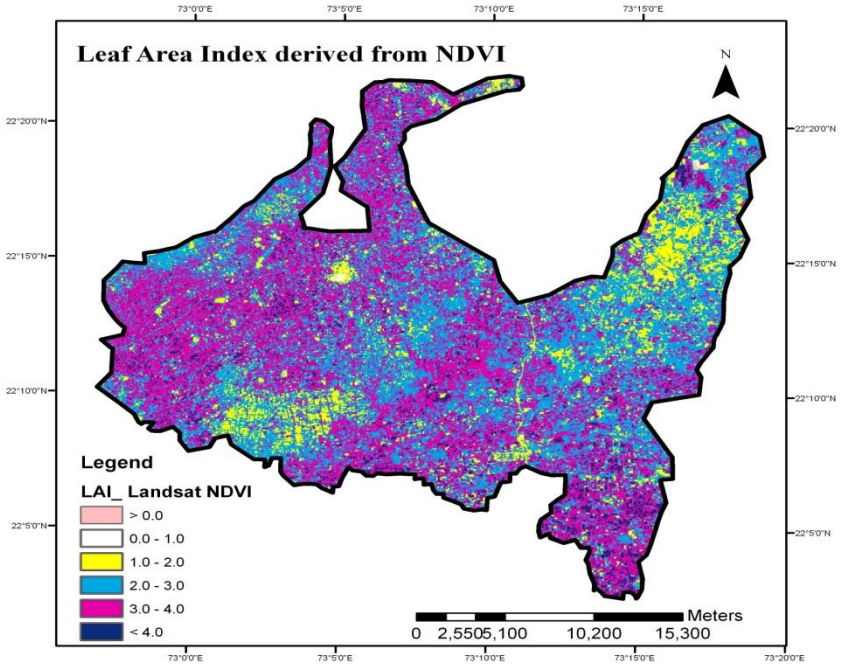

[a]

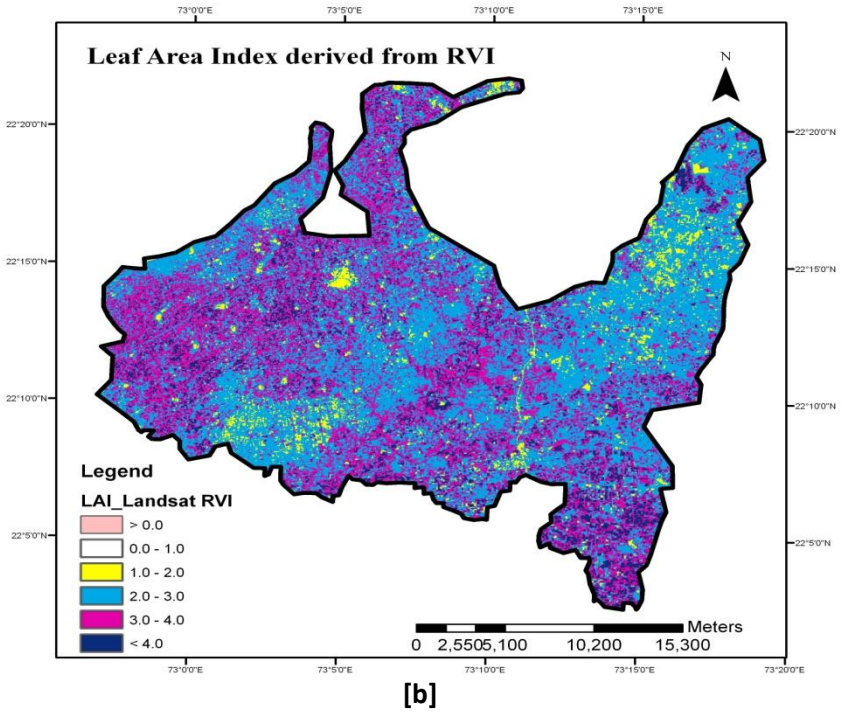

[b]

Plate 14. LAI Map generated from [a] Landsat 5 TM derived NDVI [b] Landsat 5 TM derived RVI (Oct 2009) for castor agricultural fields of Vadodara

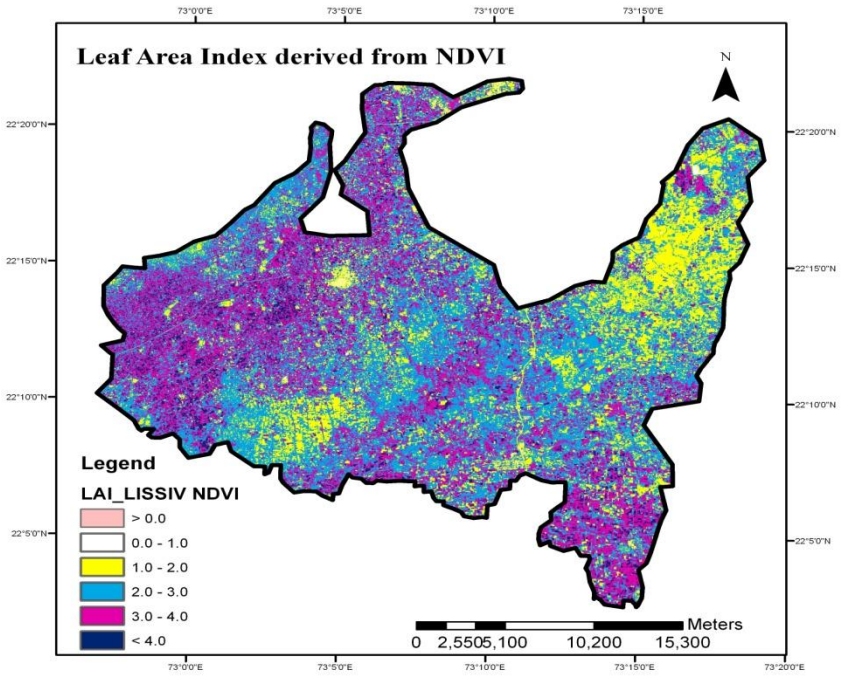

[a]

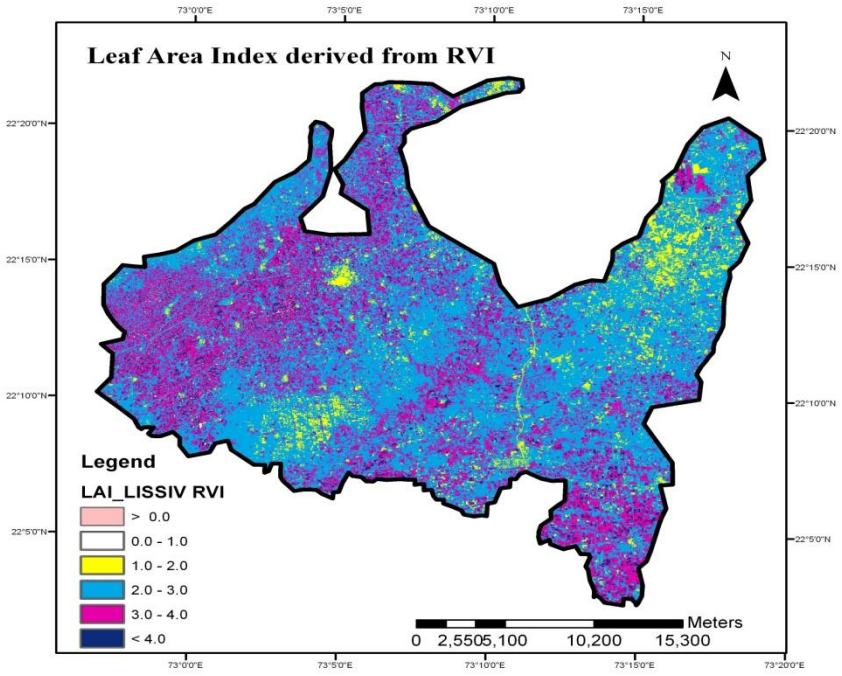

[b]

Plate 15. LAI Map generated from [a] LISS IV derived NDVI [b] LISS IV derived RVI (Oct 2009) for castor agricultural fields of Vadodara

Banana LAI

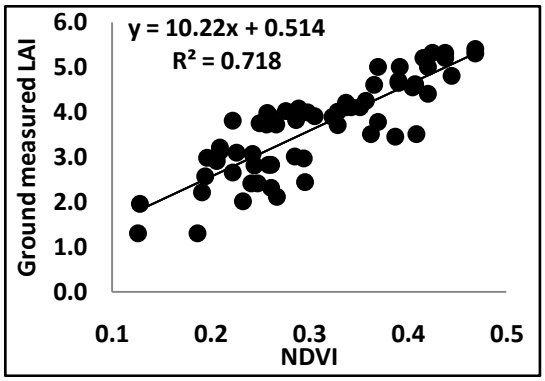

Fig 54. The linear relationship between Landsat 5 TM derived NDVI and banana LAI

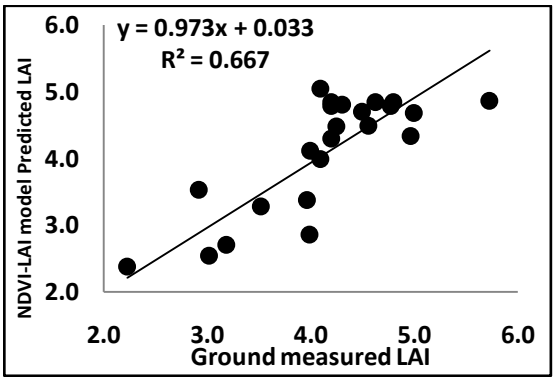

Fig 55. Validation of Landsat NDVI–LAI model using ground measured banana LAI

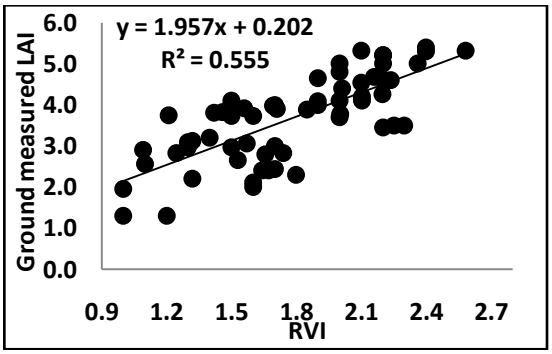

Fig 56. The linear relationship between Landsat 5 TM derived RVI and banana LAI

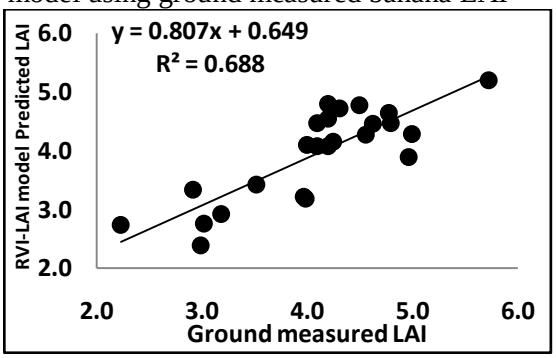

Fig 57. Validation of Landsat RVI–LAI model using ground measured banana LAI

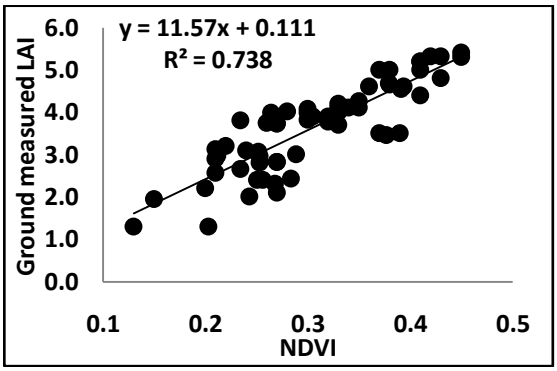

Fig 58. The linear relationship between LISS IV derived NDVI and banana LAI

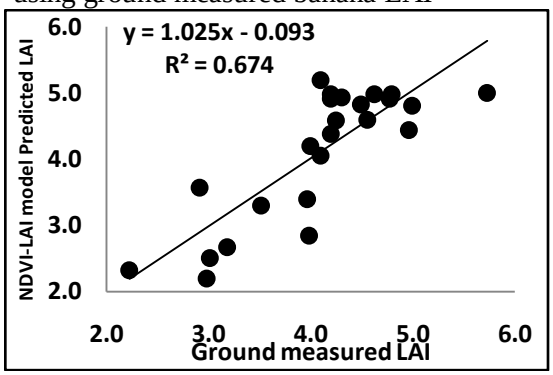

Fig 59. Validation of LISS IV NDVI–LAI model using ground measured banana LAI

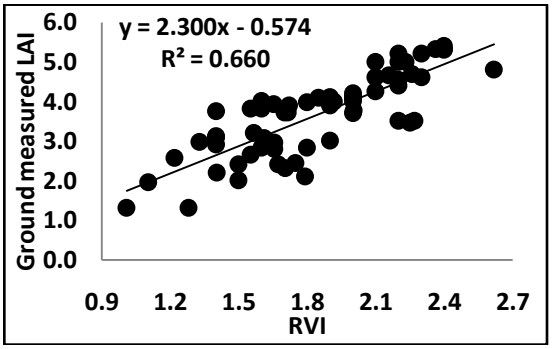

Fig 60. The linear relationship between LISS IV derived RVI and banana LAI

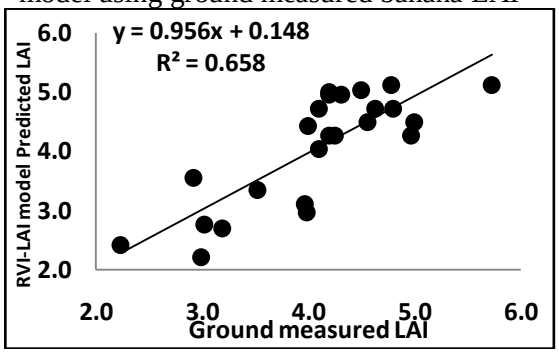

Fig 61. Validation of LISS IV RVI–LAI model using ground measured banana LAI

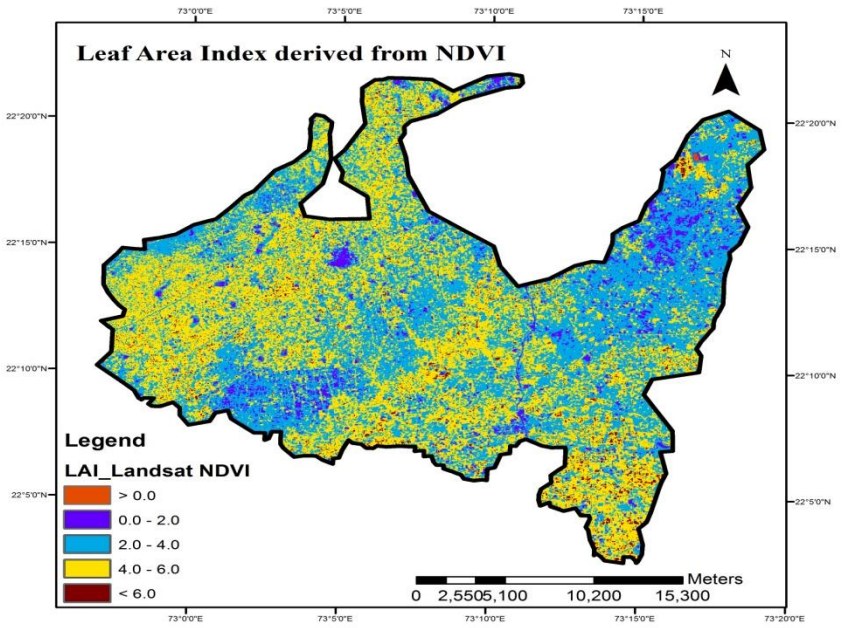

[a]

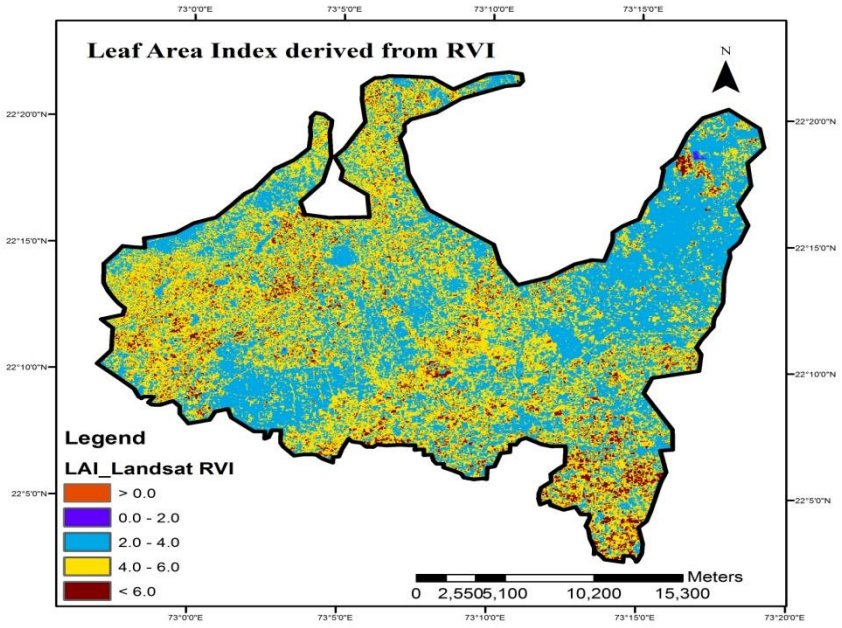

[b]

Plate 16. LAI Map generated from [a] Landsat 5 TM derived NDVI [b] Landsat 5 TM derived RVI for banana agricultural fields of Vadodara

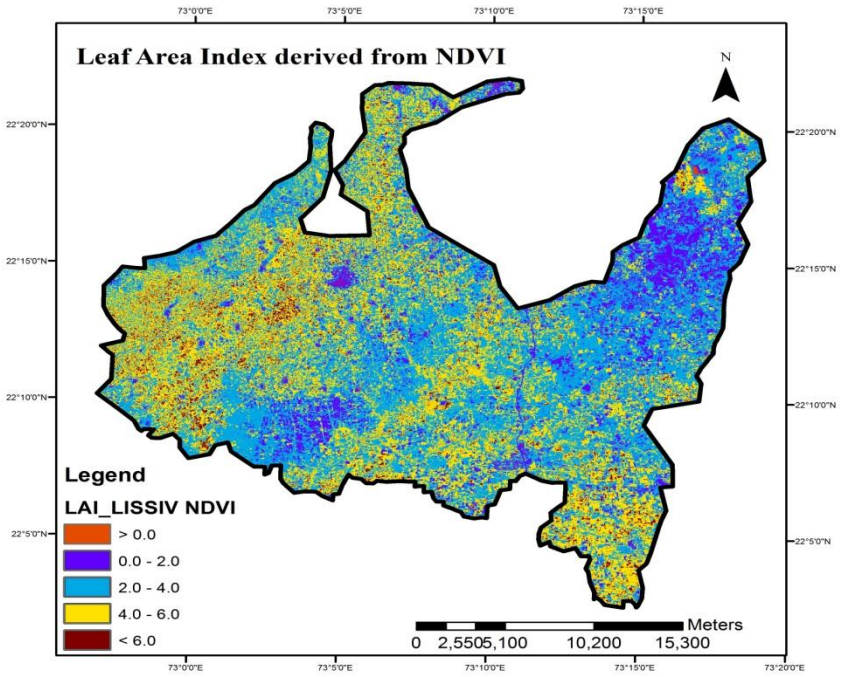

[a]

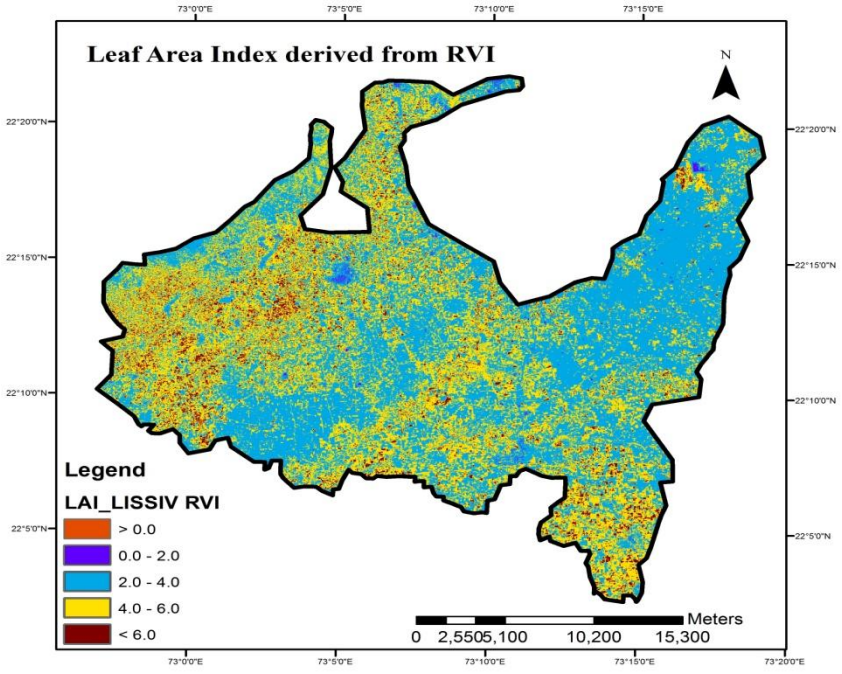

[b]

Plate 17. LAI Map generated from [a] LISS IV derived NDVI [b] LISS IV derived RVI (Oct 2009) for banana agricultural fields of Vadodara

4.5.2.1.4 RWC estimation in different crops using Landsat 5 TM:

Vegetation index, NDWI is correlated to RWC and NDWI-RWC model was formed for the selected crops.

NDWI-RWC model: NDWI-RWC, RS based empirical model showed good correlation of RWC of Cotton, Castor and Banana with NDWI (**Figure 62, 64 & 66**). The t-test for correlation coefficient was carried out and it proved a significant relationship between estimated RWC and RWC derived using NDWI-RWC model (p=0.01) (**Figure 63, 65 & 67**). Accuracies for NDWI-RWC models developed for Cotton, Castor and Banana crop were found to be 86.7 %, 83.3 % and 83.3% respectively. Empirical-statistical models developed were used to make RWC maps for these crops (**Plate 18(a, b & c)**).

Cotton RWC

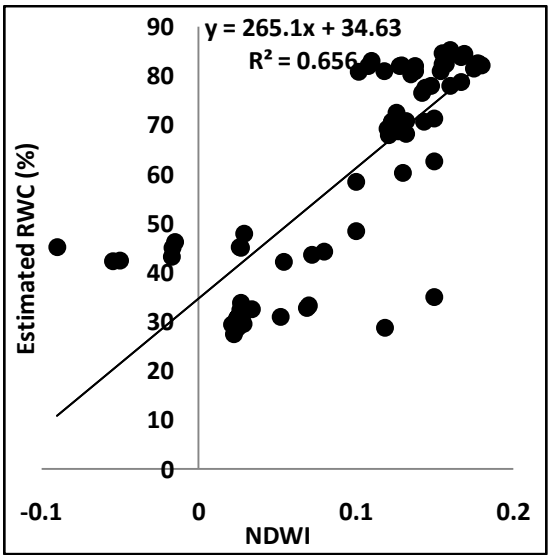

Fig 62. The linear relationship between Landsat 5 TM derived NDWI and cotton RWC

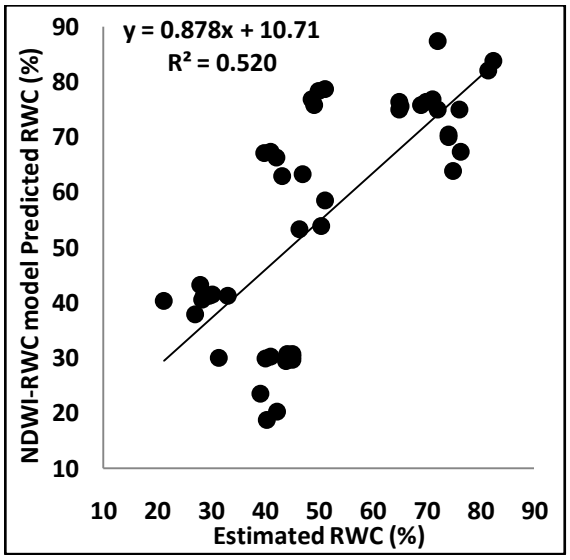

Fig 63. Validation of NDWI–RWC model using estimated cotton RWC

Castor RWC

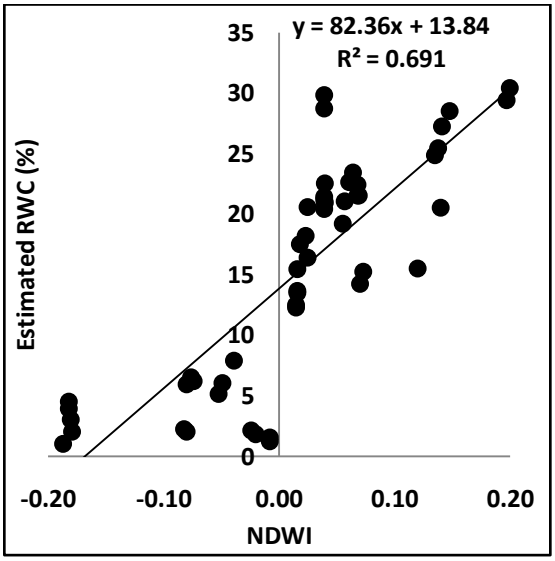

Fig 64. The linear relationship between Landsat 5 TM derived NDWI and castor RWC

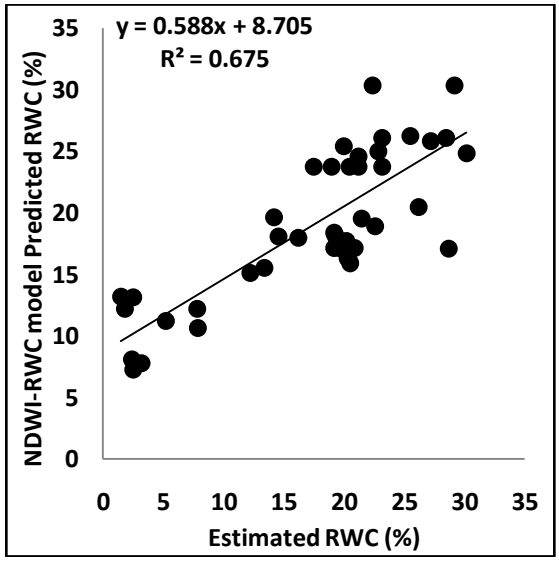

Fig 65. Validation of NDWI–RWC model using estimated castor RWC

Banana RWC

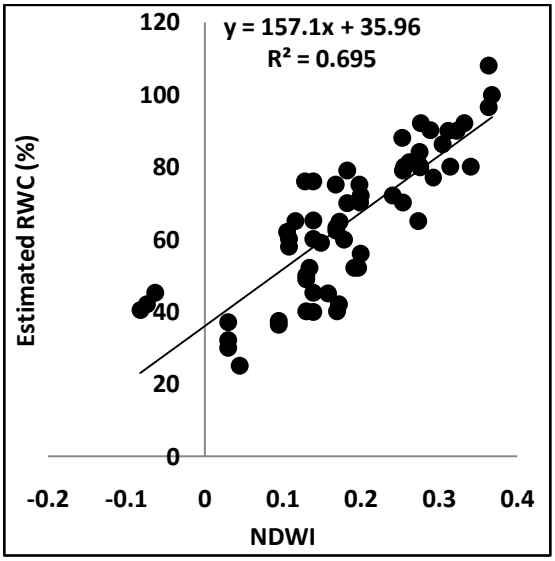

Fig 66. The linear relationship between Landsat 5 TM derived NDWI and banana RWC

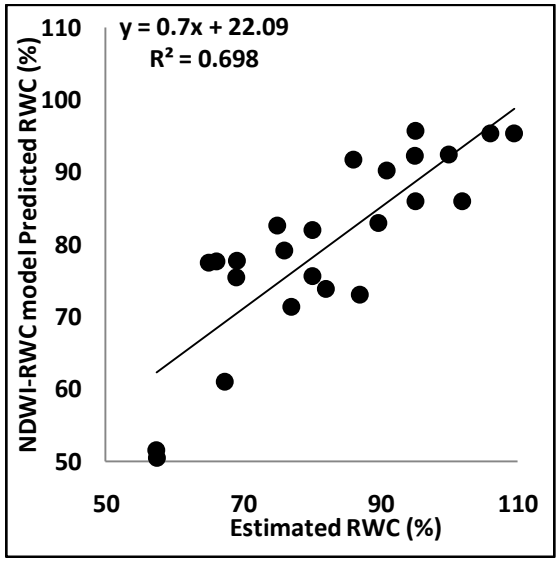

Fig 67. Validation of NDWI–RWC model using estimated banana RWC

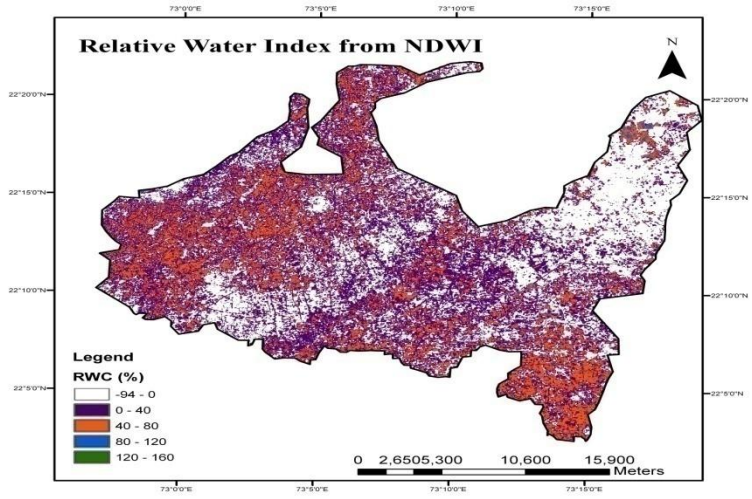

[a]

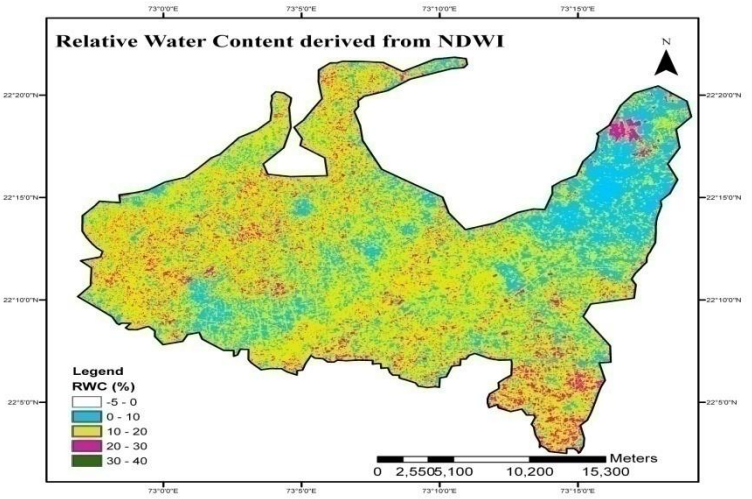

[b]

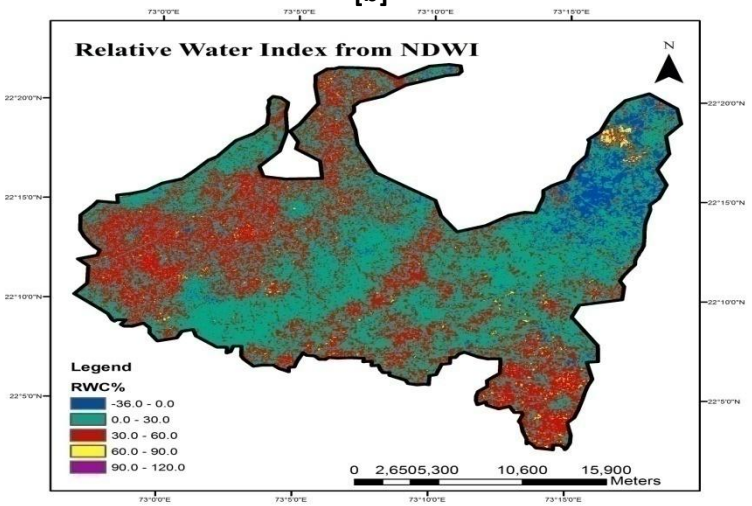

[c]

Plate 18. RWC Map generated from [a] Landsat 5 TM derived cotton NDWI [b] Landsat 5 TM derived castor NDWI [c] Landsat 5 TM derived banana NDWI (Oct 2009) for agricultural fields of Vadodara

4.5.2.1.5 CC estimation in different crops using Landsat 5 TM and LISS IV:

The importance of chlorophyll study in vegetation has been recognized for decades (Danks et al., 1984). Accurate estimates of spatially distributed CC in agricultural crops are of key importance for regional and global studies of carbon balance and responses to nitrogen application (Gitelson et al., 2005). In the present work, optical RS based empirical statistical models were developed for remotely estimating chlorophyll in cotton, castor and banana canopies. CC was retrieved from Landsat 5 TM and LISS IV by establishing empirical-statistical relationships between estimated CC and Optical RS derived vegetation indices**.** Both the indices, NDVI and RVI were related to pigment, CC in different selected crops for development of NDVI-CC and RVI-CC models.

NDVI-CC model: The biochemical feature i.e. leaf CC when correlated with Landsat 5 TM derived NDVI exhibited a positive correlation with R^2, 0. 697, 0.648 and 0.666 in Cotton, Castor and Banana crop respectively (**Figure 68, 76 & 84)**. A positive and comparatively higher correlation was found between pigment CC and LISS IV derived NDVI with R^2, 0. 746, 0.653 and 0.674 in Cotton, Castor and Banana crop respectively (**Figure 72, 80 & 88)**. Ground measured CC and CC derived using NDVI-CC models were linearly related and it showed good correlation (**Figure 69, 77, 85, 73, 81 & 89**). Accuracies for these models were estimated and for Landsat 5 TM data, it was 85.4%, 90.2% and 87.5%; and for LISS IV data it was 82.9%, 87.8% and 95.1% for Cotton, Castor and Banana respectively. These optical RS-based empirical-statistical models were further used for making CC maps of Cotton, Castor and Banana (**Plate 19a, 20a, 21a, 22a, 23a and 24a**).

RVI-CC model: For different crops, linear regression between pigment CC and RVI extracted from Landsat 5 TM was established and empirical-statistical regression equations were formed. Fitted regression relationships showed good correlations with R^2 of 0.643, 0.606 and 0.567 in case of Cotton, Castor and Banana respectively as shown in **Figure 70, 78 & 86**. Empirical-statistical regression equations were also formed by linearly correlating CC and RVI extracted from LISS IV. Fitted regression relationships emphasized comparatively good correlations with R^2 of 0.585, 0.614 and 0.597 in case of Cotton, Castor and Banana respectively as shown in **Figure 74, 82 & 90**. Validation for these models built for all three crops showed good relationship between CC estimated on ground and CC predicted using RVI-CC models (**Figure 71, 79, 87, 75, 83 & 91**). Accuracy test for these RS based models was found good. For Landsat data, 90.2% accuracy for cotton, 87.8% for castor and 83.3% for banana was obtained and for LISS IV data, 65.9% accuracy in case of Cotton, 92.7% in case of Castor and 79.2% in case of Banana was obtained. Using established empirical-statistical relationship between CC and RVI, CC maps were generated for Cotton, Castor and Banana crops (**Plate 19b, 20b, 21b, 22b, 23b and 24b**).

Based on R^2 values NDVI was seen to be more closely related to LAI than RVI exhibiting the former's potential in estimation of CC.

Cotton Chlorophyll

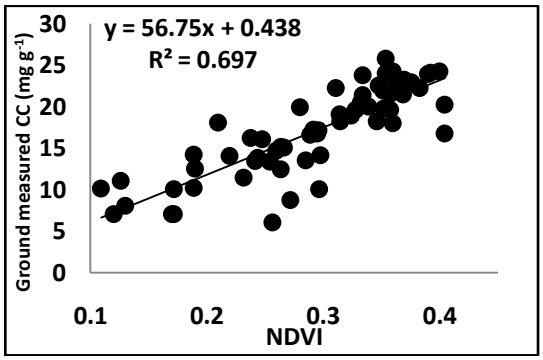

Fig 68. The linear relationship between Landsat 5 TM derived NDVI and cotton CC

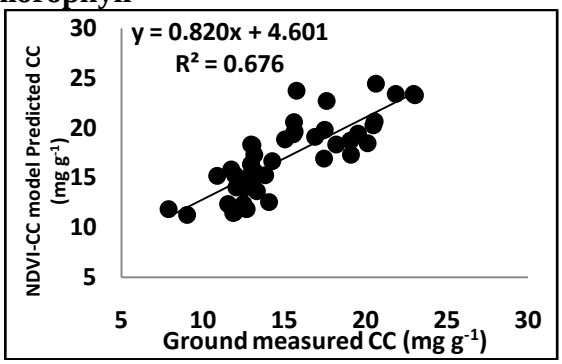

Fig 69. Validation of Landsat NDVI–CC model using ground measured cotton CC

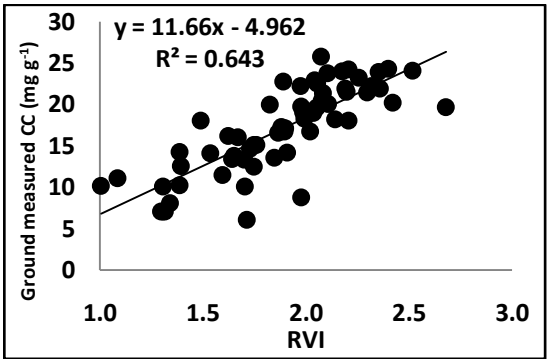

Fig 70. The linear relationship between Landsat 5 TM derived RVI and cotton CC

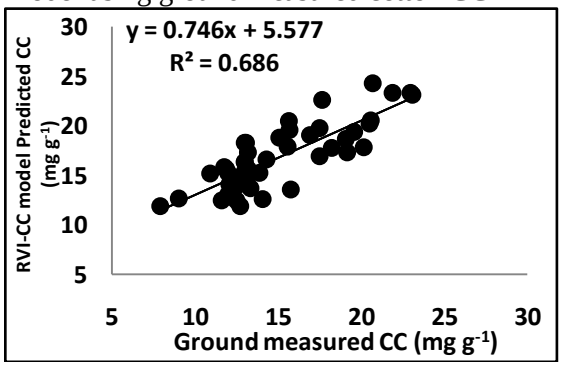

Fig 71. Validation of Landsat RVI–CC model using ground measured cotton CC

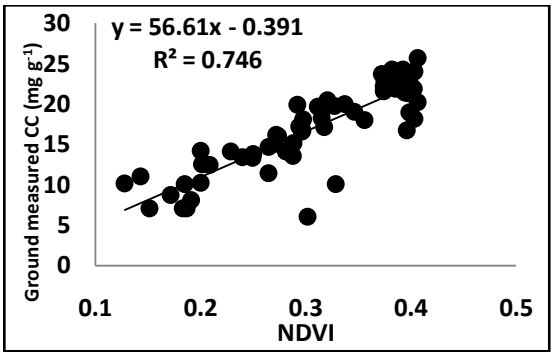

Fig 72. The linear relationship between LISS IV derived NDVI and cotton CC

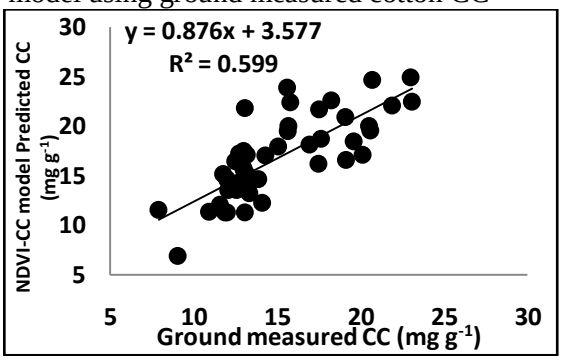

Fig 73. Validation of LISS IV NDVI–CC model using ground measured cotton CC

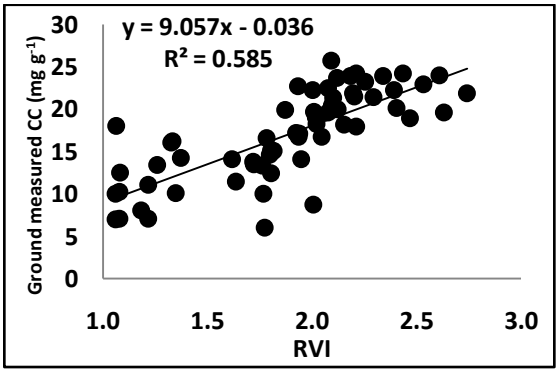

Fig 74. The linear relationship between LISS IV derived RVI and cotton CC

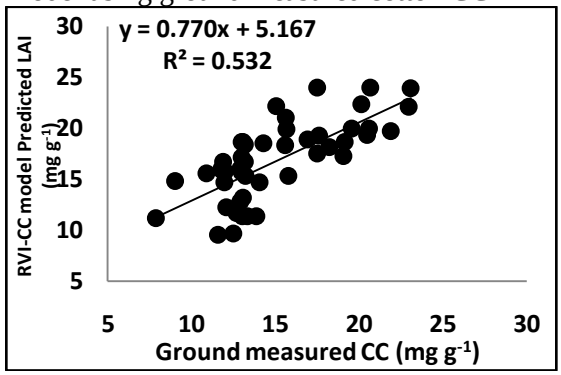

Fig 75. Validation of LISS IV RVI–CC model using ground measured cotton CC

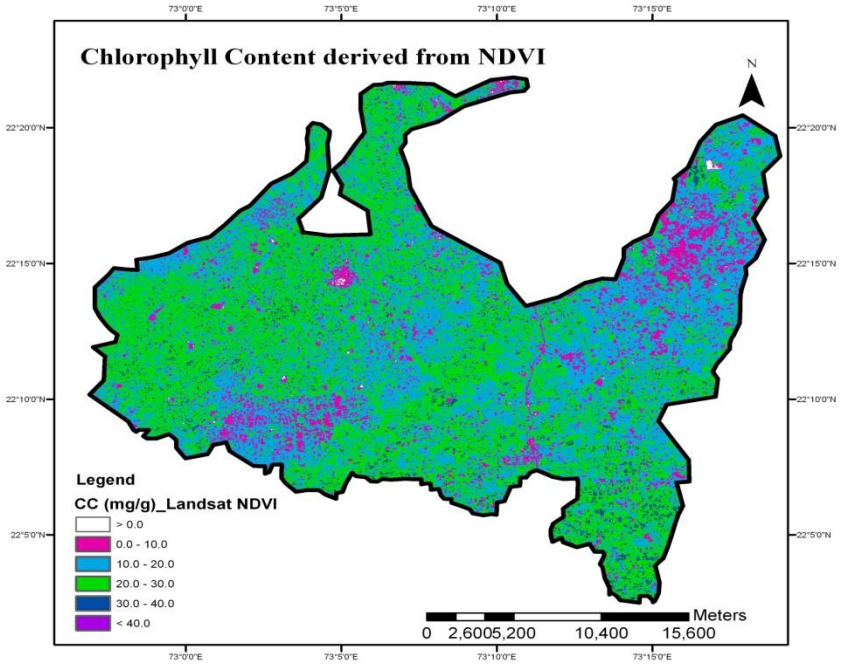

[a]

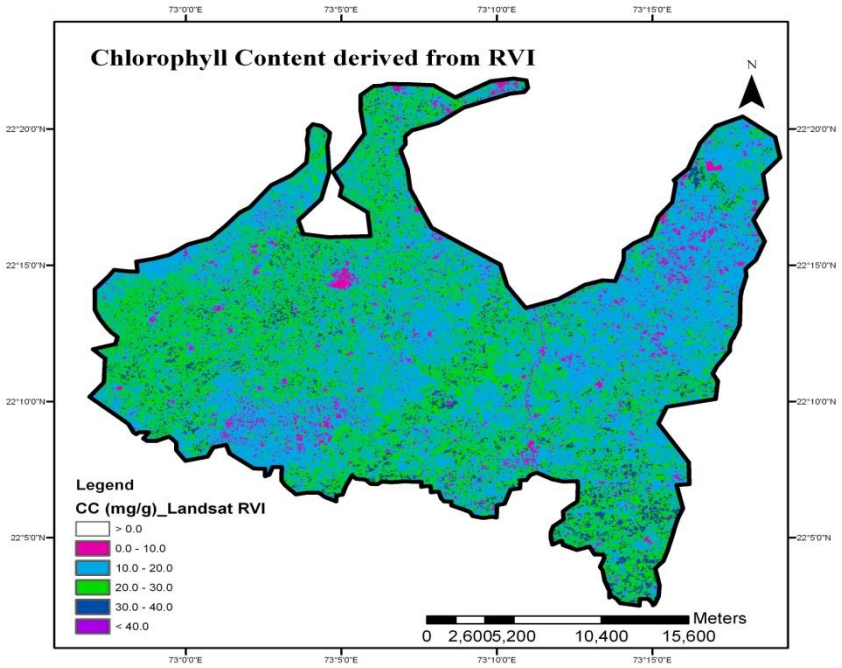

[b]

Plate 19. CC Map generated from [a] Landsat 5 TM derived NDVI [b] Landsat 5 TM derived RVI (Oct 2009) for cotton agricultural fields of Vadodara

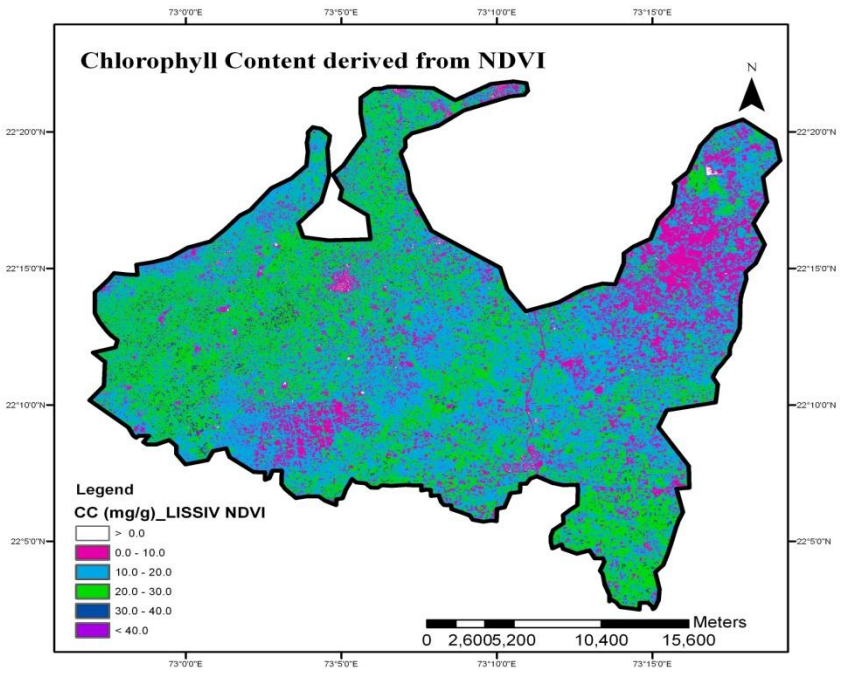

[a]

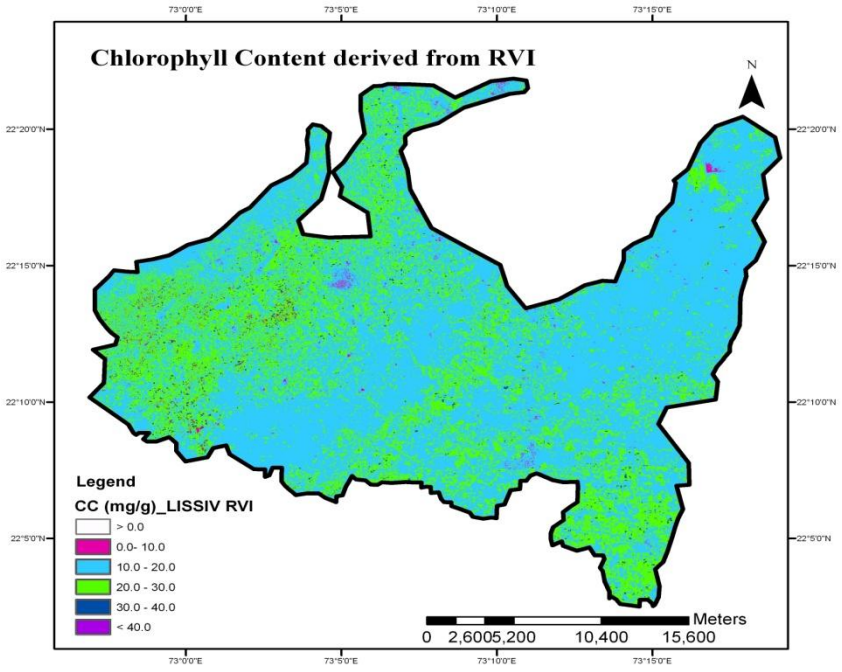

[b]

Plate 20. CC Map generated from [a] LISS IV derived NDVI [b] LISS IV derived RVI (Oct 2009) for cotton agricultural fields of Vadodara

Castor Chlorophyll

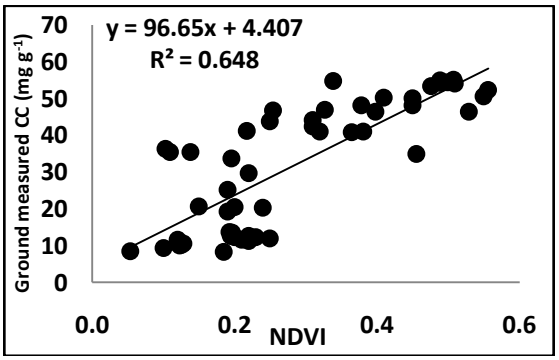

Fig 76. The linear relationship between Landsat 5 TM derived NDVI and castor CC

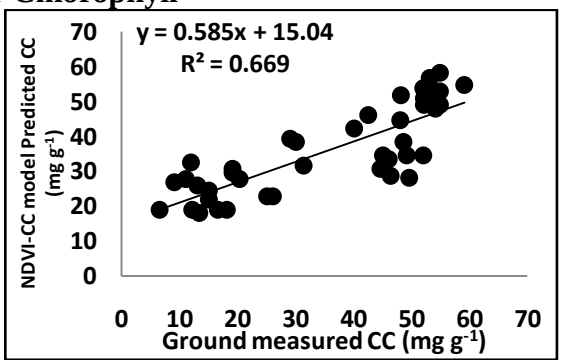

Fig 77. Validation of Landsat NDVI–CC model using ground measured castor CC

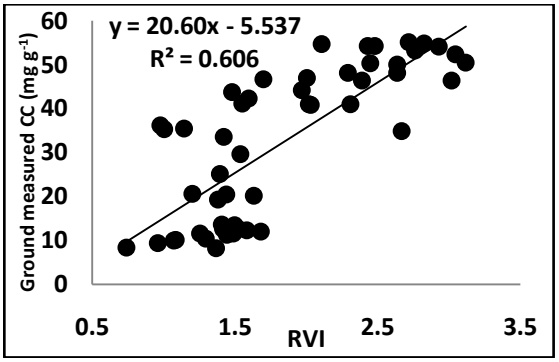

Fig 78. The linear relationship between Landsat 5 TM derived RVI and castor CC

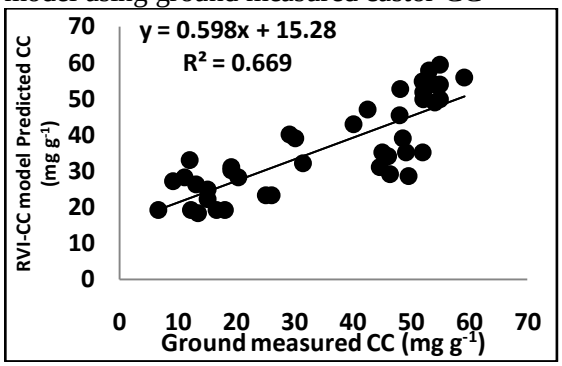

Fig 79. Validation of Landsat RVI–CC model using ground measured castor CC

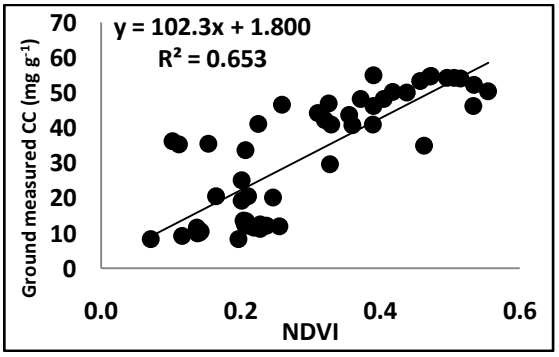

Fig 80. The linear relationship between LISS IV derived NDVI and castor CC

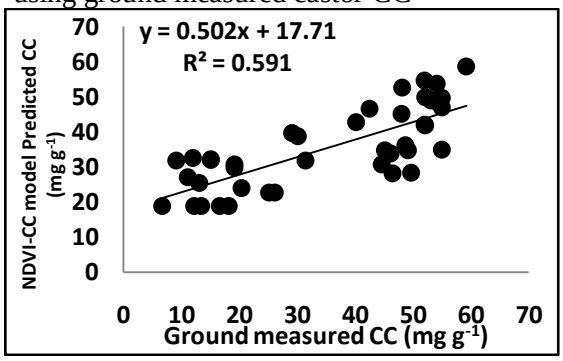

Fig 81. Validation of LISS IV NDVI–CC model using ground measured castor CC

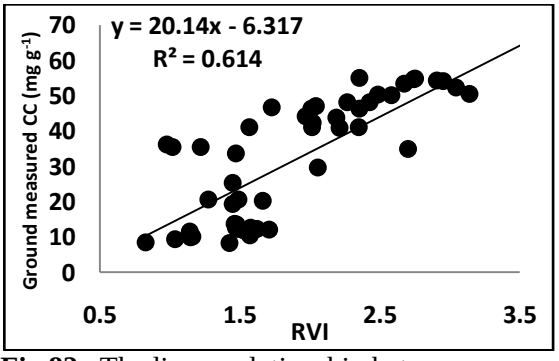

Fig 82. The linear relationship between LISS IV derived RVI and castor CC

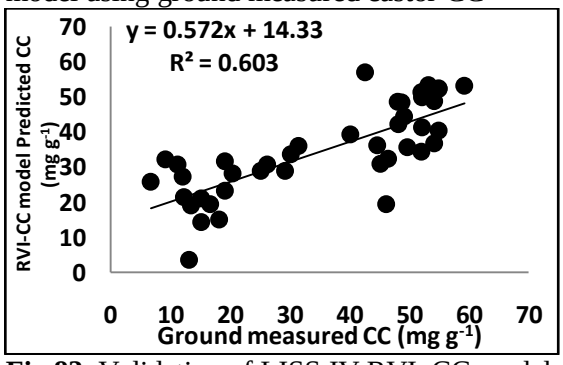

Fig 83. Validation of LISS IV RVI–CC model using ground measured castor CC

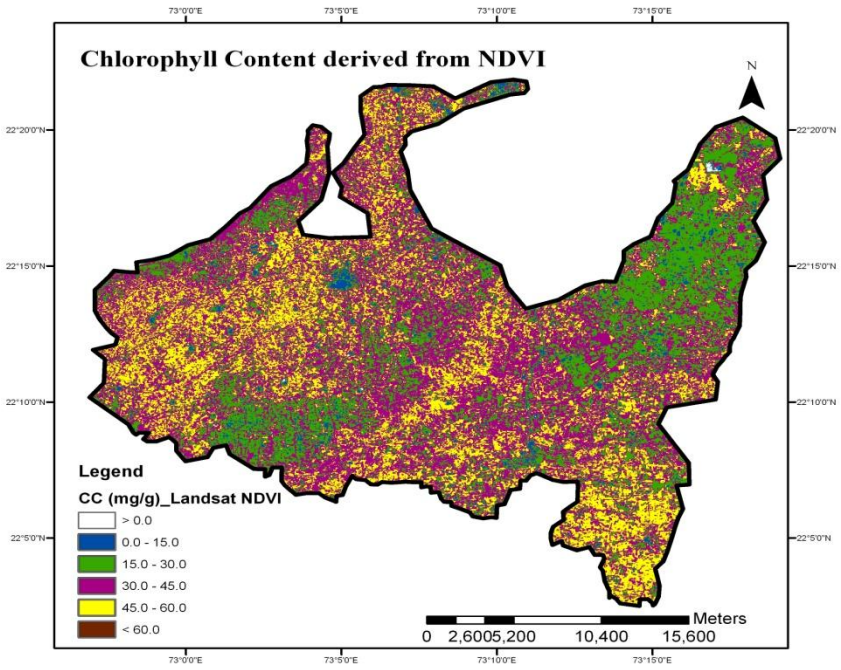

[a]

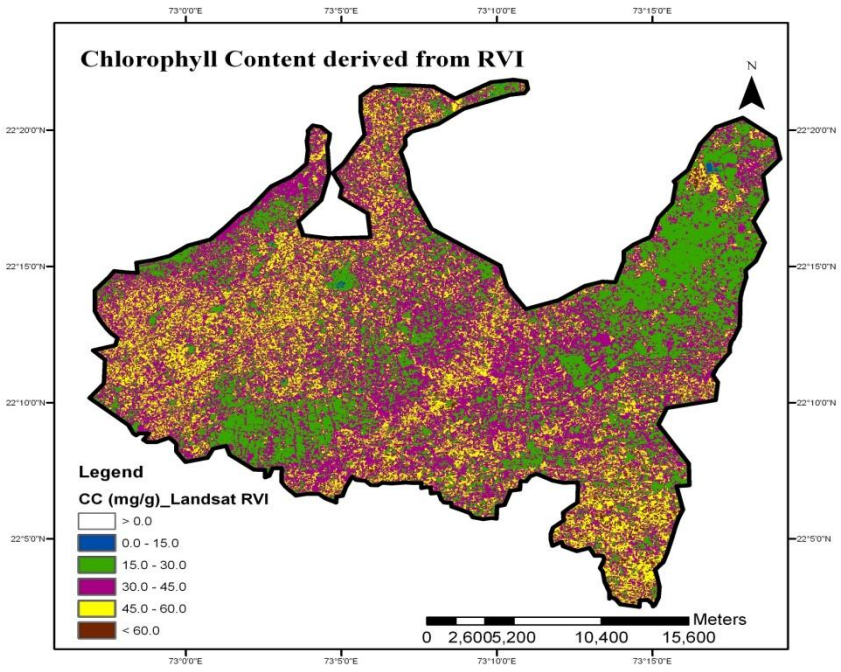

[b]

Plate 21. CC Map generated from [a] Landsat 5 TM derived NDVI [b] Landsat 5 TM derived RVI (Oct 2009) for castor agricultural fields of Vadodara

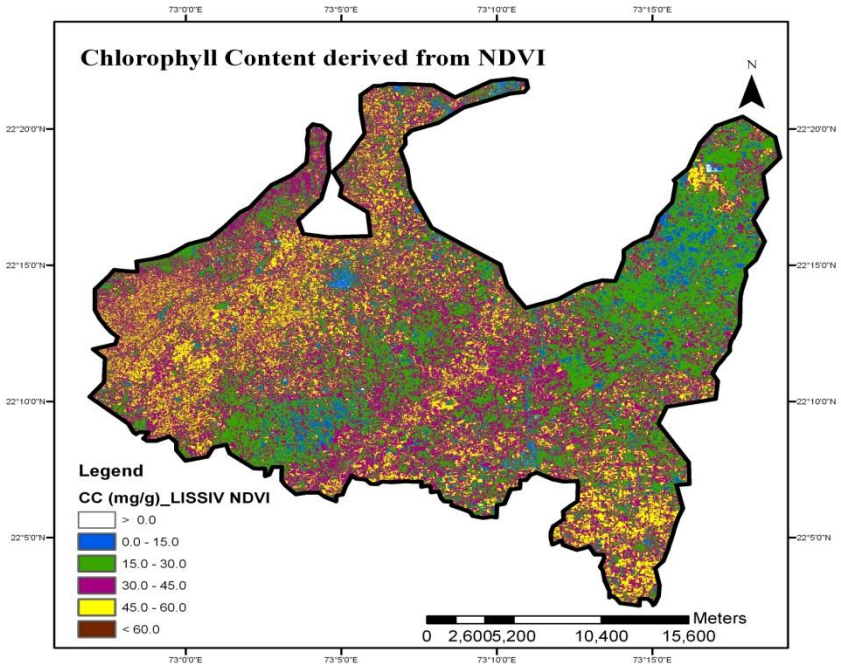

[a]

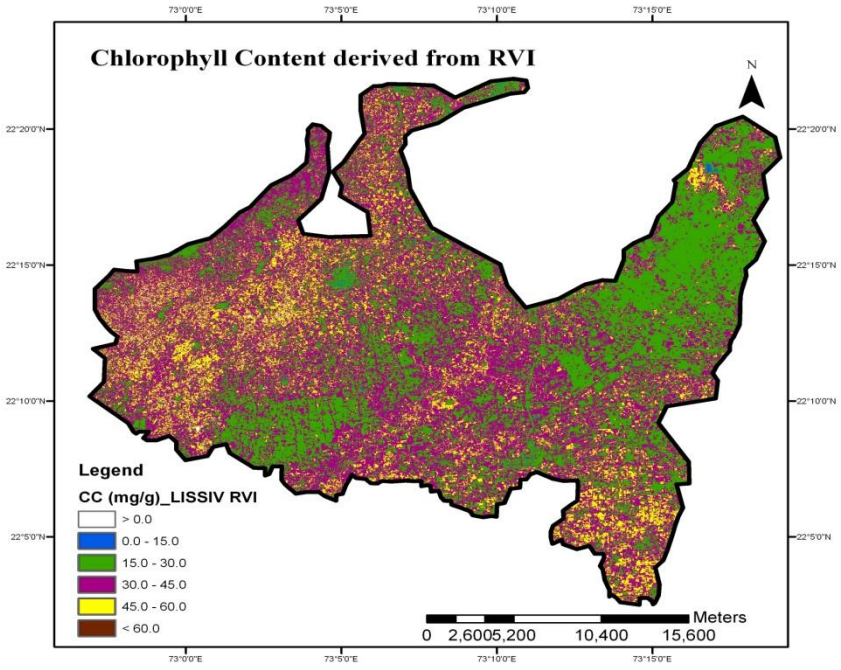

[b]

Plate 22. CC Map generated from [a] LISS IV derived NDVI [b] LISS IV derived RVI (Oct 2009) for castor agricultural fields of Vadodara

Banana Chlorophyll

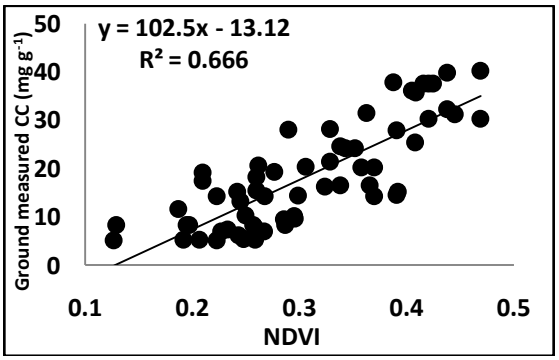

Fig 84. The linear relationship between Landsat 5 TM derived NDVI and banana CC

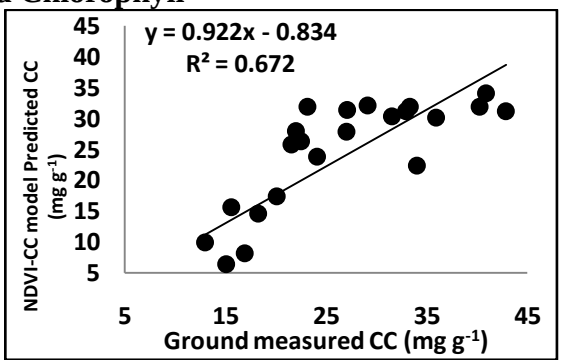

Fig 85. Validation of Landsat NDVI–CC model using ground measured banana CC

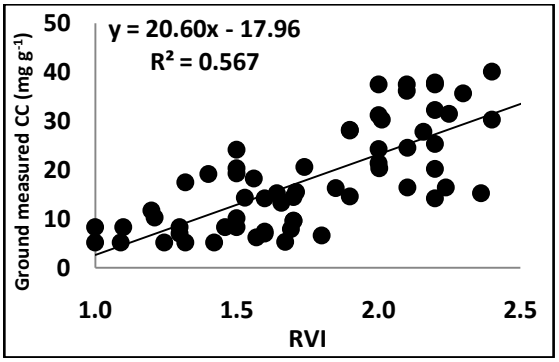

Fig 86. The linear relationship between Landsat 5 TM derived RVI and banana CC

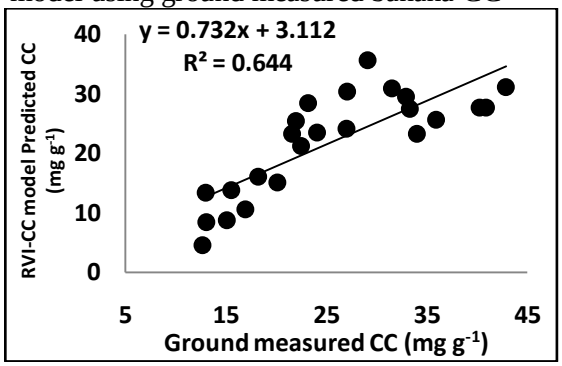

Fig 87. Validation of Landsat RVI–CC model using ground measured banana CC

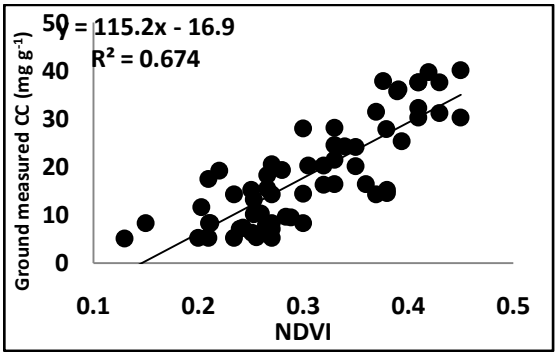

Fig 88. The linear relationship between LISS IV derived NDVI and banana CC

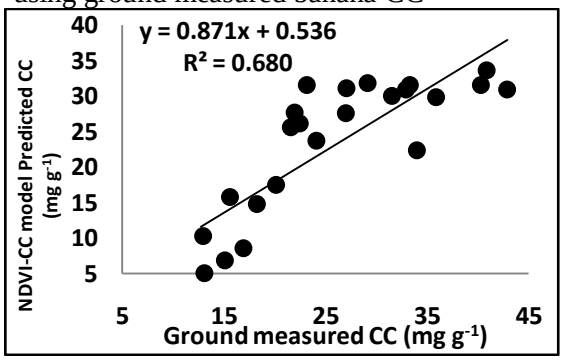

Fig 89. Validation of LISS IV NDVI–CC model using ground measured banana CC

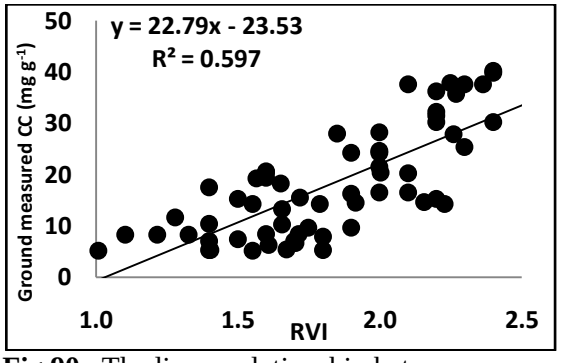

Fig 90. The linear relationship between LISS IV derived RVI and banana CC

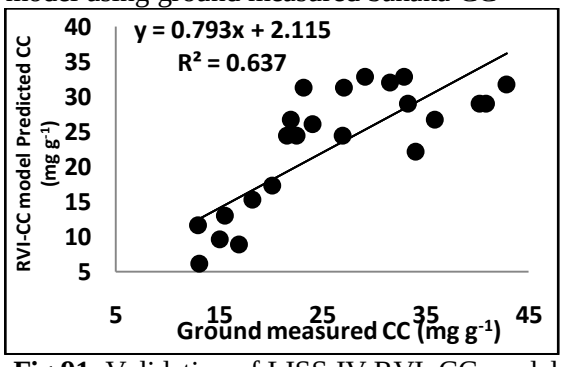

Fig 91. Validation of LISS IV RVI–CC model using ground measured banana CC

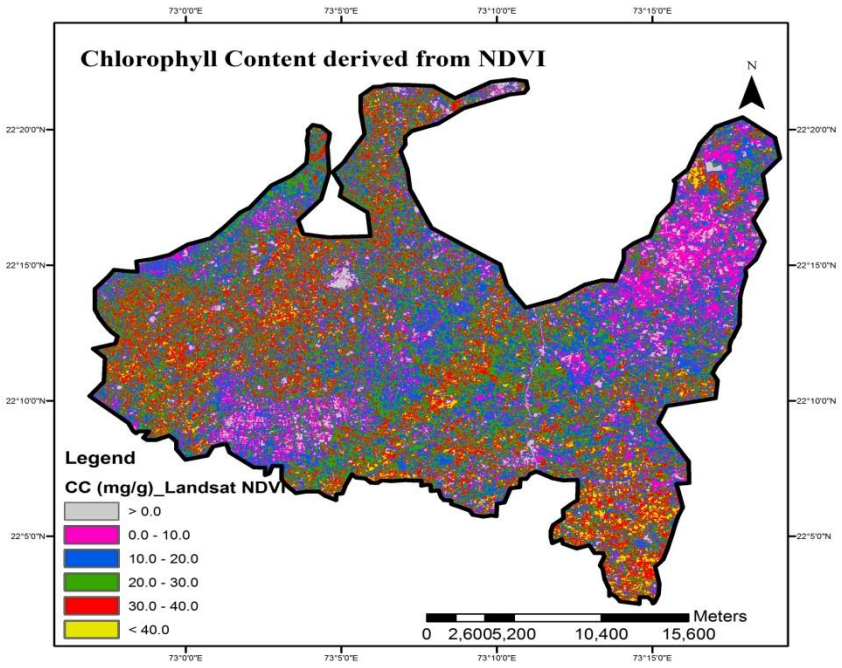

[a]

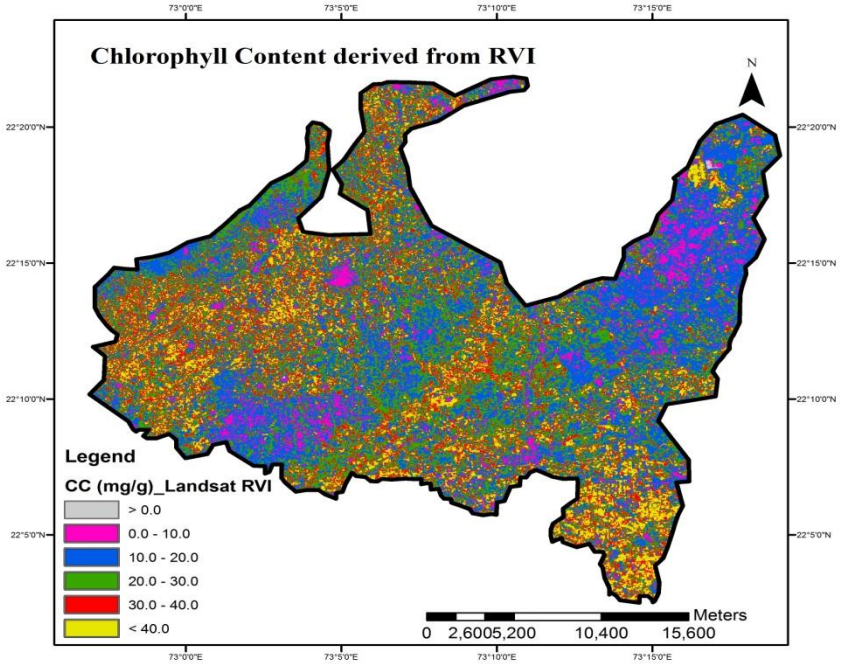

[b]

Plate 23. CC Map generated from [a] Landsat 5 TM derived NDVI [b] Landsat 5 TM derived RVI (Oct 2009) for banana agricultural fields of Vadodara

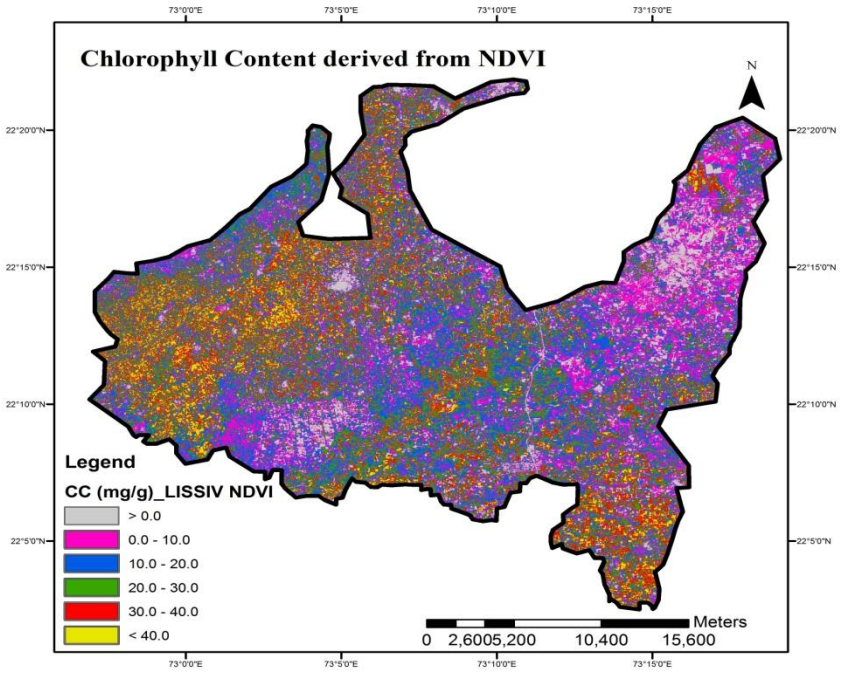

[a]

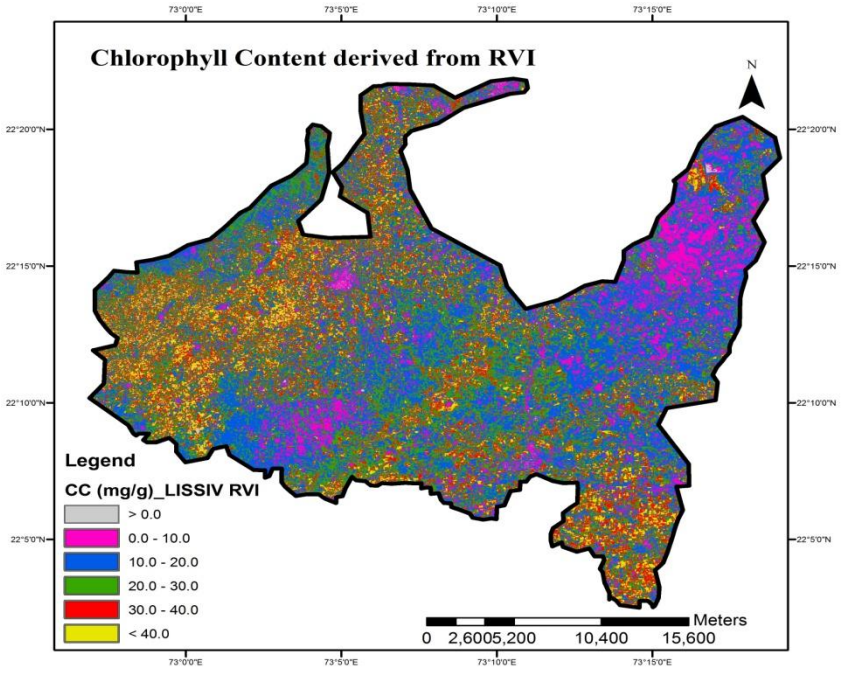

[b]

Plate 24. CC Map generated from [a] LISS IV derived NDVI [b] LISS IV derived RVI (Oct 2009) for banana agricultural fields of Vadodara

4.5.2.1.6 Biomass estimation in different crops using Landsat 5 TM and LISS IV:

Crop biomass, one of the key indicators for crop growth monitoring has a decisive influence on the final crop yield (Jiao et al., 2010). In the present study, biomass estimation is done via statistical empirical modelling. Regression analysis is carried out between ground measured biomass and vegetation indices (NDVI and RVI derived from Landsat 5 TM and LISS IV data). The obtained regression equations are used as NDVI-Biomass and RVI-Biomass models for the retrieval of biomass from an optical data.

NDVI-Biomass model: Biomass of cotton and banana crop when linearly correlated to its corresponding Landsat derived NDVI suggested good correlation between this biophysical parameter and vegetation index. R^2 obtained for this relationship are 0.670 and 0.704 for cotton and banana respectively. **Figure 92 and 96** shows the scatter plot of the relationships obtained by regression analysis: Biomass of Cotton and Banana plotted against Landsat derived NDVI displayed a positive trend as scatter is significant. Likewise, scatter plot between crop biomass and NDVI derived from LISS IV indicated good relationship. In this case slightly higher correlation was obtained with R^2 0.712 and 0.734 for Cotton and Banana crop respectively (**Figure 94 & 98)**. The equations obtained using regression analysis were utilized as inputs for the generation of biomass maps for Cotton and Banana (**Plate 25a, 26a, 27a and 28a**).

RVI-Biomass model: Landsat 5 TM extracted RVI has a positive correlation with biomass of cotton and banana crops. It means increasing of RVI values correspond to increasing biomass. R^2 values for these fitted relationships were 0.581 and 0.697 in the case of Cotton and Banana respectively (**Figure 93 & 97**). Cotton and banana biomass were also estimated by linearly correlating crop biomass and RVI derived from LISS

IV. Fitted regression relationships suggested comparatively higher correlations with R^2 of 0.607 and 0.701 in the case of Cotton and Banana respectively (**Figure 95 & 99)**. Using established relationship between crop biomass and RVI, Biomass maps were developed for Cotton and Banana crops (**Plate 25b, 26b, 27b and 28b**).

Results highlighted better potential of LISS IV data in the retrieval of biomass. NDVI, performed on optical images confirmed itself as a better predictor of biomass.

Cotton Biomass

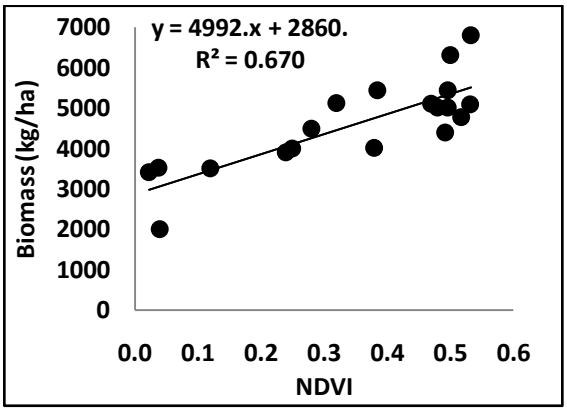

Fig 92. The linear relationship between Landsat 5 TM derived NDVI and cotton biomass

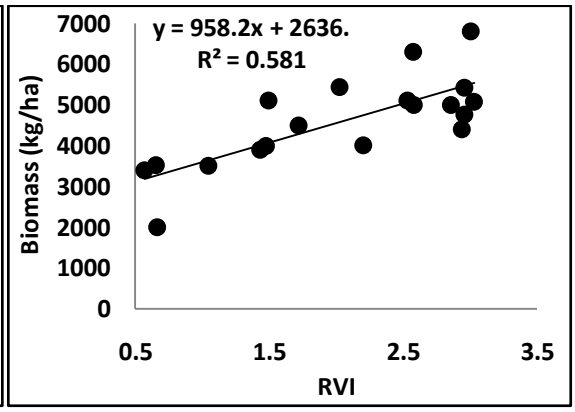

Fig 93. The linear relationship between Landsat 5 TM derived RVI and cotton biomass

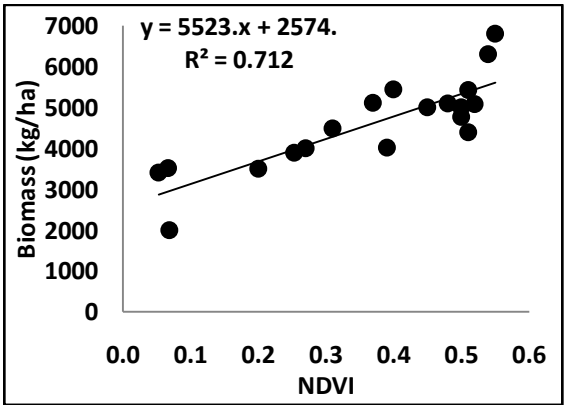

Fig 94. The linear relationship between LISS IVderived NDVI and cotton biomass

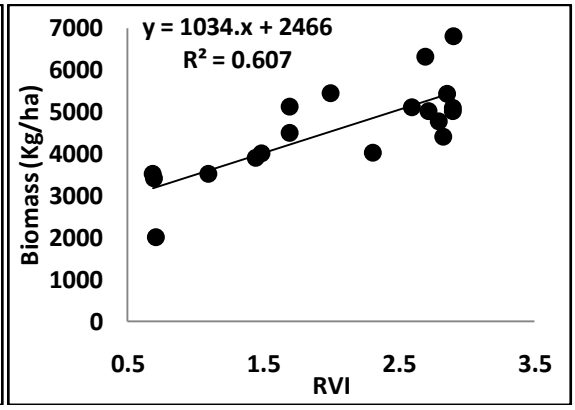

Fig 95. The linear relationship between LISS IV derived RVI and cotton biomass

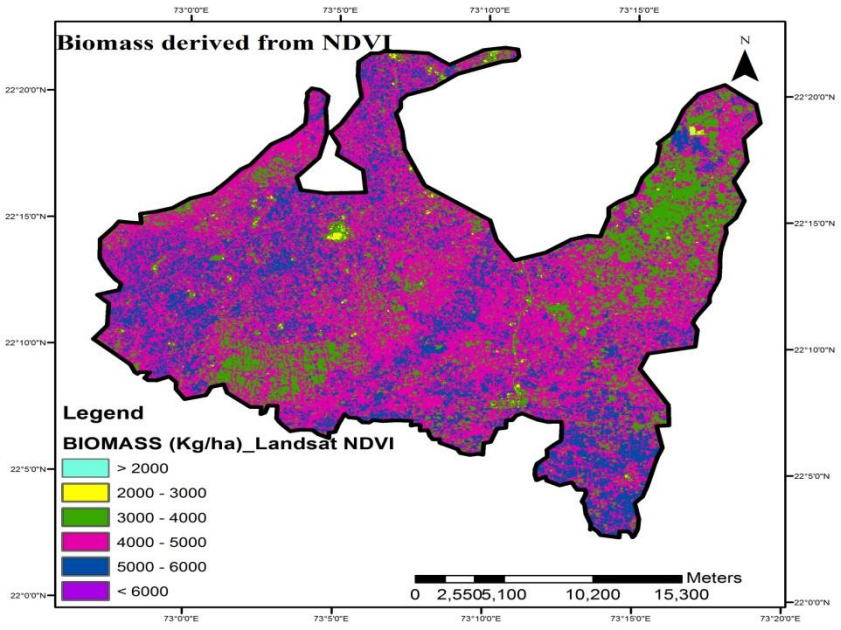

[a]

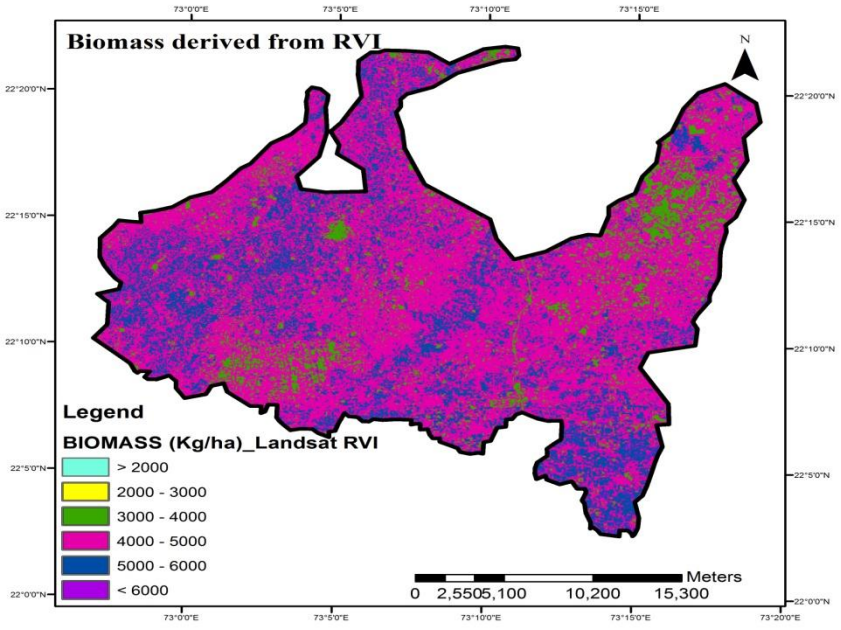

[b]

Plate 25. Biomass Map generated from [a] Landsat 5 TM derived NDVI [b] Landsat 5 TM derived RVI (Oct 2009) for cotton agricultural fields of Vadodara

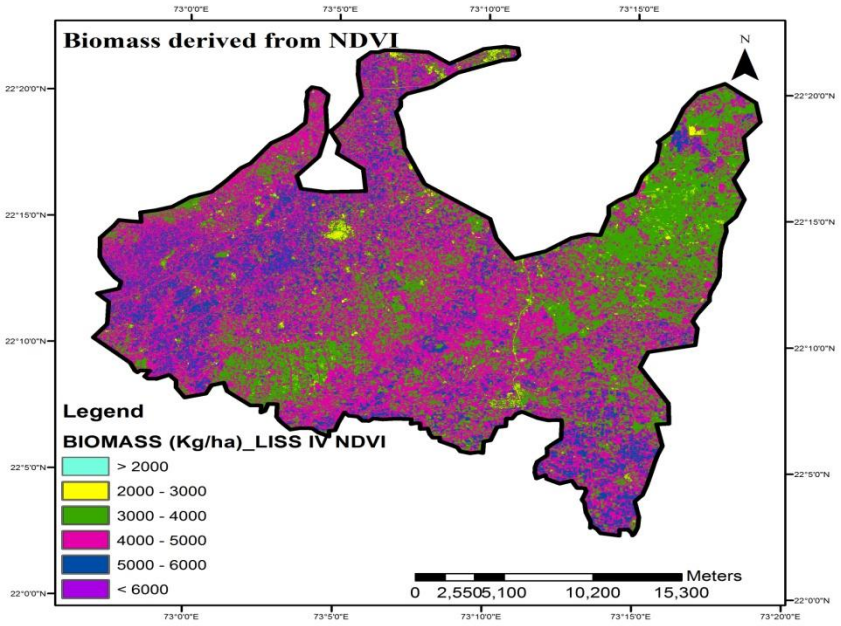

[a]

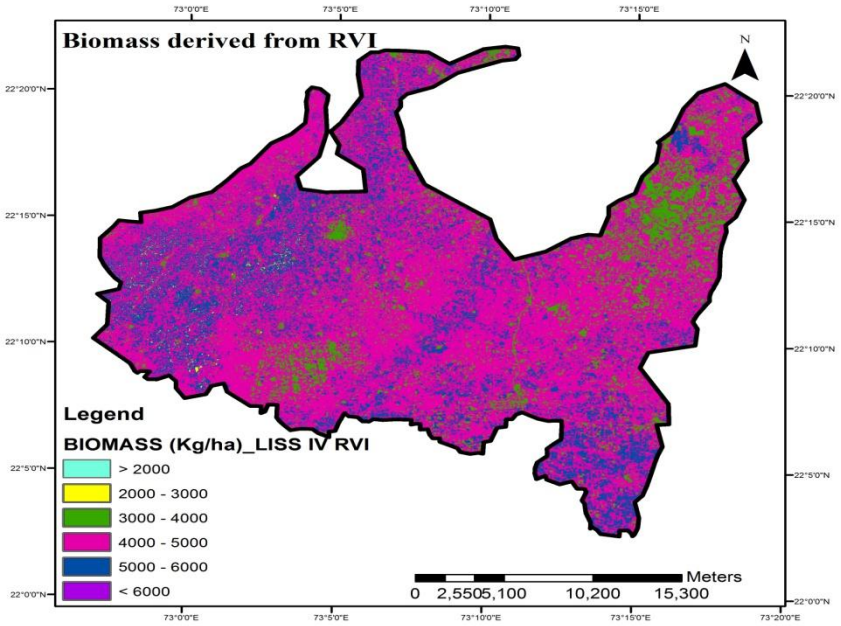

[b]

Plate 26. Biomass Map generated from [a] LISS IV derived NDVI [b] LISS IV derived RVI (Oct 2009) for cotton agricultural fields of Vadodara

Banana Biomass

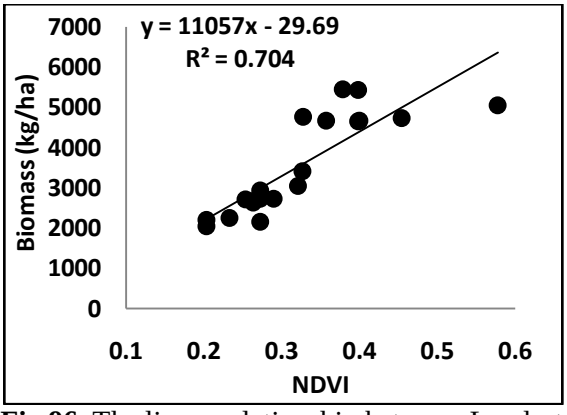

Fig 96. The linear relationship between Landsat 5 TM derived NDVI and banana biomass

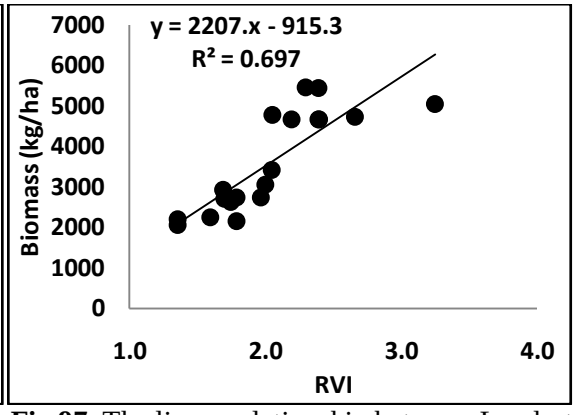

Fig 97. The linear relationship between Landsat 5 TM derived RVI and banana biomass

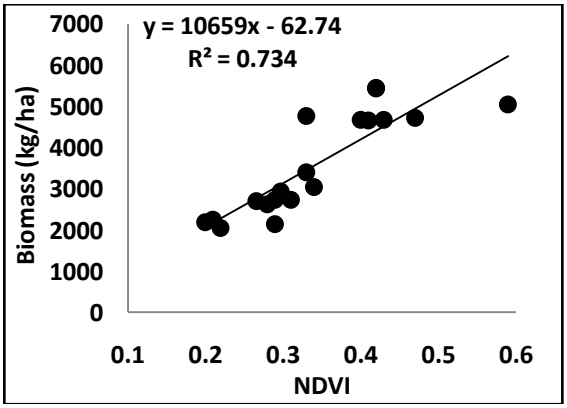

Fig 98. The linear relationship between LISS IV derived NDVI and banana biomass

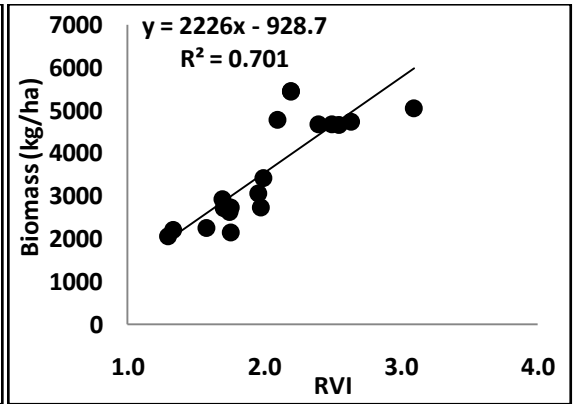

Fig 99. The linear relationship between LISS IV derived RVI and banana biomass

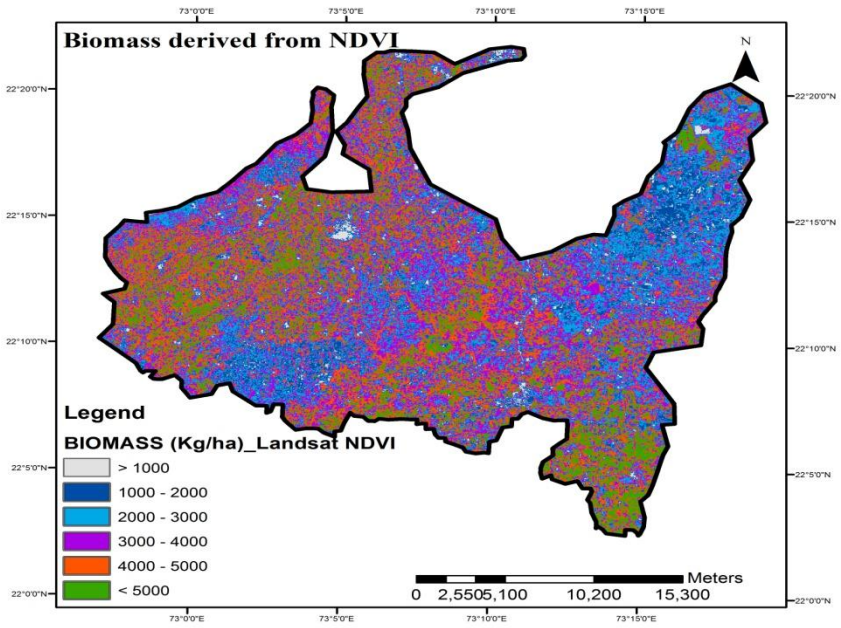

[a]

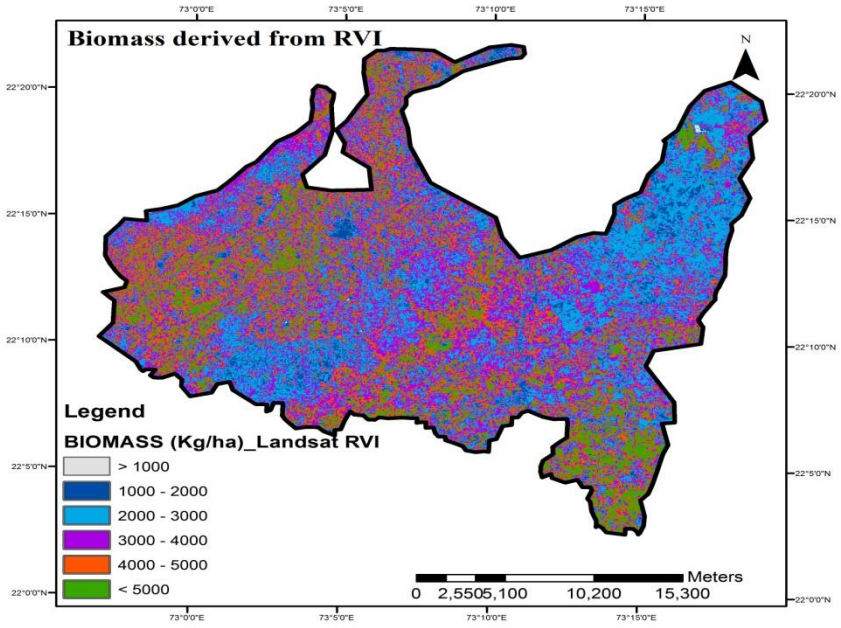

[b]

Plate 27. Biomass Map generated from [a] Landsat 5 TM derived NDVI [b] Landsat 5 TM derived RVI (Oct 2009) for banana agricultural fields of Vadodara

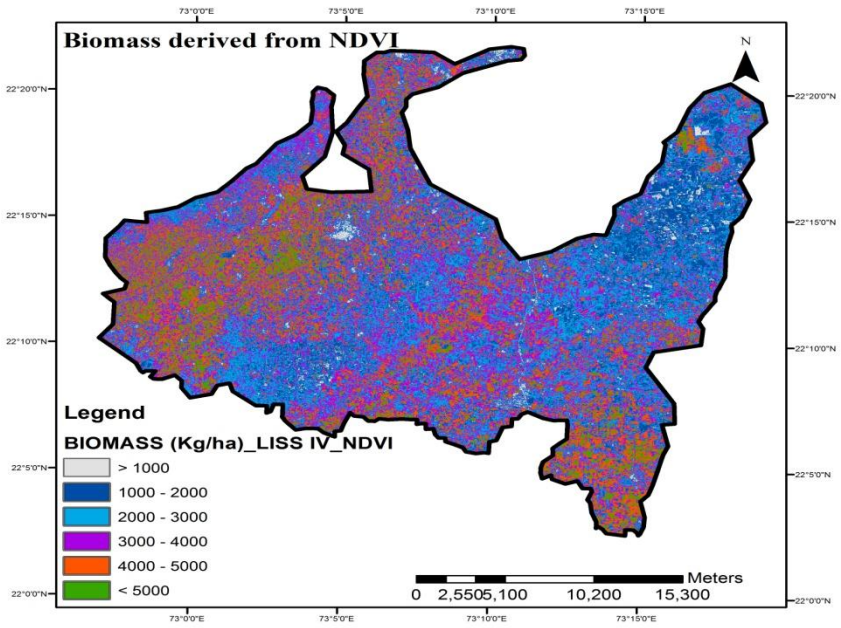

[a]

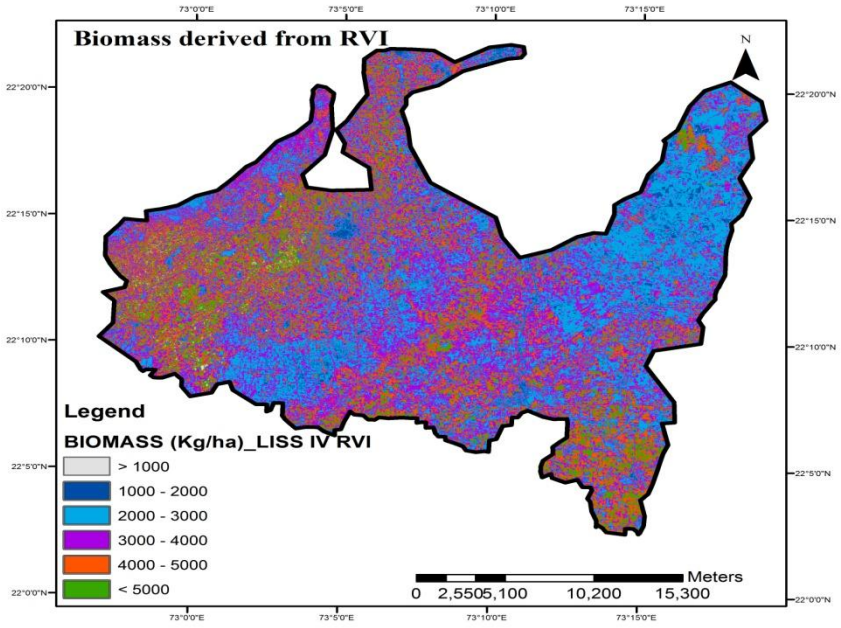

[b]

Plate 28. Biomass Map generated from [a] LISS IV derived NDVI [b] LISS IV derived RVI (Oct 2009) for banana agricultural fields of Vadodara

As in all the estimated parameters NDVI performed better than RVI thus, the parameters viz. LAI and Chlorophyll from Landsat 5 TM derived NDVI and RWC from Landsat 5 TM derived NDWI was further used to determine the health of the selected crops. These parameters were combined together to determine Vegetation Health Index (VHI) that will help in indicating the crop health of these crops in the fields.

4.5.2.1.7 Vegetation Health Index for the Selected Crops:

Crop health, one of the most dynamic crop attributes is early indicator of crop yield, crop risk and ultimately the degree of crop success or failure. Its assessment is critical in determining early yield forecasts that could avert a disastrous situation. It can thereby help in strategic planning that would ensure good agricultural productivity to meet demands of population for food. Early detection of any stress on crop can provide an opportunity for the farmer to mitigate the crop damages. Different crops having their own growth cycles have standard trend of crop vigor variation. The present study determining vegetation health index of different crops viz. Cotton, Castor and Banana reported crop conditions of these crops in agricultural fields of different villages of the study area. This index which is an integration of NDVI derived LAI and CC and NDWI derived RWC, is unitless and ranges between 0 and 1. Based on the VHI, the study region was divided into four classes corresponding to four growth conditions of crop (**Table 19**). Vegetation health index maps developed for Cotton, Castor and Banana in different villages are shown respectively in **Plate 29, 30 and 31**. Vegetation Health of the selected crops in the selected villages can be known by referring these generated maps which will help the farmers in knowing conditions of their crops in the fields and thereby help in crop monitoring. Results indicated that the cotton fields of all five

selected villages are with varying crop health. Cotton crops present in these villages were in unhealthy to very healthy conditons (**Table 20**). Castor health in ranu village also showed variation in their health. Crops were in very poor to very good condition. Castor VHI of other four villages indicated castor health ranging from poor to very good crop condition (**Table 21**). Banana crops of Luna, Dabhasa and Mahapura, Sherkhi were found with poor to very good health whereas banana of Sevasi fall under poor to good health condition categories (**Table 22**). This can be clearly observed in the maps generated.

Table 19. Four classes of crop growth condition based on vegetation health index

Vegetation Health Index	Crop growth condition
0.00 – 0.25	Very poor
0.25 – 0.50	Poor
0.50 – 0.75	Good
0.76 – 1.00	Very good

Table 20. Vegetation health index of cotton crops in different villages

Sr. No.	Village Name	VHI
1.	Luna	0.30 – 0.87
2.	Mahapura	0.30 – 0.87
3.	Muhavad	0.27 – 0.84
4.	Ekalbara	0.26 – 0.84
5.	Dabhasa	0.24 – 0.88

Table 21. Vegetation health index of castor crops in different villages

Sr. No.	Village Name	VHI
1.	Ranu	0.18 – 0.88
2.	Pipli	0.27 – 0.85
3.	Latipura	0.28 – 0.92
4.	Bhoj	0.29 – 0.91
5.	Dhobikuwa	0.30 – 0.83

Table 22. Vegetation health index of banana crops in different villages

Sr. No.	Village Name	VHI
1.	Luna	0.30 – 0.86
2.	Dabhasa	0.24 – 0.88
3.	Mahapura	0.30 – 0.87
4.	Sevasi	0.45 – 0.74
5.	Sherkhi	0.46 – 0.77

Vegetation Health Index for Cotton Crop

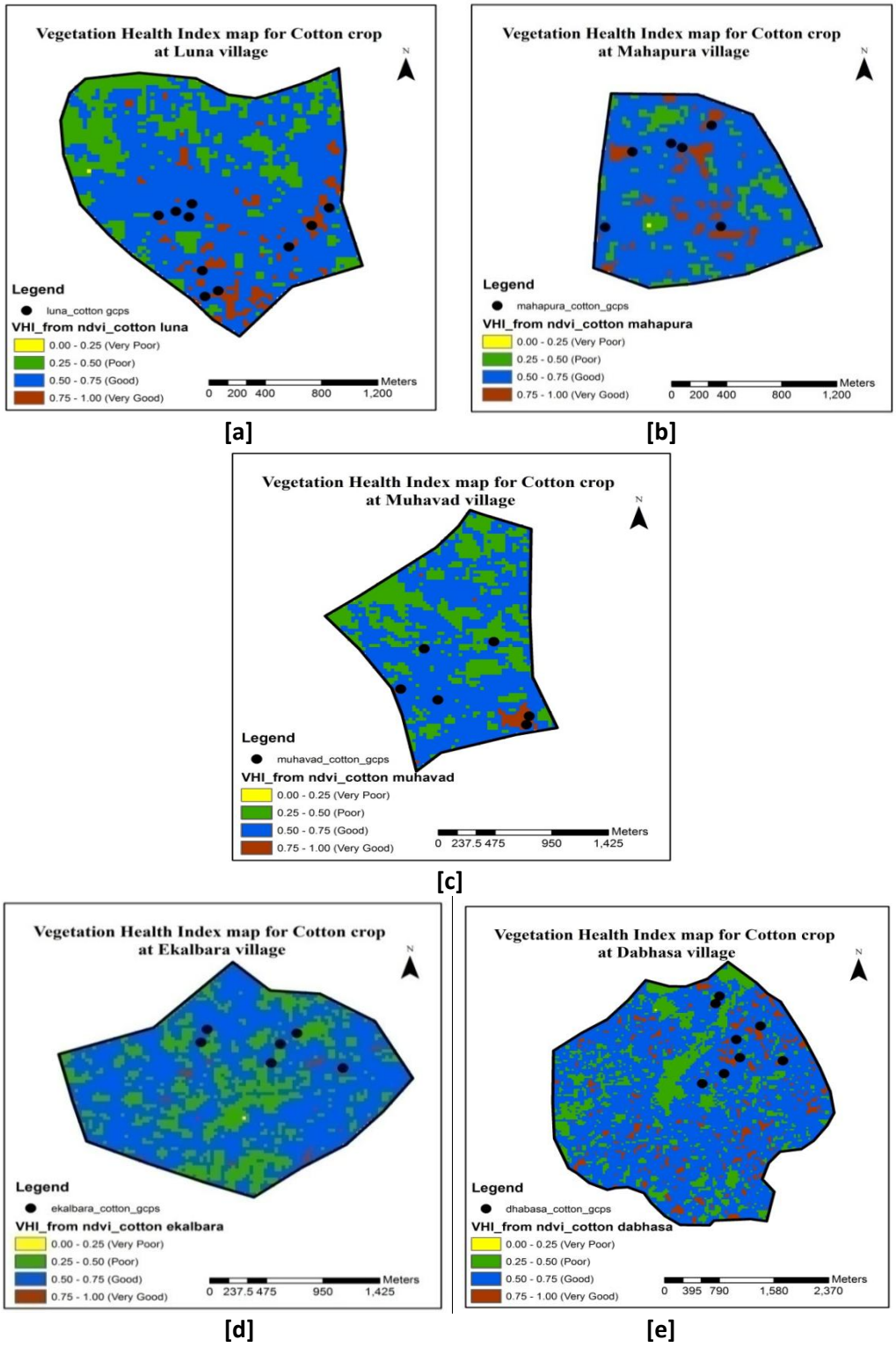

Plate 29. Vegetation Health Index Map developed by combining Landsat NDVI derived CC, Landsat NDVI derived LAI and Landsat NDWI derived RWC for cotton agricultural fields of [a] Luna [b] Mahapura [c] Muhavad [d] Ekalbara [e] Dabhasa villages

Vegetation Health Index for Castor Crop

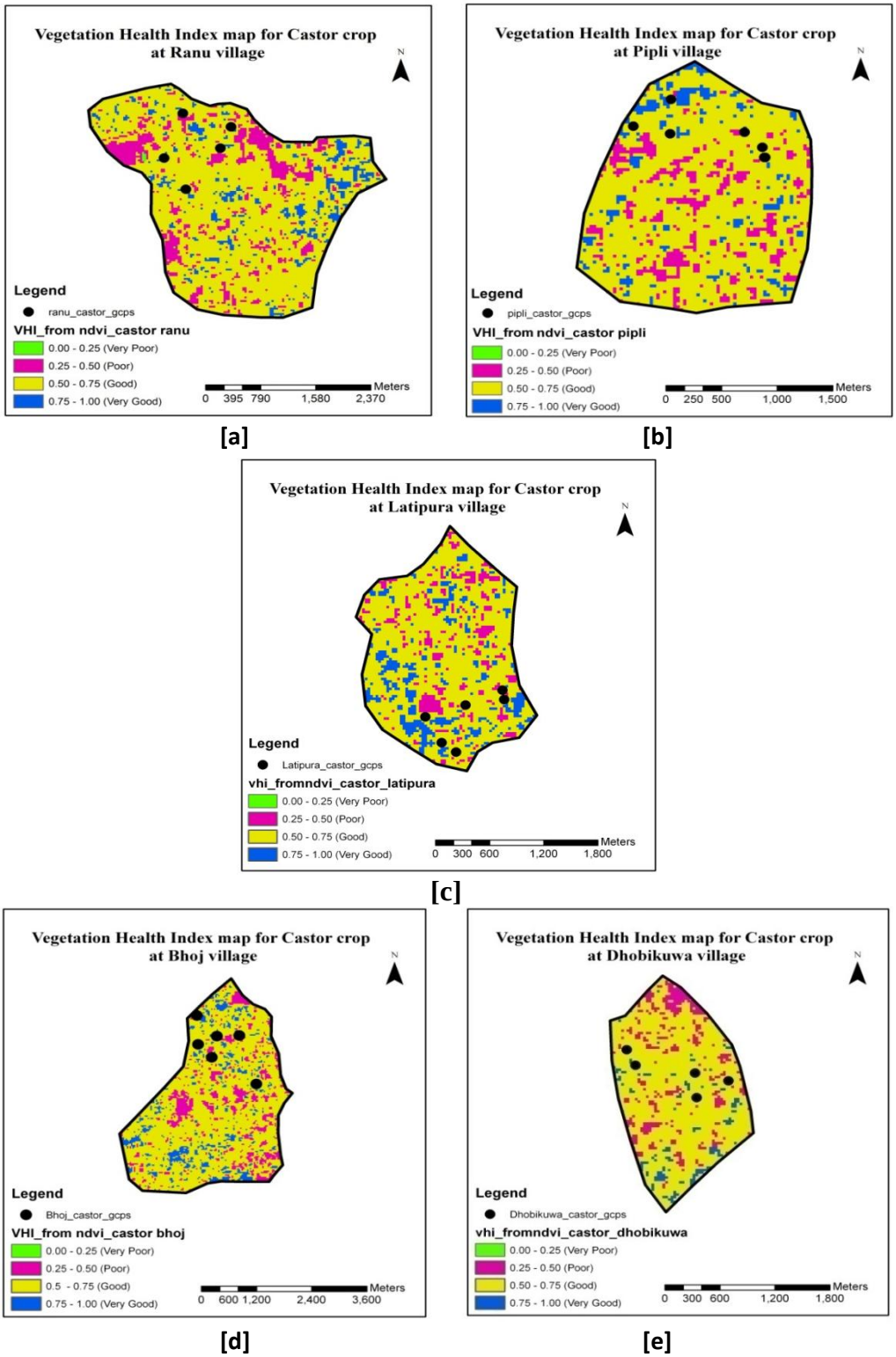

Plate 30. Vegetation Health Index Map developed by combining Landsat NDVI derived CC, Landsat NDVI derived LAI and Landsat NDWI derived RWC for castor agricultural fields of [a] Ranu [b] Pipli [c] Latipura [d] Bhoj [e] Dobikuwa village

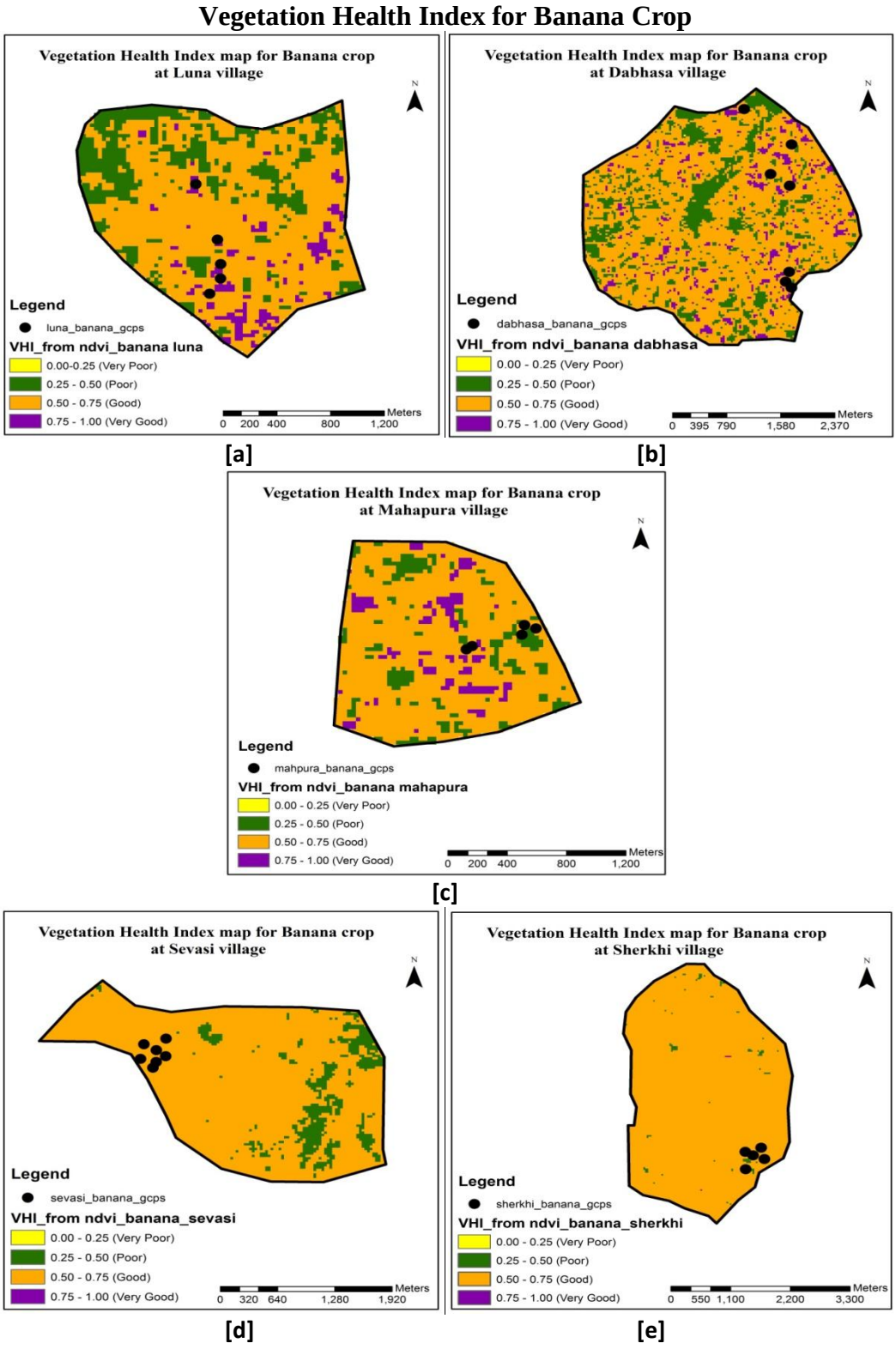

Plate 31. Vegetation Health Index Map developed by combining Landsat NDVI derived CC, Landsat NDVI derived LAI and Landsat NDWI derived RWC for banana agricultural fields of [a] Luna [b] Dabhasa [c] Mahapura [d] Sevasi [e] Sherkhi village

4.5.2.2 Crop parameters retrieval from Microwave data:

Typically, the retrieval of crop parameters like that of LAI is based on VIs calculated using an optical satellite data. As said before, the cloud cover, however, constitutes a big problem for regular acquisition of optical remote sensing data thereby making these estimations difficult in such cases. Therefore satellite SAR data based crop parameter retrieval method would be a valuable alternative and/or addition (Manninen et al., 2007). Because of all-weather imaging capability of microwave remote sensing data, several researchers have used SAR data to map and monitor rice growth (Le Toan et al., 1997, Chen et al., 2007b), and some models have been designed to explain the complex backscattering interaction mechanism and to retrieve LAI and other biophysical parameters of vegetation and crops (Wigneron et al., 1999, De Roo et al., 2001; Lin et al., 2009; Jiao et al., 2011). In the present study, data of C-band (5.3 GHz) ASAR on board of the Envisat when investigated showed its potential in the retrieval of LAI.

4.5.2.2.1 Extraction of backscatter coefficient:

The preprocessed ASAR C band data calibrated to σ° backscatter values is shown in **Plate 32**. Backscattering coefficients (HH, VV) were extracted from the selected Cotton and Banana crop fields. The average backscatter (σ°) values at both HH and VV polarizations were calculated for each selected crop and the polarization ratio (VV/HH) was calculated.

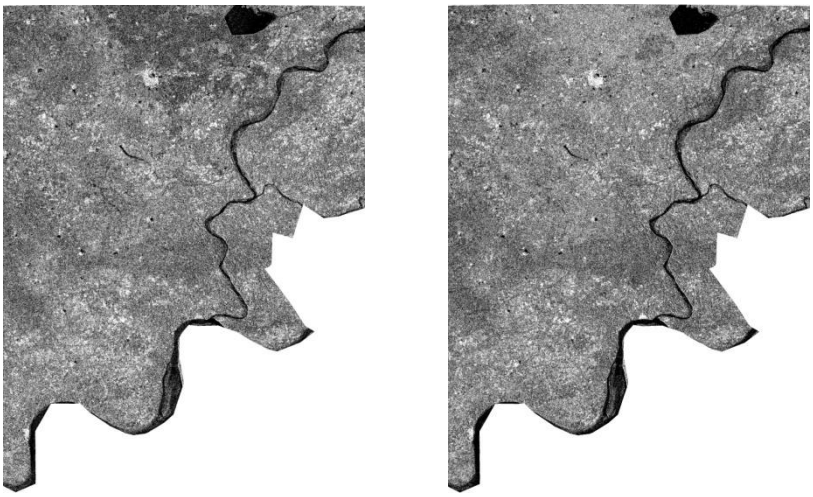

Plate 32. ENVISAT ASAR backscatter. Left: HH-polarized. Right: VV-polarized

Scatter plots of HH versus VV backscatter for cotton and banana crops were also generated (**Figure 100 & 101**). For Banana, the HH polarization backscatter intensities were slightly higher than for the VV polarization, which confirms a higher attenuation at the VV polarization for vegetation with a vertical structure.

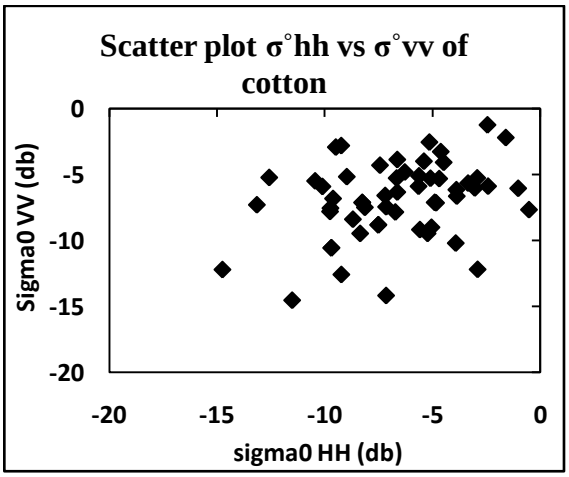

Fig 100. Scatter plots σ˚hh vs σ˚vv of cotton

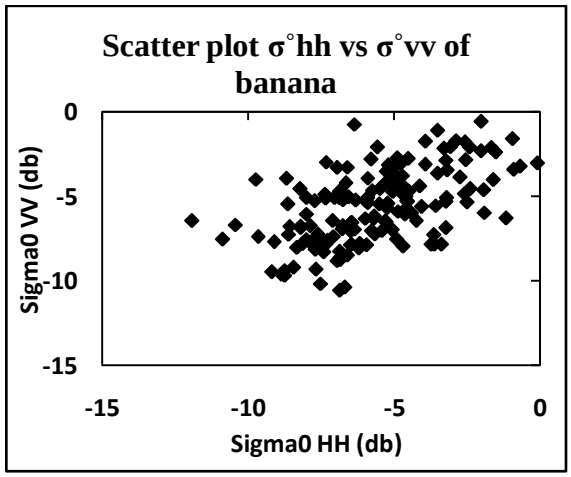

Fig 101. Scatter plots σ˚hh vs σ˚vv of banana

4.5.2.2.2 Retrieval of crop parameters using Microwave RS based Empirical-statistical models:

The backscatter values over each crop field were plotted against the corresponding crop parameters and linear regression models were developed individually for HH and VV backscattering.

4.5.2.2.3 Retrieval of LAI in different crops from ASAR data:

In the present study, LAI for Cotton and Banana crops was measured and relationships of microwave backscattering coefficient (σ°) and the vertical/horizontal (VV/HH) backscattering ratio with LAI were examined.

Correlation analysis between σ° and crop LAI:

The model relation between ASAR HH σ° and cotton LAI fitted with the linear regression, depicted in **Figure 102** did not show good correlation between HH σ° and LAI. Even, the regression analysis between VV σ° and cotton LAI did not provide sufficiently good values of R^2 (**Figure 103**). Same results were found for banana where no good correlation of HH σ° and VV σ° with banana LAI was obtained (**Figure 104 and 105**).

The VV/HH ratio can reflect the variation of cotton and banana components simultaneously, and avoid the problem of calibration, data processing, and soil backscattering effects. Thus, for discriminating the soil and crop properties of the scattering surface, VV/HH polarization ratio has proved to be useful.

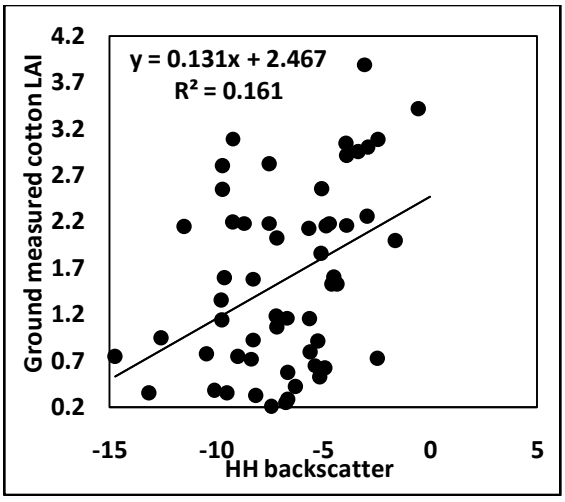

Fig 102. Cotton LAI versus ENVISAT ASAR HH backscatter

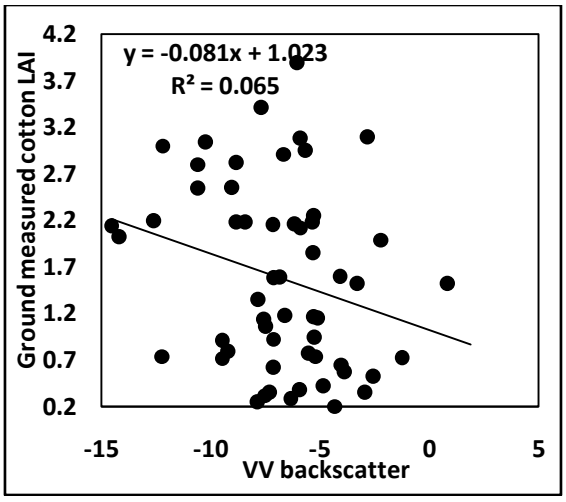

Fig 103. Cotton LAI versus ENVISAT ASAR VV backscatter

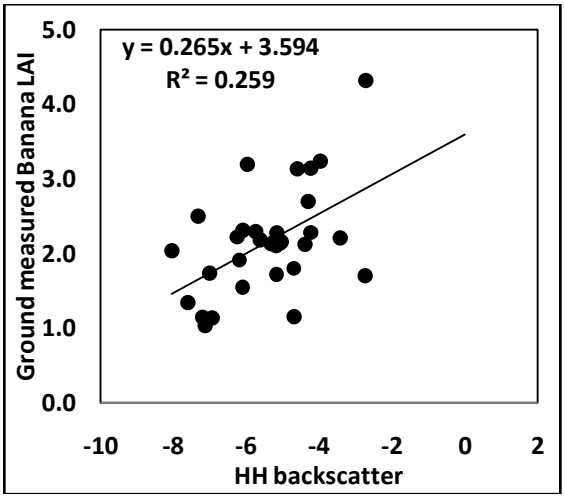

Fig 104. Banana LAI versus ENVISAT ASAR HH backscatter

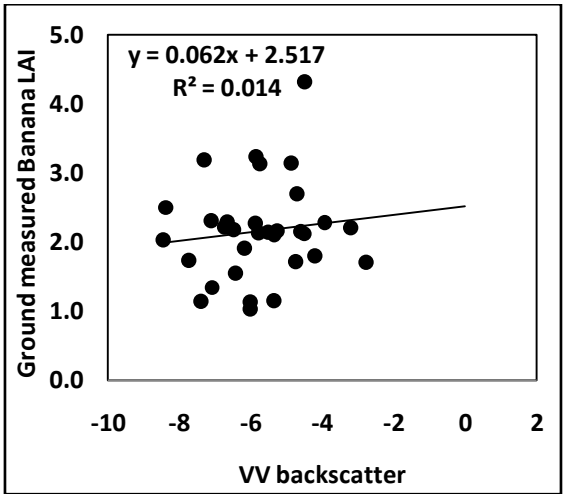

Fig 105. Banana LAI versus ENVISAT ASAR VV backscatter

Correlation analysis between polarization ratio and crop parameters:

It was interesting to study the relationship between polarization ratio and ground measured crop LAI. **Figure 106** shows the results of correlation between Cotton LAI and ASAR VV/HH polarization ratio whereas **Figure 107** shows correlation between Banana LAI and VV/HH polarization ratio. Although some sample errors affected the accuracy of ground data, good correlations were found between polarization ratio of crop fields and their LAI.

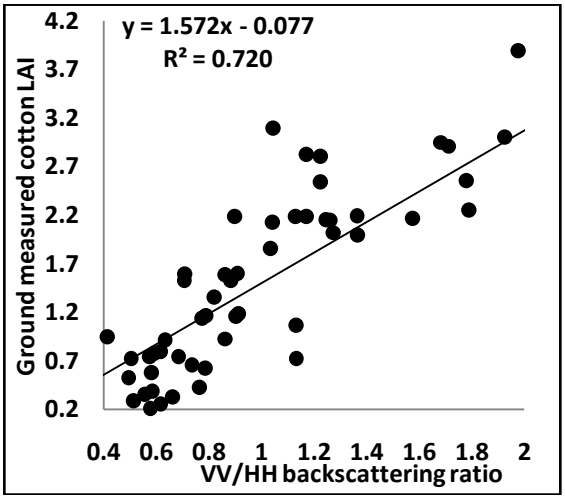

Fig 106. Cotton LAI versus VV/HH backscatter ratio

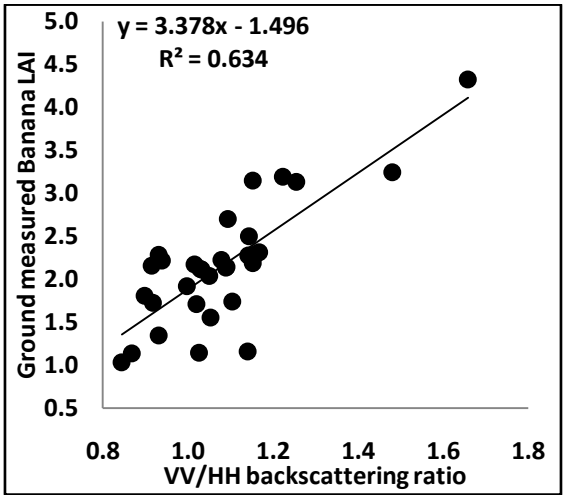

Fig 107. Banana LAI versus VV/HH backscatter ratio